2-P (mix)

NASA CR-134619
WANL-M-FR-74-001

FINAL REPORT

TDNiCr (Ni-20Cr-2ThO$_2$) FORGING STUDIES

BY
A. M. FILIPPI

WESTINGHOUSE ASTRONUCLEAR LABORATORY

PREPARED FOR
NATIONAL AERONAUTICS AND SPACE ADMINISTRATION
NASA-LEWIS RESEARCH CENTER
CONTRACT NAS3-15548

WESTINGHOUSE ELECTRIC CORPORATION - P. O. BOX 10864 - PITTSBURGH, PENNSYLVANIA 15236

154

NOTICE

This report was prepared as an account of Government-sponsored work. Neither the United States nor the National Aeronautics and Space Administration (NASA), nor any person acting on behalf of NASA:

A) Makes any warranty or representation, expressed or implied, with respect to the accuracy, completeness, or usefulness of the information contained in this report, or that the use of any information, apparatus, method, or process disclosed in this report may not infringe privately-owned rights; or

B) Assumes any liabilities with respect to the use of, or for damages resulting from the use of any information, apparatus, method or process disclosed in this report.

As used above, "person acting on behalf of NASA" includes any employee or contractor of NASA, or employee of such contractor, to the extent that such employee or contractor of NASA or employee of such contractor prepares, disseminates, or provides access to, any information pursuant to his employment or contract with NASA, or his employment with such contractor.

1. Report No.	2. Government Accession No.	3. Recipient's Catalog No.
NASA CR-134619		

4. Title and Subtitle	5. Report Date
TDNiCr (Ni-20Cr-2ThO_2) FORGING STUDIES	February, 1974
	6. Performing Organization Code

7. Author(s)	8. Performing Organization Report No.
A. M. Filippi	WANL-M-FR-74-001
	10. Work Unit No.

9. Performing Organization Name and Address	11. Contract or Grant No.
Westinghouse Astronuclear Laboratory P. O. Box 10864 Pittsburgh, Pennsylvania 15236	NAS 3-15548
	13. Type of Report and Period Covered
12. Sponsoring Agency Name and Address	Contractor Report
National Aeronautics and Space Administration Washington, DC 20546	14. Sponsoring Agency Code

15. Supplementary Notes

Project Manager, A. E. Anglin, NASA Lewis Research Center, Cleveland, Ohio

16. Abstract

Elevated temperature tensile and stress-rupture properties were evaluated for forged TDNiCr (Ni-20Cr-2ThO_2) and related to thermomechanical history and microstructure. Forging temperature and final annealed condition had pronounced influences on grain size which, in turn, was related to high temperature strength. Tensile strength improved by a factor of 8 as grain size changed from 1 to 150 μm. Stress-rupture strength was improved by a factor of 3 to 5 by a grain size increase from 10 to 1000 μm. Some contributions to the elevated temperature strength of very large grain material may also occur from the development of a strong texture and a preponderance of small twins. Other conditions promoting the improvement of high temperature strength were: an increase of total reduction, forging which continued the metal deformation inherent in the starting material, a low forging speed, and prior deformation by extrusion. The mechanical properties of optimally forged TDNiCr compared favorably to those of high strength sheet developed for space shuttle application.

17. Key Words (Suggested by Author(s))	18. Distribution Statement
High temperature mechanical properties Thermomechanical and grain size effects Strength optimization	

19. Security Classif. (of this report)	20. Security Classif. (of this page)	21. No. of Pages	22. Price*
UNCLASSIFIED	UNCLASSIFIED		

* For sale by the National Technical Information Service, Springfield, Virginia 22151

NASA-C-168 (Rev. 6-71)

FOREWORD

The work described herein was performed at the Astronuclear Laboratory, Westinghouse Electric Corporation, under NASA Contract NAS3-15548. Messrs. A. Anglin, P. Sikora, and M. Quatinetz, NASA-Lewis Research Center, functioned as project advisors.

The author wishes to acknowledge Mr. Subash Gupta, Utica Division of the Kelsey-Hayes Company, for coordinating the many and varied subcontracted forging experiments, and Dr. Arthur Holms, NASA-Lewis Research Center, for providing the statistical analysis of mechanical property data.

TABLE OF CONTENTS

Section	Title	Page No.
1.0	SUMMARY	1
2.0	INTRODUCTION	2
3.0	MATERIALS AND EXPERIMENTAL PROCEDURES	4
4.0	RESULTS AND DISCUSSION	8
4.1	THERMOMECHANICAL STUDIES	8
	4.1.1 Strength and Forging Conditions	8
	4.1.2 Strength and Microstructure	12
4.2	AN EVALUATION OF OPTIMIZED MATERIAL	19
	4.2.1 Tensile and Stress-Rupture Properties	19
	4.2.2 Microstructure	21
	4.2.3 Dispersed Phase Characteristics	25
	4.2.4 Preferred Orientation	28
4.3	FORGING VELOCITY, PRIOR DEFORMATION, AND SHOCK TREATMENT EFFECT	30
	4.3.1 Tensile Properties	30
	4.3.2 Stress-Rupture Properties	37
5.0	CONCLUSIONS	39
6.0	REFERENCES	40
	APPENDIXES	
A	STARTING MATERIALS	A-1
B	DEFINITIONS OF MATERIAL TERMS	B-1

TABLE OF CONTENTS
(Continued)

Section		Page No.
C	DEFORMATION PROCEDURES	C-1
D	METHODS OF EVALUATION	D-1
E	A SUMMARY OF EXPERIMENTS, TEST DATA, AND STATISTICAL ANALYSIS	E-1
F	AN EXPERIMENT RELATING MICROSTRUCTURE TO FORGING HISTORY	F-1
G	REFERENCES	G-1

LIST OF ILLUSTRATIONS

Figure No.		Page No.
1	A Schematic Representation of Channel Die Forgings	5
2	The Influence of Forging Temperature and Total Deformation on As-forged Tensile Strength	9
3	The Influence of Forging Temperature and Total Deformation on Tensile Strength After Annealing	10
4	Stress-Rupture Properties of Representative Forgings and TDNiCr Sheet	13
5	The Relationship Between Forging Temperature and Rupture Strength	14
6	The Influence of Forging Temperature and Condition on Grain Size	15
7	The Influence of Grain Size and Condition on Tensile Strength	17
8	The Influence of Grain Size on Rupture Strength	18
9	The Influence of Temperature on the Tensile Properties of Optimally Forged TDNiCr	20
10	The Influence of Stress and Temperature on the Rupture Life of Optimally Forged TDNiCr	22
11	The Influence of Temperature on the Rupture Strength of Optimally Forged and Rolled TDNiCr	23
12	The Optical Microstructure of Optimally Forged TDNiCr	24
13	A Transmission Electron Micrograph of Optimally Forged TDNiCr	26
14	ThO_2 Particle Size Distribution in Optimally Forged TDNiCr	27
15	The (200) Pole Figure for Optimally Forged TDNiCr	29
16	The Influence of Total Deformation History on Tensile Properties	31

LIST OF ILLUSTRATIONS (Continued)

Figure No.		Page No.
17	The Influence of Forging Velocity on Tensile Properties	33
18	The Influence of Shock Treatment on the Strength and Hardness of Optimized Material	35
19	A Transmission Electron Micrograph of Optimally Forged and Single Shock Treated Material	36
20	How Forging Velocity, Deformation History, and Shock Treatment Influence Stress-Rupture Strength	38

LIST OF TABLES

Table No.		Page No.
1	The Ranges of Forging Variables Studied	6

1.0 SUMMARY

The high temperature tensile and stress-rupture properties of forged TDNiCr were evaluated and related to thermomechanical variables and microstructure. Test material was produced in the form of nominally 0.38 cm (0.15 inch) thick channel die forged plates. Over 60 test plates were prepared to examine different conditions of forging temperature and reduction and in-process and final annealing conditions.

Forging temperature and final annealed condition had pronounced influences on grain size which, in turn, was related to high temperature strength. The grain size developed in forged material spanned ~1 to 1000 μm depending upon the combination of these two fabrication variables. An increase of grain size from 1 to 150 μm was followed by a 1366°K (2000°F) tensile strength improvement from 14 to 128 MN/m^2 (2 to 17 ksi). The stress to rupture material in 100 hours at 1366°K (2000°F) increased from 14 to > 49 MN/m^2 (2 to > 7 ksi) as grain size changed from 10 to 1000 μm. A strong texture and numerous very small twins were observed for large grain material and may also contribute to strengthening. Thermomechanical conditions, mechanical properties, and microstructure were related in the same manner for test plates forged from preform material (thick TDNiCr plate commonly used for rolling stock), or from round extruded bar.

Forging in the temperature range of 1255 to 1477°K (1800 to 2200°F) followed by annealing at 1616°K (2450°F), an increase of total reduction, forging to continue the deformation inherent in the starting material, a low forging speed, and prior deformation by extrusion, were conditions which acted to optimize high temperature strength. The program results demonstrated that the mechanical properties of TDNiCr sheet developed for space shuttle applications can be achieved in forged material. Data were also obtained which indicated that the high temperature strength of optimally forged material might possibly be increased further by shock treatment.

2.0 INTRODUCTION

Materials of interest for advanced turbojet engine components must have a high strength to weight ratio at temperatures of 1366°K (2000°F) and higher. One of the most promising types of materials for meeting these property goals are dispersion strengthened alloys. The use of TD-Nichrome (TDNiCr) had been considered by NASA for thermal protection of space shuttle vehicles and a manufacturing development program was undertaken to prepare suitable sheet for this application.[1,2] The properties of dispersion strengthened alloys depend on both the nature of the dispersoid distribution and thermomechanical processing. The properties of TDNiCr sheet are very dependent on rolling history. Most dispersion alloys have been produced by extrusion and swaging or rolling but very little work has been reported on the effects forging has on these materials. Therefore, this program was sponsored by NASA to determine whether a novel forging procedure could be developed that would permit achievement of properties in TDNiCr comparable to those produced by extrusion or rolling.

The purpose of the program described was to study the effect of various forging methods and variables on the properties of TDNiCr which was used as a "model system" for dispersion strengthened materials. The program emphasis was placed on relating forging variables to mechanical properties, not on the ability to produce a specific part.

The specific objectives of this program were to determine: (1) Whether stress relieved dispersion strengthened powder metallurgy preforms could be converted into high strength plates by semi-conventional or novel forging techniques, (2) Whether the properties of high strength bar materials could be retained or improved by semi-conventional or novel forging techniques either with or without controlled thermomechanical processing, (3) Which forging variables enhance the strengthening mechanisms of dispersion-strengthened alloys.

A statistical approach using the Box Wilson method[3,4] was employed to minimize the number of forgings required to determine the optimum conditions. Emphasis was placed upon defining the relationships between elevated temperature tensile and stress-rupture properties and forging and annealing conditions. The role of microstructure in this relationship was examined. A forging procedure that optimized high temperature strength was established, and a thorough evaluation was made of material in this condition. This included the measurement of preferred orientation, thoria particle characteristics, and the temperature dependence of mechanical properties. In addition, experiments were run to determine how the mechanical properties of forged material are influenced by prior deformation, forging velocity, and shock wave treatment.

3.0 MATERIALS AND EXPERIMENTAL PROCEDURES

The starting materials were obtained in the form of forged preforms measuring 30.5 cm x 30.5 cm x 3.8 cm (12 in. x 12 in. x 1.5 in), and 2.85 cm (1-1/8 in.) diameter extruded bar. Preforms are commonly used for rolling stock. Both starting materials were prepared from powders, and consolidated by hydrostatic compaction, sintering, and fabrication. Detailed manufacturing, chemical analysis, mechanical property, and microstructure data are reported for these materials in Appendixes A and B.

A major program effort involved establishing the relationship between thermomechanical conditions, microstructure, and the high temperature strength of forged TDNiCr. This was accomplished by forging the starting materials into nominally 15 - 30 cm x 3.8 cm x 0.38 cm (6 - 12 in. x 1.5 in. x 0.15 in.) test plates under a wide range of temperature and reduction conditions. Forging was done in a slotted or channel die schematically shown in Figure 1. Detailed descriptions of channel die forged plates and the forging equipment used are given in Appendixes B and C. The thermomechanical variables of forging temperature and reduction, in-process annealing temperature, and final annealed condition were examined over the ranges given in Table 1. These variables were correlated with results of tensile and stress-rupture tests made at 1366°K (2000°F) to measure their influence on high temperature strength. The assessment of how each individual variable influenced strength was assisted by applying some techniques of statistical analysis. Selected material was examined metallographically to determine if and how microstructure and strength were related. Detailed descriptions of the evaluation methods used are given in Appendix D.

A second major program effort involved a thorough metallurgical characterization of material channel die forged to optimize high temperature strength. The temperature dependencies of tensile and stress-rupture properties were evaluated. Microstructure and thoria particle

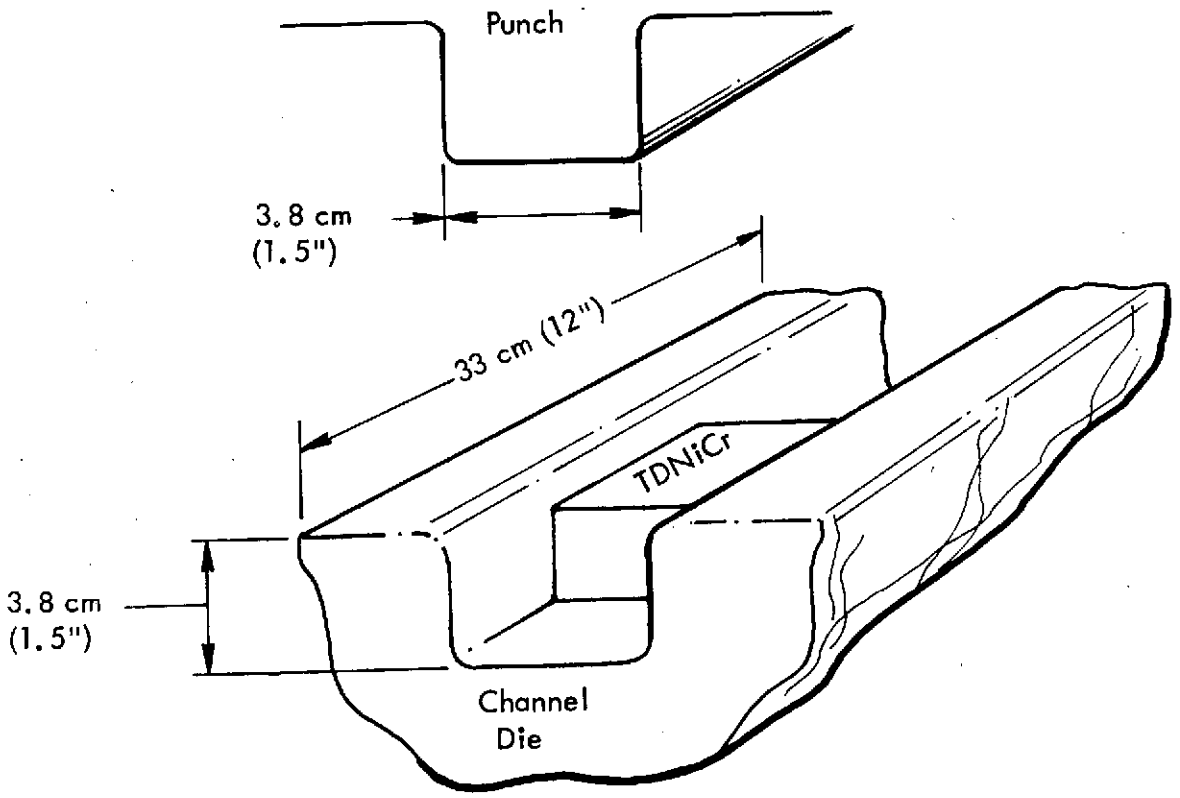

Figure 1. A Schematic Representation of Channel Die Forging. Test plates measuring 15-30 cm x 3.8 cm x 0.38 cm (6-12 in. x 1.5 in. x 0.15 in.) were forged in this setup.

Table 1. The Ranges of Forging Variables Studied

Forging Temperature	Forging Reduction			In-process Annealing Condition	Final Annealed Condition
	%/step	No. of Steps	% total		
922 - 1477°K* (1200-2200°F)	10 to 48	4 to 14	60 to 90	0.5 hr. at** 1089 or 1144°K (1500 or 1600°F)	As-forged or Annealed 0.5 - 1.0 hour at 1589 - 1616°K (2400 - 2450°F)

* Two temperatures, a primary forging temperature used for initial breakdown and a secondary forging temperature used for finish forging operations, were employed in the preparation of several test forgings.

** Used in conjunction with lower forging temperatures.

characteristics were examined by transmission electron microscopy. Preferred orientation was measured. This material was also used to determine if a shock wave treatment of $2.3 \times 10^4 MN/m^2$ (3.3×10^3 ksi) would impart additional high temperature strength.

The test material prepared on the two major projects discussed above was channel die forged on a Mechanical Press. The individual experiments comprising these projects are detailed in Appendix E. Included are the experiments of smaller companion projects such as the actual forging of a turbine vane, and studies of how mechanical properties are influenced by forging velocity (a comparison of Mechanical Press with Dynapak forging), and by the deformation history of the starting material. The results of statistical analyses, where performed, and tabulated mechanical property data are also given in Appendix E.

A separate investigation relating microstructure to forging history was also undertaken. This involved upset forging cylindrical coupons of TDNiCr followed by microstructural examination of the material as-forged and after high temperature heat treatment. A wide range of forging and annealing temperatures and reductions were investigated. The results of this work provided a basis for guiding some aspects of the major forging experiments mentioned previously. This entire project (experimental approach, results, and discussion) is reported in Appendix F.

4.0 RESULTS AND DISCUSSION

Data obtained on the program are summarized in graphic presentations and discussed under three subsections entitled: 1) Thermomechanical Studies; 2) An Evaluation of Optimized Material; 3) Forging Velocity, Prior Deformation and Shock Treatment Effects. Brief introductory and/or summary statements are given at the beginning of each subsection. Data are tabulated in Appendix E.

4.1 THERMOMECHANICAL STUDIES

Preform material and extruded bar stock were channel die forged (Figure 1) on a Mechanical Press under a wide range of thermomechanical conditions (Table 1). Only forging temperature, final annealed condition, and to a lesser extent total reduction, had significant influences on high temperature strength. Relationships between strength and grain size were observed.

4.1.1 Strength and Forging Conditions

The relationships observed between high temperature tensile strength and the thermomechanical variables of forging temperature, total reduction, and final annealed condition are illustrated in Figures 2 and 3. Tensile strength at 1366°K (2000°F) is presented as functions of forging temperature for as-forged material in Figure 2, and annealed material in Figure 3. A total of 49 test forgings are represented in these figures. An average tensile strength value was used where more than one forging was fabricated at a given temperature. Where primary and secondary forging temperatures were used in fabrication, the latter was defined as the forging temperature. Fabrication differences related to the amount of reduction taken on each forging step, the number of steps used, or use of primary forging and in-process annealing were ignored.

The influence total reduction had on high temperature strength was examined by comparing preform material forged 60% and 80 to 90% at 977 and 1089°K (1300 and 1500°F). The results obtained demonstrated, regardless of final condition, that material given the smaller total forging reduction was lower in strength by ~15 - 20 MN/m^2 (~2 - 3 ksi).

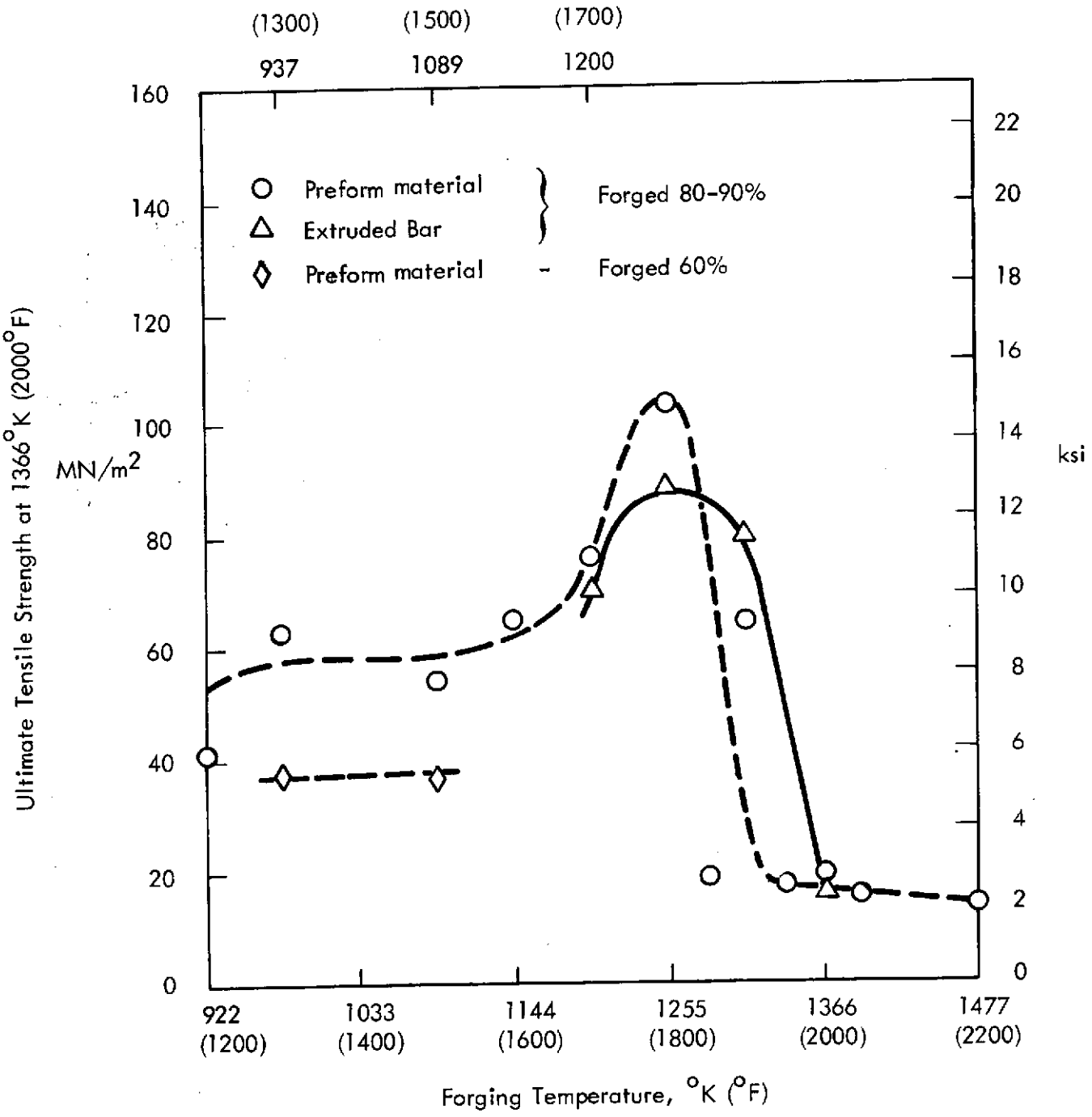

Figure 2. The Influence of Forging Temperature and Total Deformation on As-forged Tensile Strength

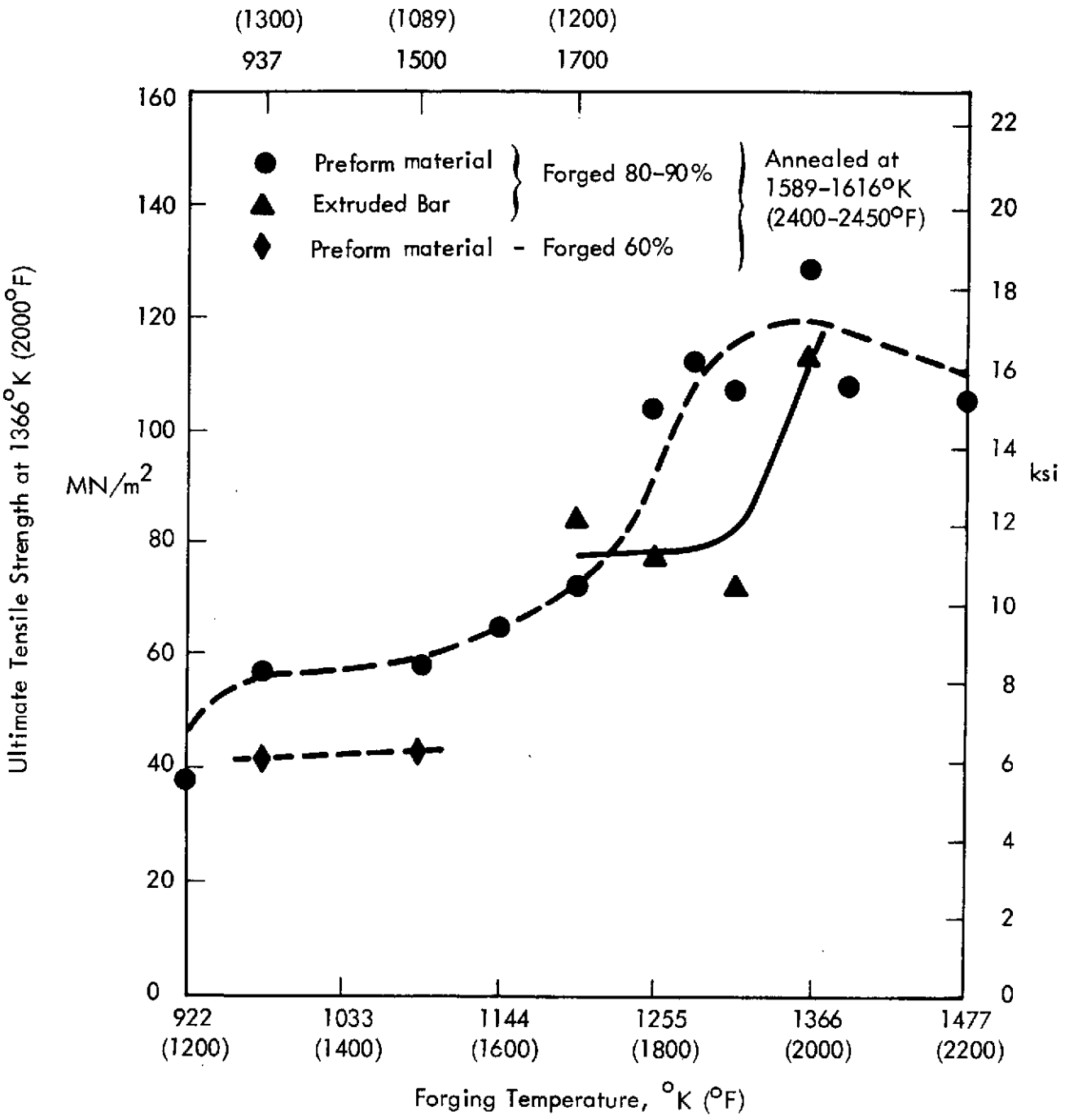

Figure 3. The Influence of Forging Temperature and Total Deformation on Tensile Strength After Annealing

Forging temperatures ranging in 56°K (100°F) increments from 922 to 1477°K (1200 to 2200°F) were investigated for preform material reduced 80 - 90%. This data represents the majority of test forgings prepared on the experimental task. Only a few forgings were produced using extruded bar stock, and forging temperatures from 1200 to 1366°K (1700 to 2000°F) were investigated. Where comparison was made, forging temperature generally had a similar influence on tensile strength, regardless of which forging stock was used. The results representing each starting material do reveal some differences in strength at comparable forging temperatures and in the relative positioning of each curve. These differences are believed due primarily to insufficient results obtained on extruded bar material to accurately define its behavior. The more detailed discussion of how elevated temperature tensile strength and forging temperature are related, which is presented below, refers to the preform data.

The tensile strength of as-forged material measured at 1366°K (2000°F) improved from ~40 to 104 MN/m^2 (~6 to 15 ksi) as forging temperature was increased from 922 to 1255°K (1200 to 1800°F); Figure 2. Further increase of forging temperature caused strength in the as-forged condition to decrease to ~14 MN/m^2 (~2 ksi). The tensile strength of annealed material improved with increased forging temperature until a relatively constant level of ~111 MN/m^2 (~16 ksi) was reached for material forged at or above 1255°K (1800°F); Figure 3.

The tensile strength of TDNiCr sheet processed to optimize high temperature mechanical properties is 139 MN/m^2 at 1366°K (20 ksi at 2000°F)[1]. The information summarized in Figures 2 and 3 demonstrates that this strength level can be closely approached by properly forged material.

Forgings fabricated from preform material and selected to cover the 1144 to 1477°K (1600 to 2200°F) forging temperature range were stress-rupture tested at 1366°K (2000°F). Data were gathered for the annealed condition. These results are summarized in Figure 4 where rupture life and test stress are related. Included in the figure are data for optimally processed TDNiCr sheet.

A general improvement in rupture strength occurred with increase of forging temperature, and a maximum in this property was achieved at ~1366°K (~2000°F). Furthermore, the rupture strength of material forged at or above 1255°K (1800°F) equaled or surpassed that of optimized sheet. These points are more clearly illustrated in Figure 5 where 100 hour rupture strength levels (obtained from Figure 4) are plotted against forging temperature.

4.1.2 Strength and Microstructure

Tensile tested samples representing the entire range of strength observed and all forging temperatures and material conditions investigated were examined metallographically. Relationships between grain size, forging temperature, and final annealed condition emerged and are illustrated in Figure 6.

The grain size of material forged between 922 and 1255°K (1200 and 1800°F) was influenced primarily by forging temperature and not by the final annealed condition or the type of starting stock used. A grain size increase from ~5 to ~175 μm occurred with increase of forging temperature over this range. Forging temperature and final annealed condition both influenced the grain size of material forged above 1255°K (1800°F), but this microstructural parameter remained unrelated to the type of starting stock. Material forged at these temperatures and tensile tested at 1366°K (2000°F) had an ~1 μm grain size. The same material had an ~1000-2000 μm grain size if annealed before testing.

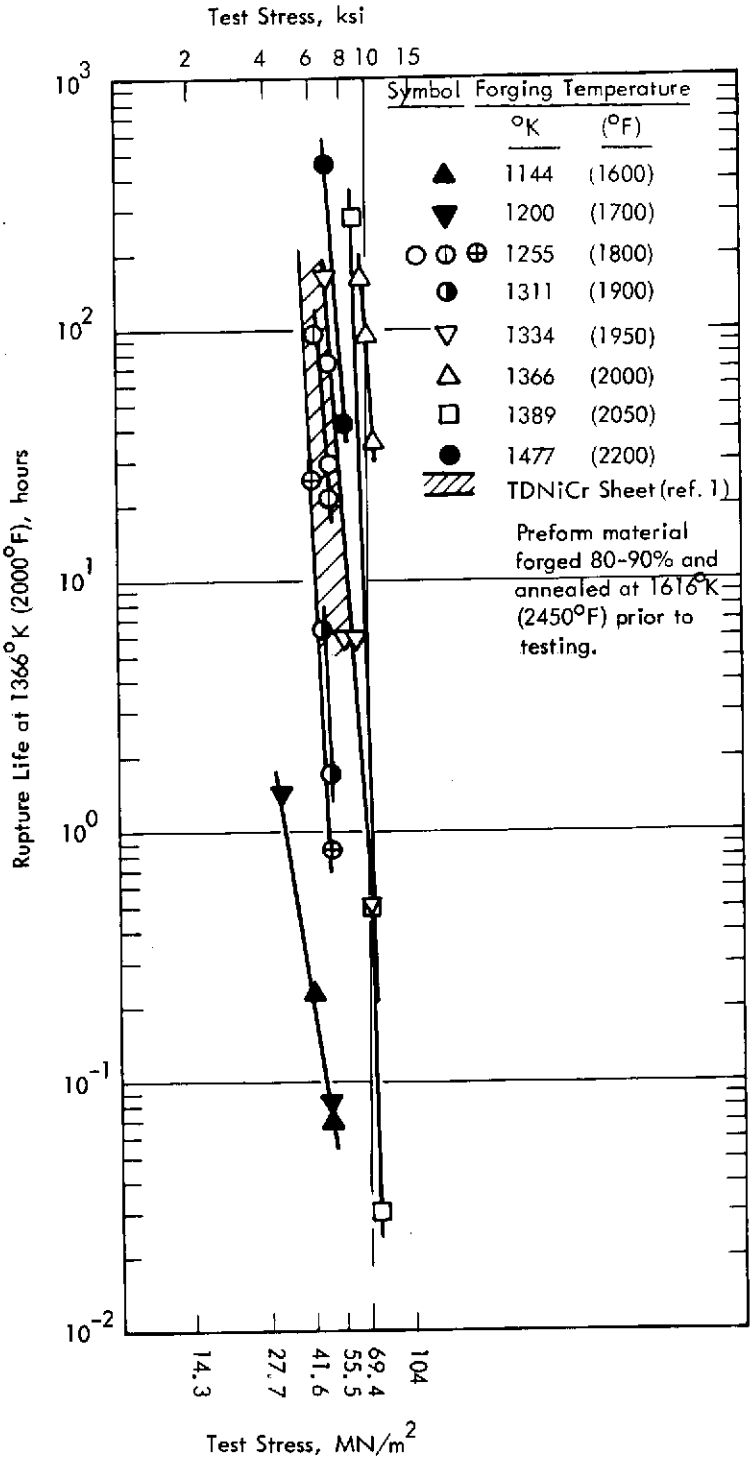

Figure 4. Stress-Rupture Properties of Representative Forgings and TDNiCr Sheet. Forgings prepared from preform material and annealed at 1616°K (2450°F) prior to testing.

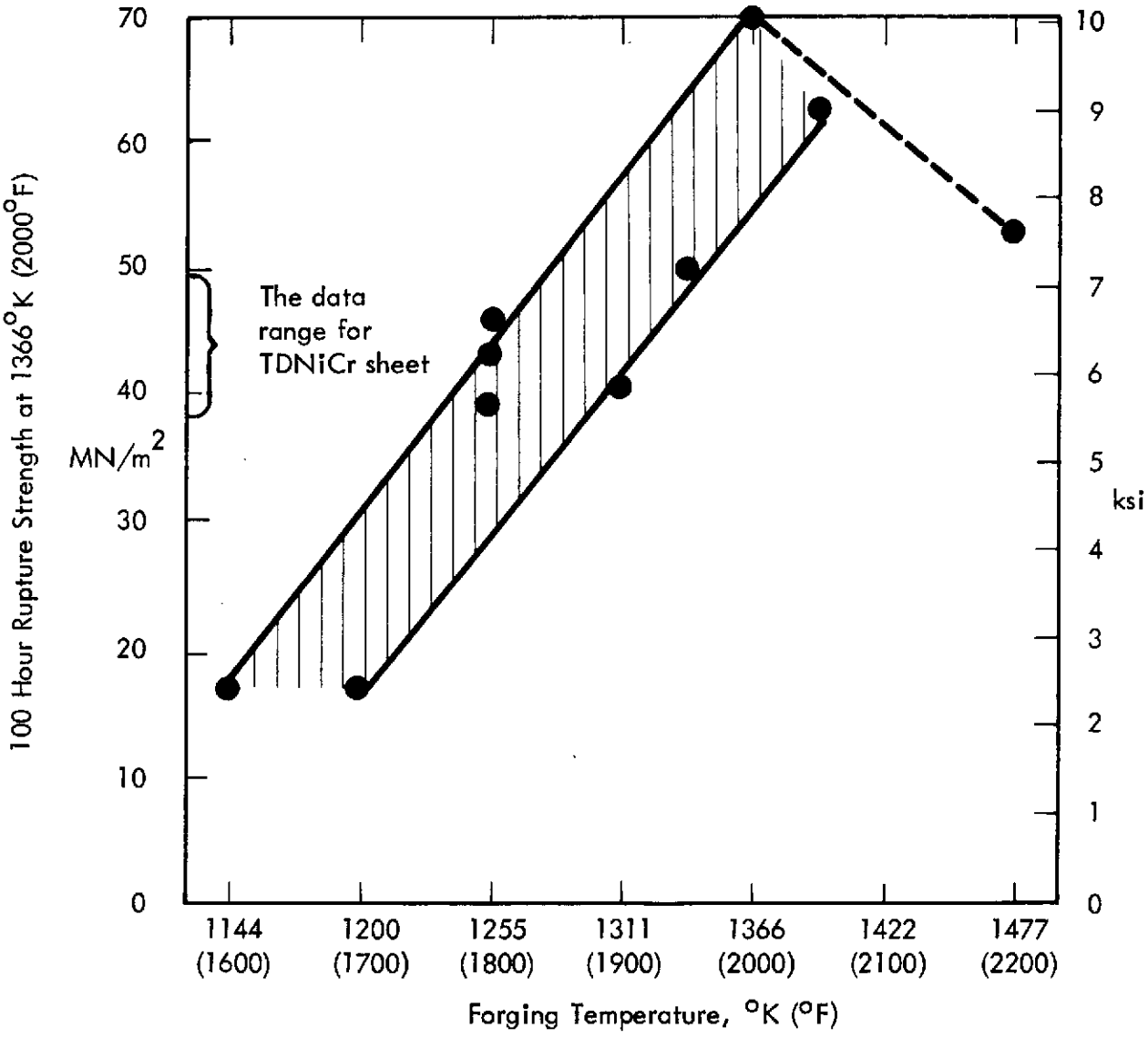

Figure 5. The Relationship Between Forging Temperature and Rupture Strength. Data derived from Figure 4.

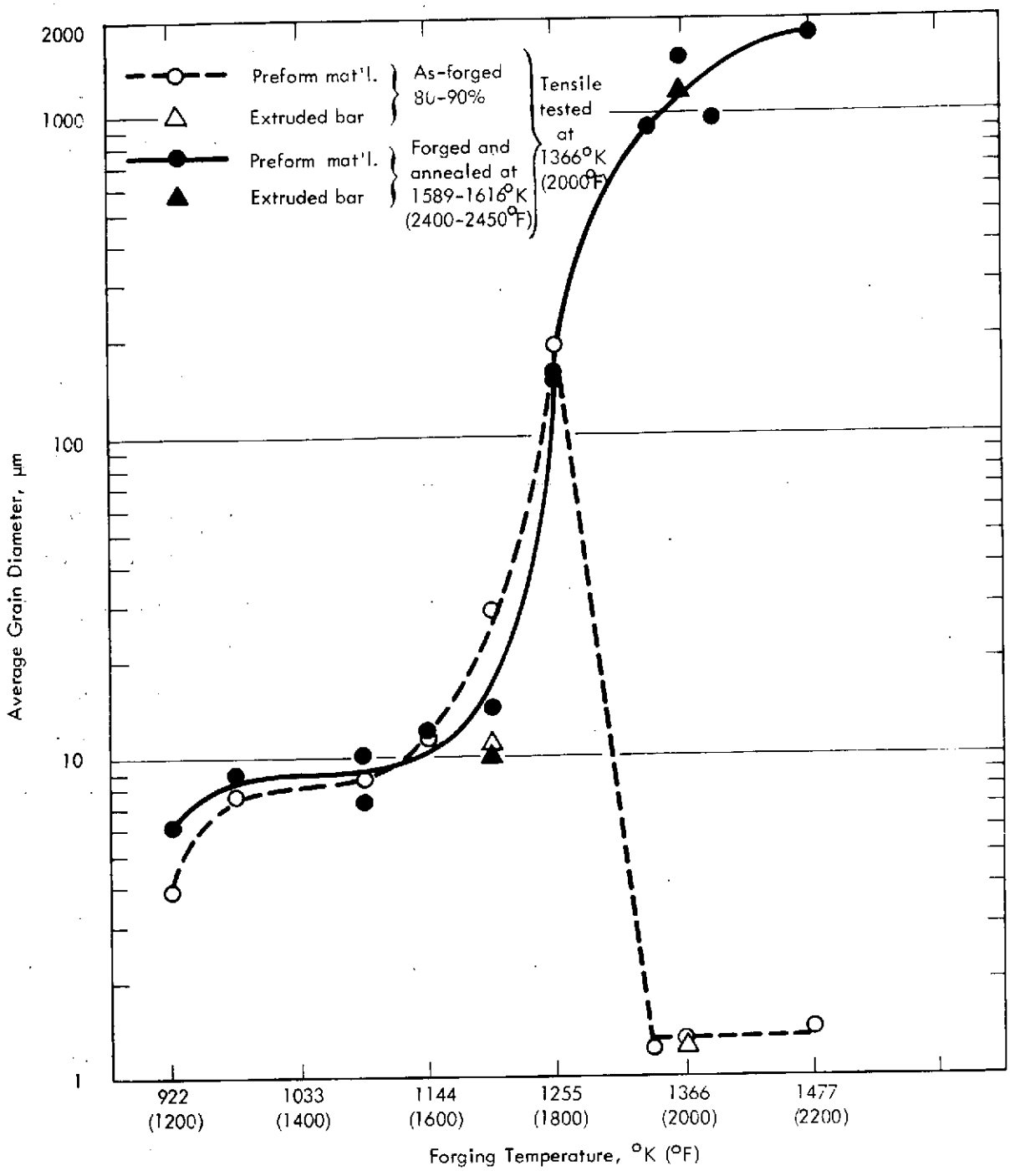

Figure 6. The Influence of Forging Temperature and Condition on Grain Size.

The data summarized in Figures 2, 3, and 6 indicated an obvious relationship between grain size and tensile strength at 1366°K (2000°F), which is illustrated in Figure 7. The strength values of those tensile tested samples examined metallographically to obtain the data presented in Figure 6, are plotted against grain size in Figure 7. Included in the figure are whatever data were available for the two starting materials.

Tensile strength improved with increasing grain size until an asymptotic level of ~111 - 125 MN/m^2 (~16 - 18 ksi) was reached for grain sizes of ~150 μm or larger. This grain size dependency of tensile strength was followed regardless of material condition or type.

The relationship between grain size and 100 hour rupture strength at 1366°K (2000°F) was also examined, and the results are illustrated in Figure 8. Eight of the ten forgings whose stress-rupture properties are summarized in Figures 4 and 5 are represented. An improvement of rupture strength from ~17 to 44 MN/m^2 (2.4 to 6.3 ksi) accompanied a 13 to 150 μm grain size increase. Rupture strength was further improved by an increase of grain size to ~1000 μm, but the response measured was markedly greater in two of the four cases examined. This material displayed a rupture strength range of ~49 to 69 MN/m^2 (~7 to 10 ksi). Some of the results obtained for extremely large grain material may have been biased toward lower values due to an insufficient number of grains in the gauge section of the test specimens.

The grain shape developed in forged material was generally similar regardless of grain size. Grain dimensions measured parallel and perpendicular to the major deformation direction did reveal aspect ratios which ranged up to 4.5, but in the majority of cases, large grain included, they fell between 1 and 2*. It follows that the influences of grain size on high temperature strength were observed under relatively constant conditions of grain shape. A direct dependency of high temperature strength on grain aspect ratio, however, has been demonstrated for thoria dispersion hardened nickel alloys including TDNiCr [5]. The results of the present work indicates that grain size alone can have a potent influence on the strength of TDNiCr.

* See Table E-19.

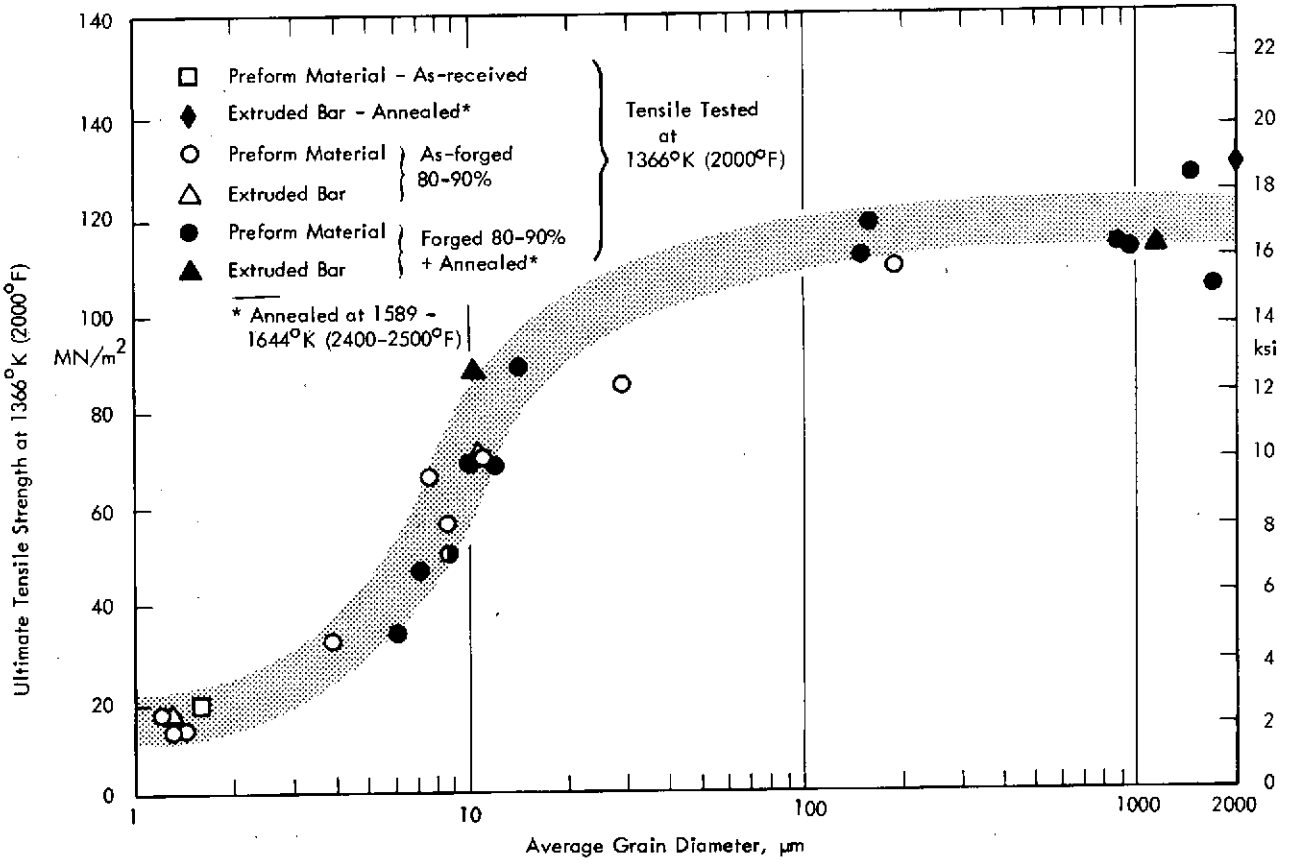

Figure 7. The Influence of Grain Size and Condition on Tensile Strength

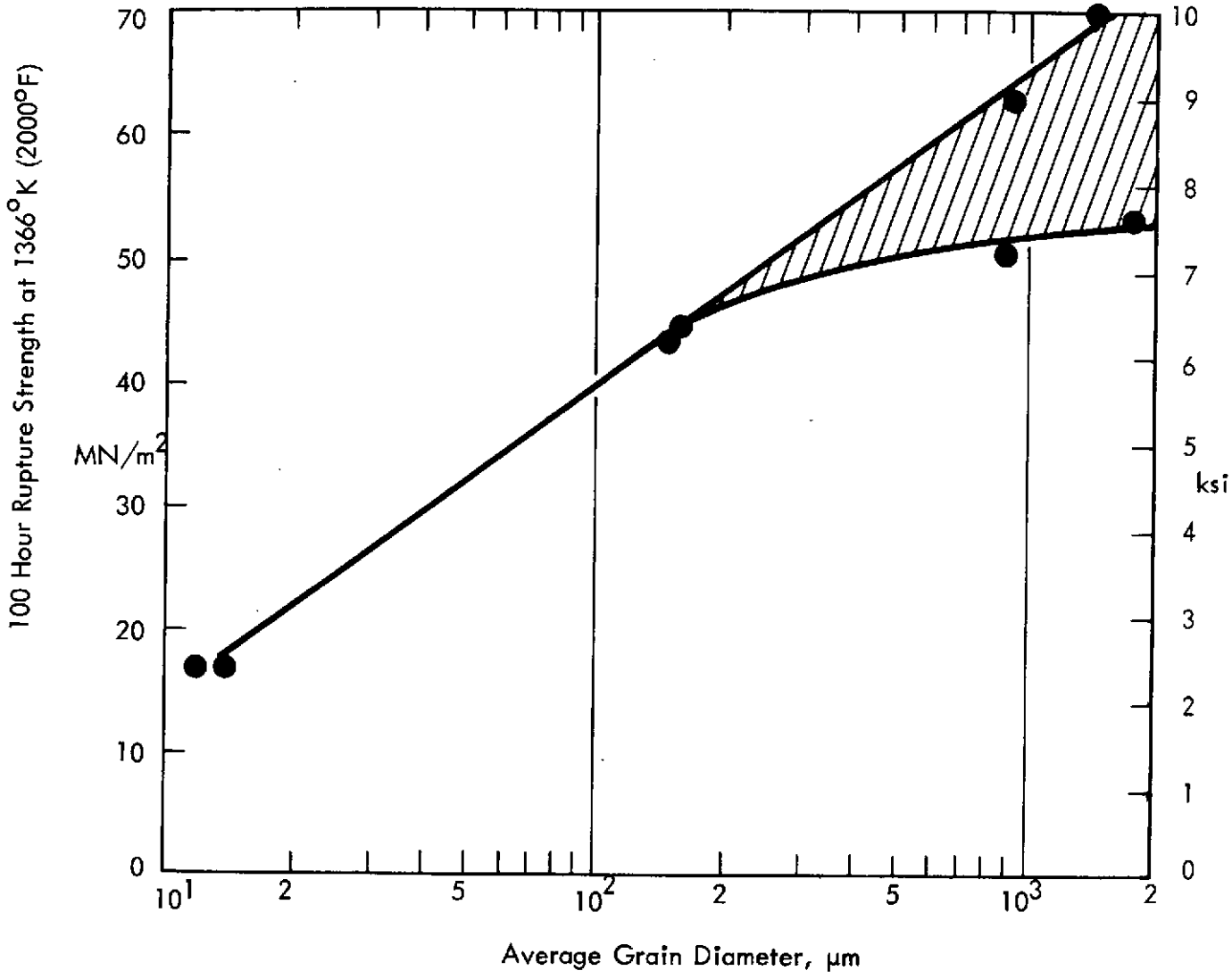

Figure 8. The Influence of Grain Size on Rupture Strength

4.2 AN EVALUATION OF OPTIMIZED MATERIAL

From data presented in the previous section, it was concluded that forging at 1366°K (2000°F) through an 80 to 90% reduction followed by annealing at 1616°K (2450°F), would be a suitable procedure for maximizing high temperature strength (see Figures 3 and 5). This formed the basis for preparing optimized material for an extensive metallurgical evaluation. It should be noted, that the work leading to this point investigated fabrication procedures on which total deformation involved anywhere from 4 forging steps each of 48%, to 14 steps of 10% (Table 1). Total deformation was taken in 7 forging steps each of 28% for optimum processing. This was thought to be a reasonable approximation to the practice typical of turbine blade or vane forging.

Material prepared according to the forging and annealing procedure outlined above is referred to as "optimally forged". It should be understood that forging variables having some influence on high temperature strength other than just temperature and reduction, which are discussed in the next report section, were also maintained at their most favorable conditions in the preparation of optimized material.

4.2.1 Tensile and Stress-Rupture Properties

Tensile properties were determined for optimally forged preform material over the temperature range from ambient to 1477°K (2200°F), and for similarly processed bar stock at 1366°K (2000°F). These data are summarized in Figure 9.

A major decrease of tensile strength and ductility began at ~811°K (1000°F). At 1366°K (2000°F) these properties for optimally forged preform material were 113 MN/m^2 (16.3 ksi) and 2.2%. By comparison, optimally forged extruded bar exhibited strength and ductility values of 128 MN/m^2 (18.5 ksi) and 7.5%. Somewhat improved properties are apparently induced by prior extrusion deformation. It should be pointed out, however, that the extruded

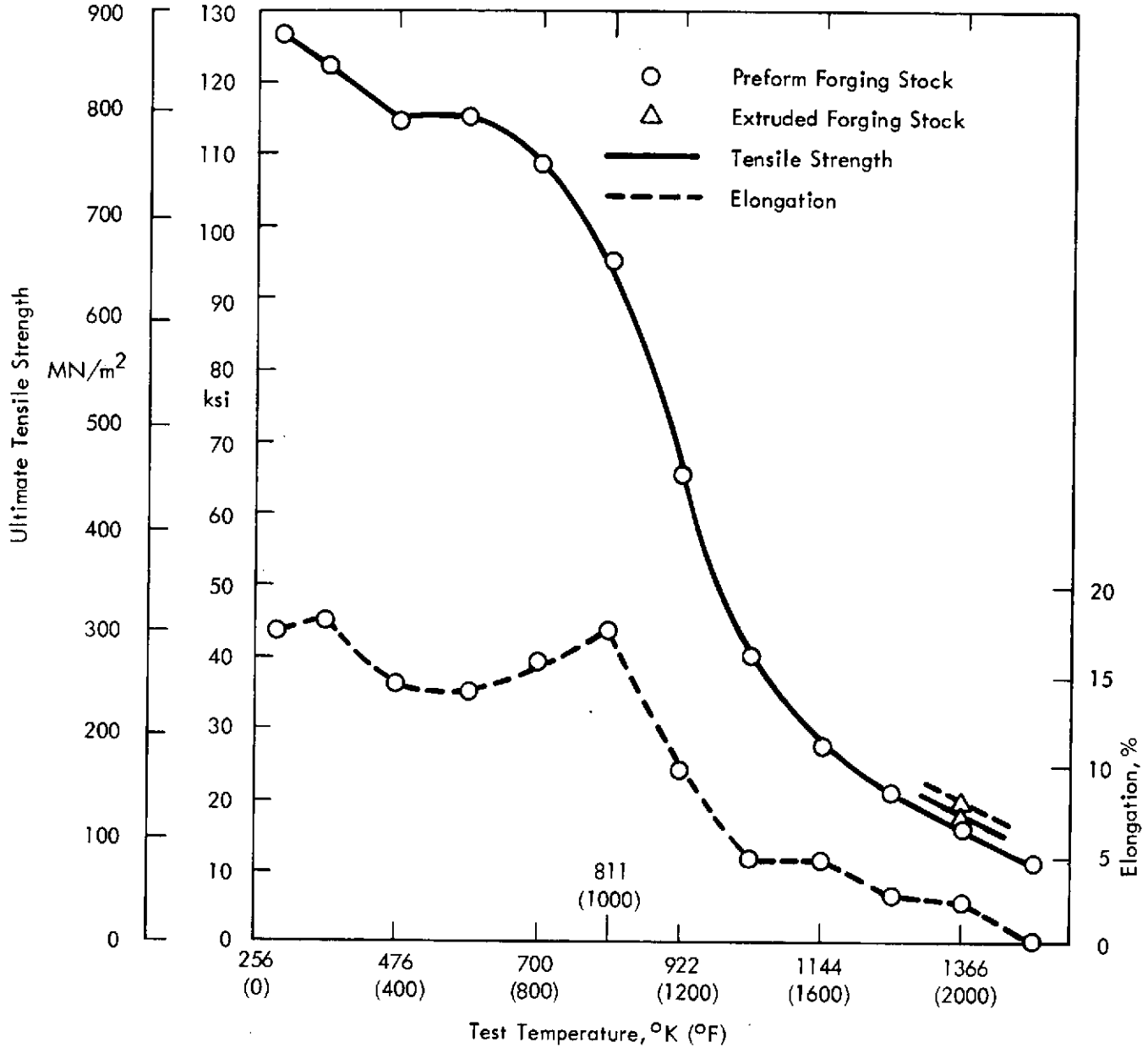

Figure 9. The Influence of Temperature on the Tensile Properties of Optimally Forged TDNiCr

stock was forged with its cylindrical axis placed along the length of the channel die. In this manner, the directions of prior extrusion and subsequent forging deformation were kept parallel. If this material is forged to produce deformation perpendicular to the original extrusion direction, strength and ductility values below preform material are obtained. A discussion of the influence that prior fabrication history has on forged properties is presented in the next report section.

Stress-rupture behavior was examined for optimally forged preform material at 1033, 1255, 1366, and 1477°K (1400, 1800, 2000, and 2200°F), and for similarly forged bar stock at 1366°K (2000°F). These results are summarized in Figure 10 where rupture life and test stress are related.

The anticipated loss of rupture strength with increased test temperature and a somewhat higher level of this property obtained on material forged from extruded bar are illustrated by this presentation. These points are more clearly made in Figure 11 where 100 hour rupture strength (obtained from Figure 10) is plotted against test temperature. The level of this property reported for optimally rolled sheet is also included in the figure for comparison.

The 100 hour rupture strengths of optimally forged preform and extruded material were 52 and 66 MN/m^2 at 1366°K (7.5 and 9.5 ksi at 2000°F). These strength values are somewhat higher than reported for optimally rolled sheet. An interesting result displayed in Figure 11 is the linear loss of rupture strength with temperature increase. The rate of change measured was -24.3 MN/m^2/+100°K (-1.94ksi/+100°F) over the investigated temperature range.

4.2.2 Microstructure

Longitudinal and forging plane optical microstructures of optimally forged preform material are displayed in parts (a) and (b) of Figure 12.* The material had an average grain diameter of 1920 μm. The results of a separate study indicated that large grain conditions similar to that of optimized material are probably caused by secondary recrystallization.**

*Terms used to describe planes and directions in materials are defined in Appendix B.

**Reported in Appendix F.

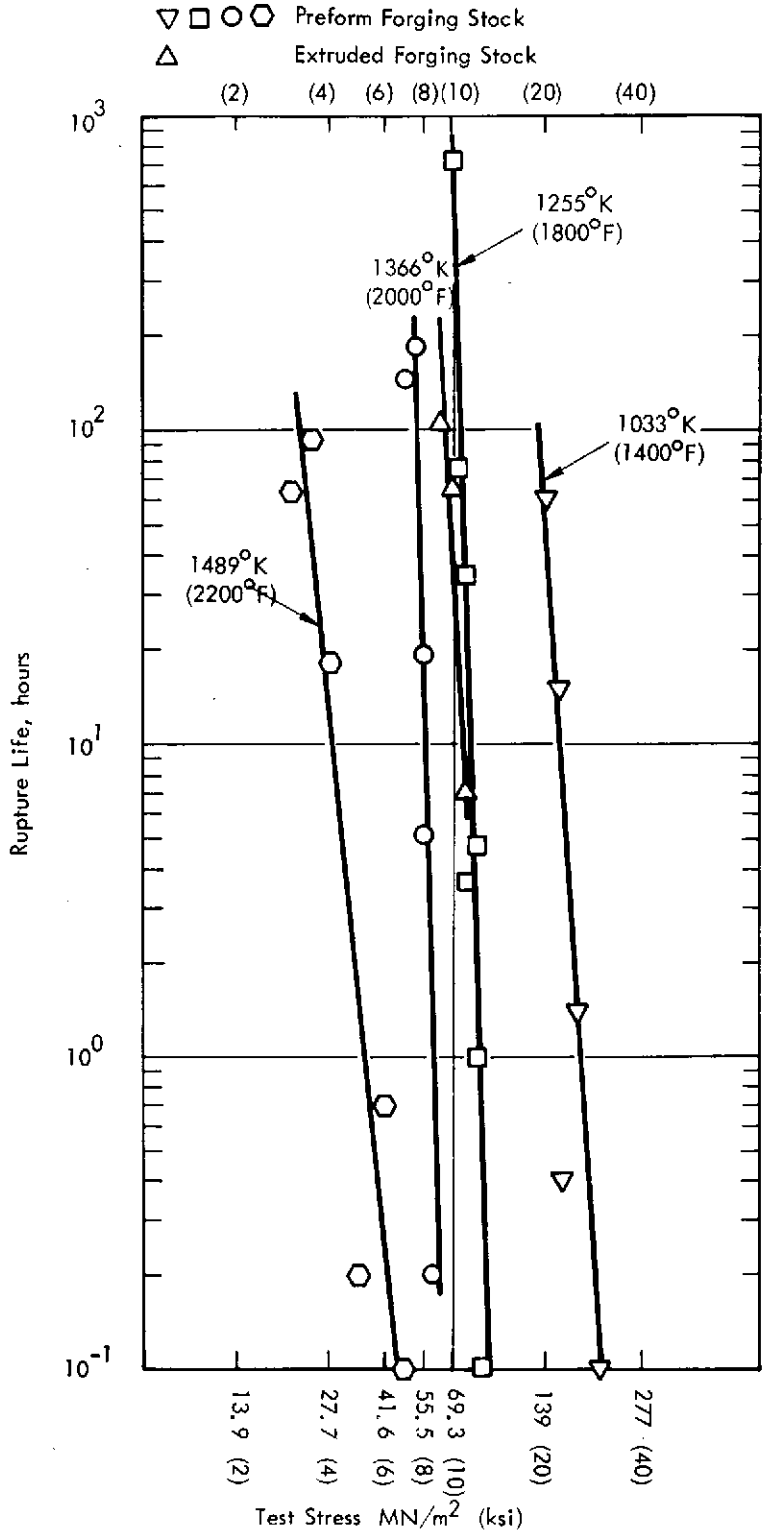

Figure 10. The Influence of Stress and Temperature on the Rupture Life of Optimally Forged TDNiCr

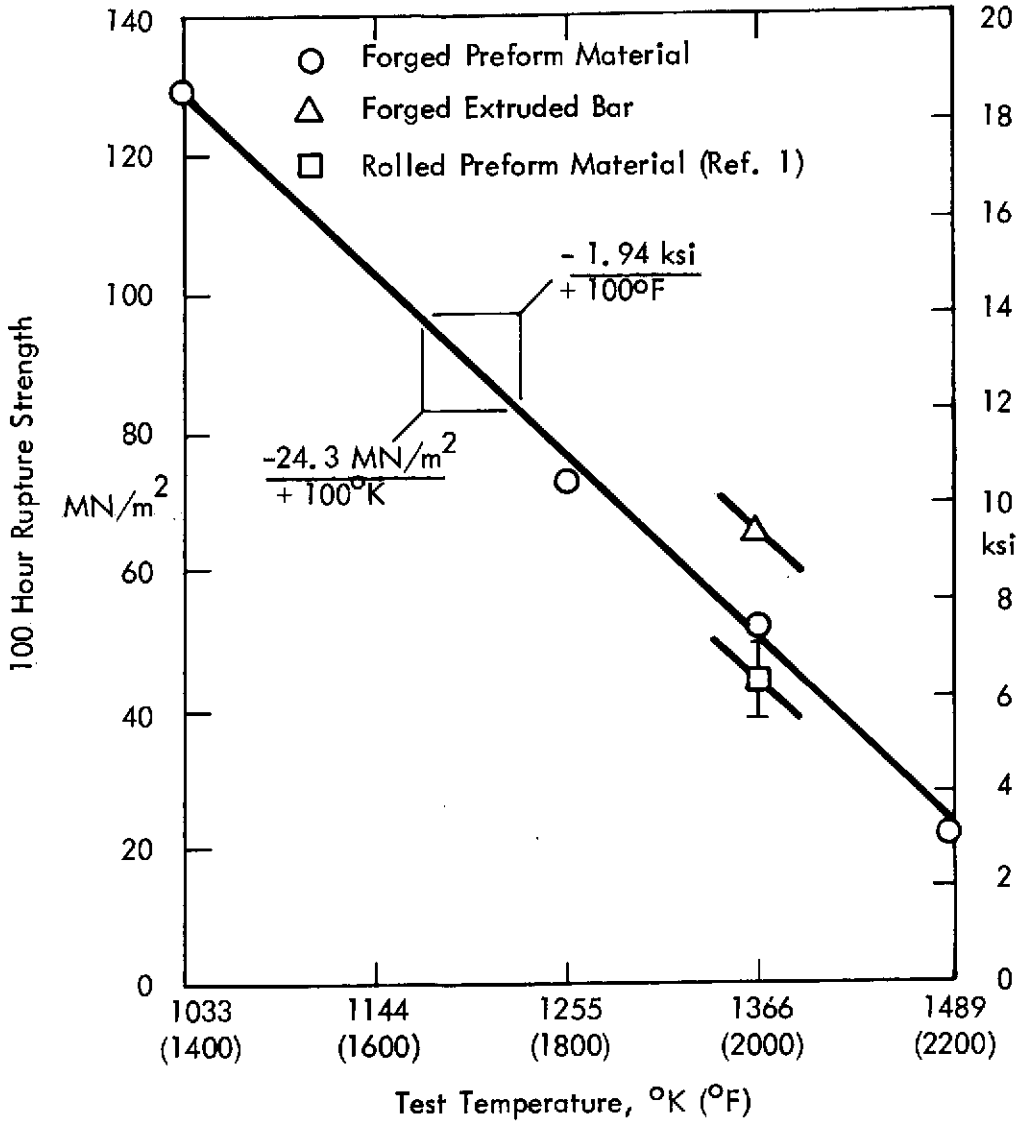

Figure 11. The Influence of Temperature on the Rupture Strength of Optimally Forged and Rolled TDNiCr

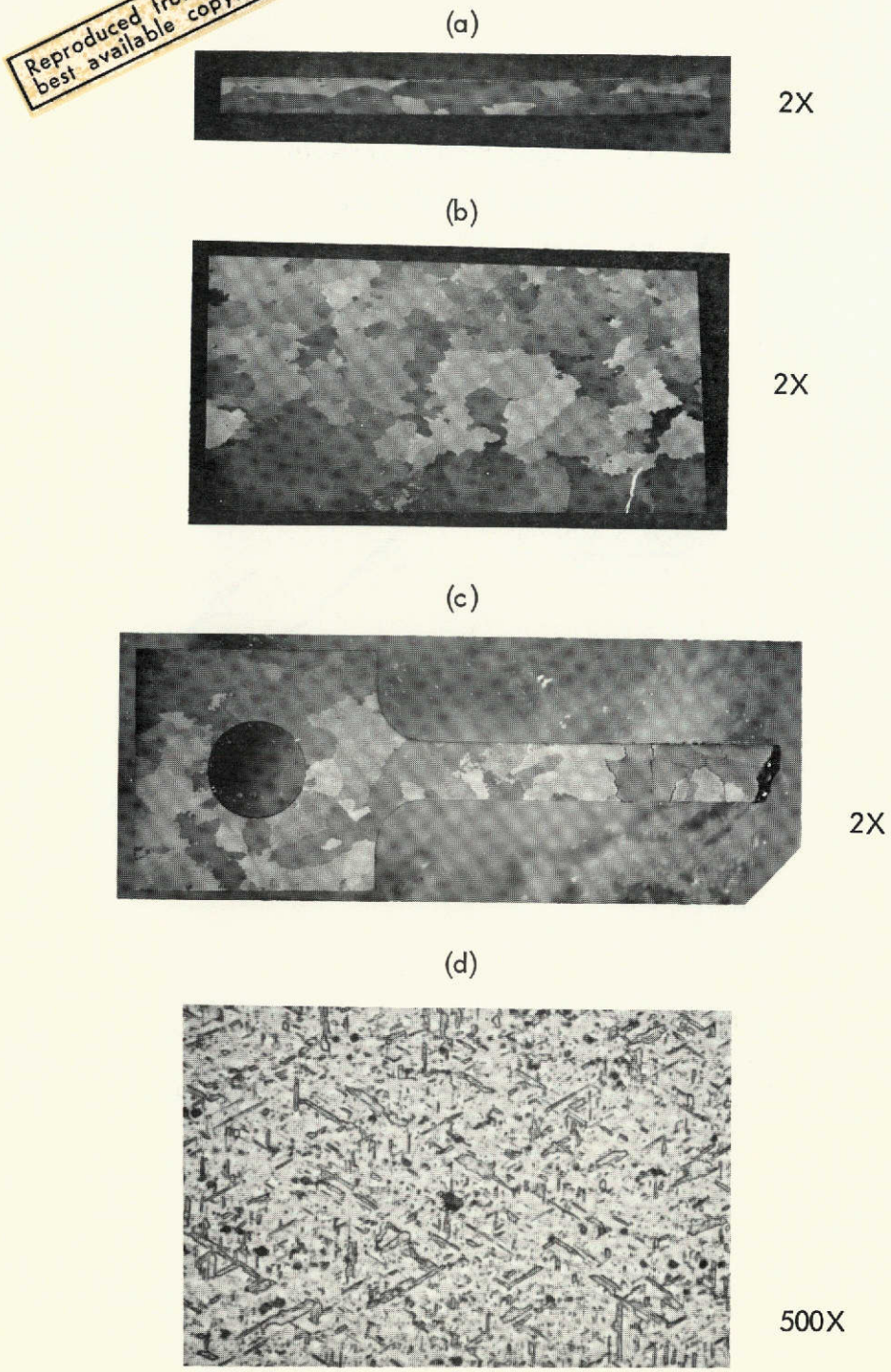

Figure 12. The Optical Microstructure of Optimally Forged TDNiCr. Preform forging stock. (a) Longitudinal view; (b) Forging plane view; (c) Stress-rupture specimen tested 140 hours at 48.5 MN/m^2 and 1366°K (140 hrs. at 7 ksi and 2000°F); (d) Twinning in optimally forged material.

A section of a rupture test specimen of optimized material is shown in part (c) of Figure 12. Grain boundary separation was the failure mechanism. This failure behavior undoubtedly accounts, in part at least, for the observed improvement in high temperature strength with increased grain size.

A higher magnification photomicrograph of optimally forged material revealing a preponderance of very small annealing twins is shown in part (d) of Figure 12. The sizes of these twins ranged from approximately 1 μm x 4 μm to 5 μm x 20 μm. Killpatrick and Young [6], reported a similar faulted microstructure for large grain highly textured TDNiCr sheet of excellent high temperature strength. As will be discussed in a latter section, optimally forged TDNiCr also displayes a strong preferred orientation. The question of whether or not the fine twin substructure and texture of large grain TDNiCr contribute to its high temperature strength remains to be answered.

The microstructure of optimally forged preform material as revealed by transmission electron microscopy is shown in Figure 13. A relatively low dislocation density, twins, and the fine thoria dispersion are apparent in the photomicrograph.

4.2.3 Dispersed Phase Characteristics

The size, distribution, and spacing of ThO_2 particles was examined for optimally forged preform material. This was accomplished by measuring the diameter of ~1000 particles in a thin film and relating an average size to the volume of material examined. The observed distribution of particle diameters is illustrated graphically in Figure 14.* A diameter of $< 200 \times 10^{-10}$ m (< 200 Å) was measured on 80% of the particles.

*The raw data is given in Table E-25.

Figure 13. A Transmission Electron Micrograph of Optimally Forged TDNiCr. Preform forging stock

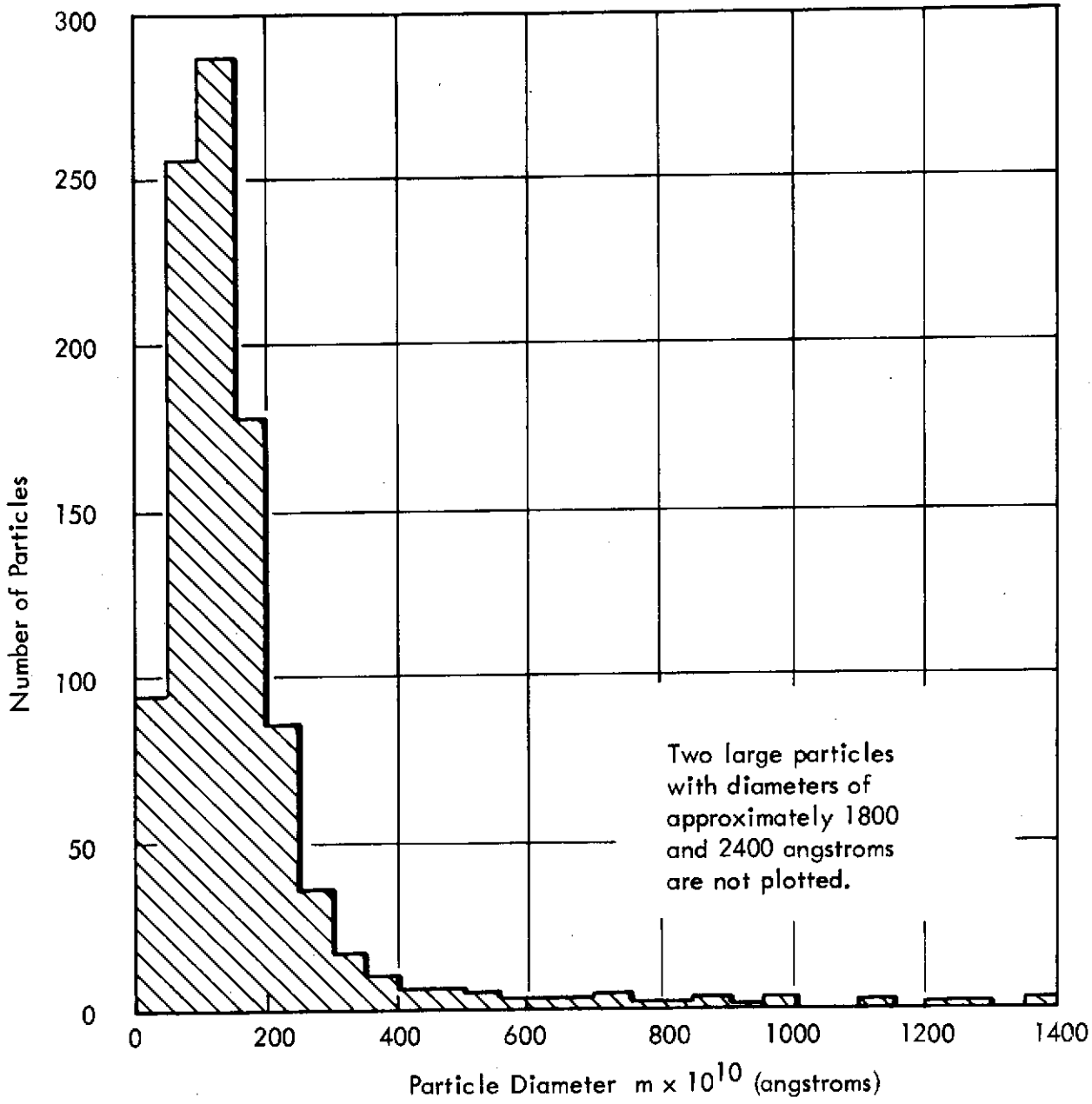

Figure 14. ThO_2 Particle Size Distribution in Optimally Forged TDNiCr. Preform forging stock

The average particle diameter calculated from this information spanned 135 - 185 x 10^{-10} m (135 - 185 Å). The amount of material in which the counted particles were enclosed was ~3 x 10^{-19} cubic meters. An estimate of interparticle spacing based upon thoria spheres of average diameter each enclosed in cubes of metal is ~500 x 10^{-10} m (~500 Å).

4.2.4 Preferred Orientation

A (200) pole figure determined on optimally forged preform material is reported in Figure 15. Pole intensities were measured for crystallographic planes lying parallel to the forging plane, and the pole figure is oriented with the north-south direction parallel to the longitudinal direction.* Pole intensities are given by contour numbers which are related to the intensity measured from a randomly oriented nickel powder standard.

The large grains formed in optimally forged material orient themselves to produce two strong texture components which approximate the {110} <100> and {110}<110>ideal conditions. Planes of {110} tilt by ~10° about the longitudinal axis. The results of a (220) pole figure determination confirmed these orientations.

A preferred orientation of {110} planes was also observed for as-forged material. (Recall that optimally forged refers to the total process of forging and annealing.) The texture developed approximated the {110}<111> ideal condition with a {110} tilt of ~15° about the longitudinal axis. This texture differs from those developed upon subsequent annealing by only a 45° rotation of direction.

*Terms describing material surfaces and directions are defined in Appendix B.

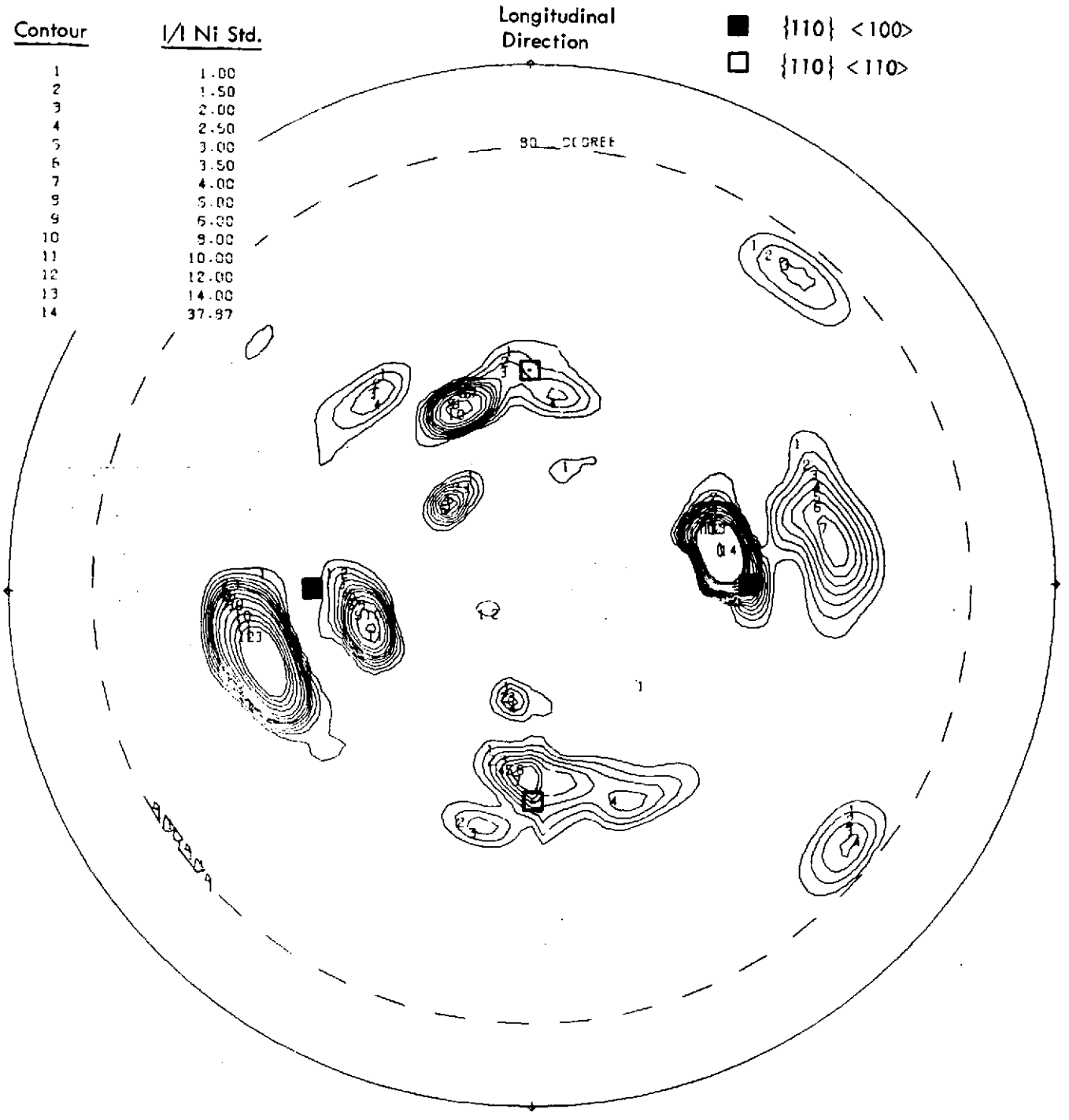

Figure 15. The (200) Pole Figure for Optimally Forged TDNiCr. Preform forging stock

4.3 FORGING VELOCITY, PRIOR DEFORMATION, AND SHOCK TREATMENT EFFECT

The stock used on forging experiments was produced by either upset forging (preform material) or extrusion (bar stock). Although slight, some mechanical property differences were observed between test plates forged under identical conditions from these starting materials (see Figures 9 through 11). This presumably resulted from differences in their prior fabrication histories.

The forgings characterized in the previous report sections were channel die forged on a Mechanical Press in a manner which continued the metal deformation inherent in the starting materials. This was accomplished by placing the extrusion axis of bar stock parallel to the channel die axis, and orienting preform material to maintain the forging direction coincident with that used in its preparation. Presentations are made in this report section to demonstrate how high temperature mechanical properties are influenced by deformation performed both to oppose as well as continue that of the starting materials. Preform material was forged perpendicular to its upset direction, and bar stock was forged with its axis placed perpendicular to that of the channel die to oppose their original deformations. Opposed and continued deformation are referred to as perpendicular forged and parallel forged. The high temperature mechanical properties of material forged on a Mechanical Press and by the higher velocity Dynapak process, and for material given shock wave treatments after optimum forging, are also reported in this section.

4.3.1 Tensile Properties

Data showing how the thermomechanical histories of the starting materials interact with that of subsequent forging to influence high temperature tensile properties are summarized in Figure 16. Both preform material and extruded bar stock were forged to continue and to oppose their original deformations. In the experiment involving the use of extruded bar,

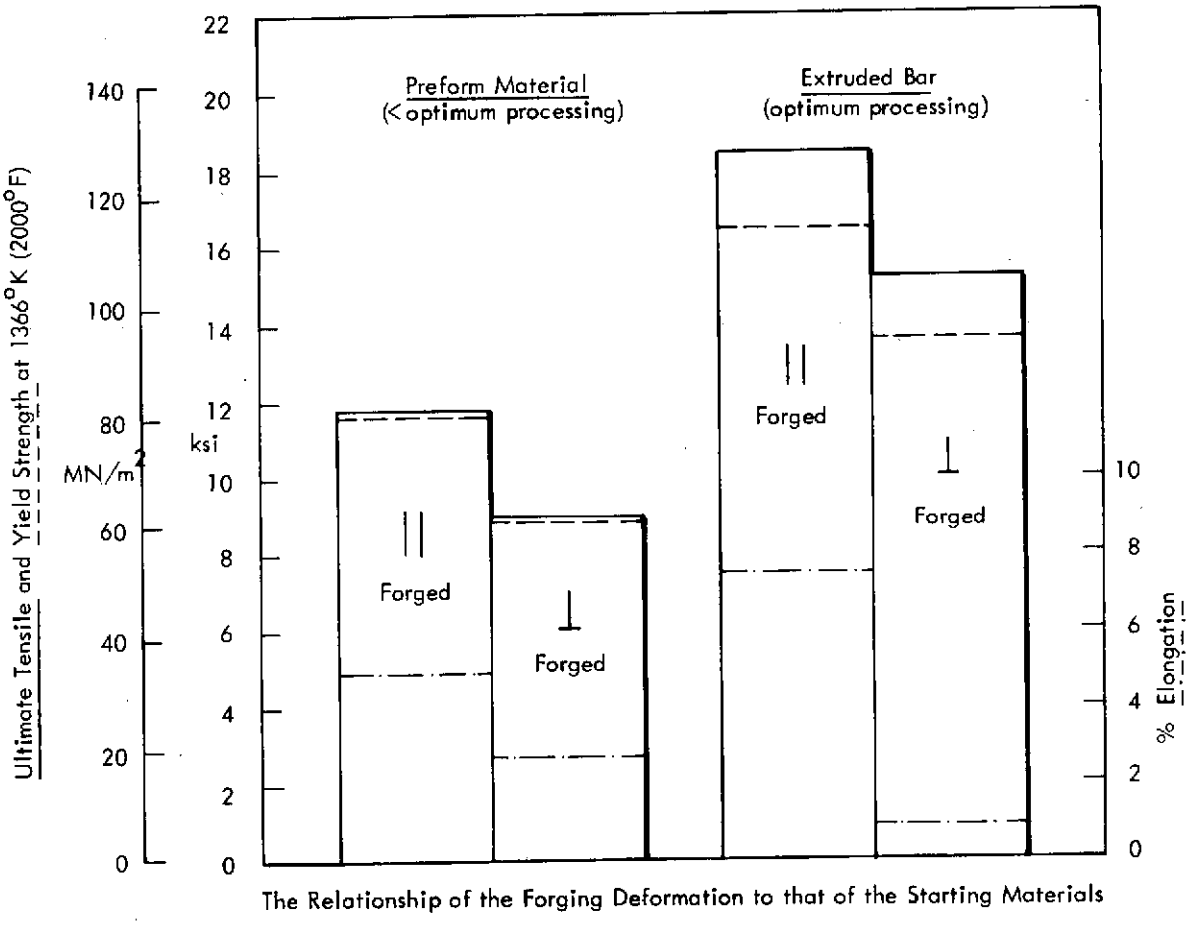

The Relationship of the Forging Deformation to that of the Starting Materials

Figure 16. The Influence of Total Deformation History on Tensile Properties. Parallel and perpendicular forged refer to deformations which continued (||) or opposed (⊥) that of the starting materials. Since the specific processing conditions differed for each pair of forgings, any cross comparison of data is invalid. Specific thermomechanical details are reported in Appendix E; forgings 36-39 and 52-54.

forging variables other than the deformation relationship examined, were fixed at conditions which would optimize high temperature strength. Optimized forging conditions were not used on the preform material experiment. The results demonstrated that for both materials higher tensile strength and ductility are obtained by parallel forging. They also revealed that a similar strength advantage is obtained by parallel forging, regardless of the starting material used, or whether forging conditions were optimized. The constant tensile strength advantage was ~20 MN/m^2 at 1366°K (~3 ksi at 2000°F). By comparison, processing temperatures have a much greater influence on strength (see Figures 2 and 3).

Wilcox, et al, reported a direct improvement in the high temperature strength of TDNiCr with increased grain aspect ratio[5]. Forging to continue the flow of metal involved in original fabrication would promote further development of any inherent grain aspect condition. Forging to oppose original deformation would obviously act to destroy the original grain shape. It should be noted, however, that although perpendicular forging of extruded bar would be expected to eliminate its favorable inherent grain aspect condition, material so forged by the optimized process did display a relatively high tensile strength of 115.5 MN/m^2 at 1366°K (15.2 ksi at 2000°F). This is undoubtedly a result of the large grain size developed in optimally forged material and emphasizes the singular importance of this microstructural parameter in determining the high temperature strength of TDNiCr.

The influence that forging velocity had on 1366°K (2000°F) tensile strength is illustrated in Figure 17. Two experiments were run using preform material and Dynapak and Mechanical Press equipment which differed in forging velocity by a factor of 19. In one case, forging variables other than speed were fixed at conditions which would optimize high temperature strength. Conditions close to optimum were used on the other experiment. Both experiments revealed that higher strength but lower ductility was obtained by forging at the lower velocity.

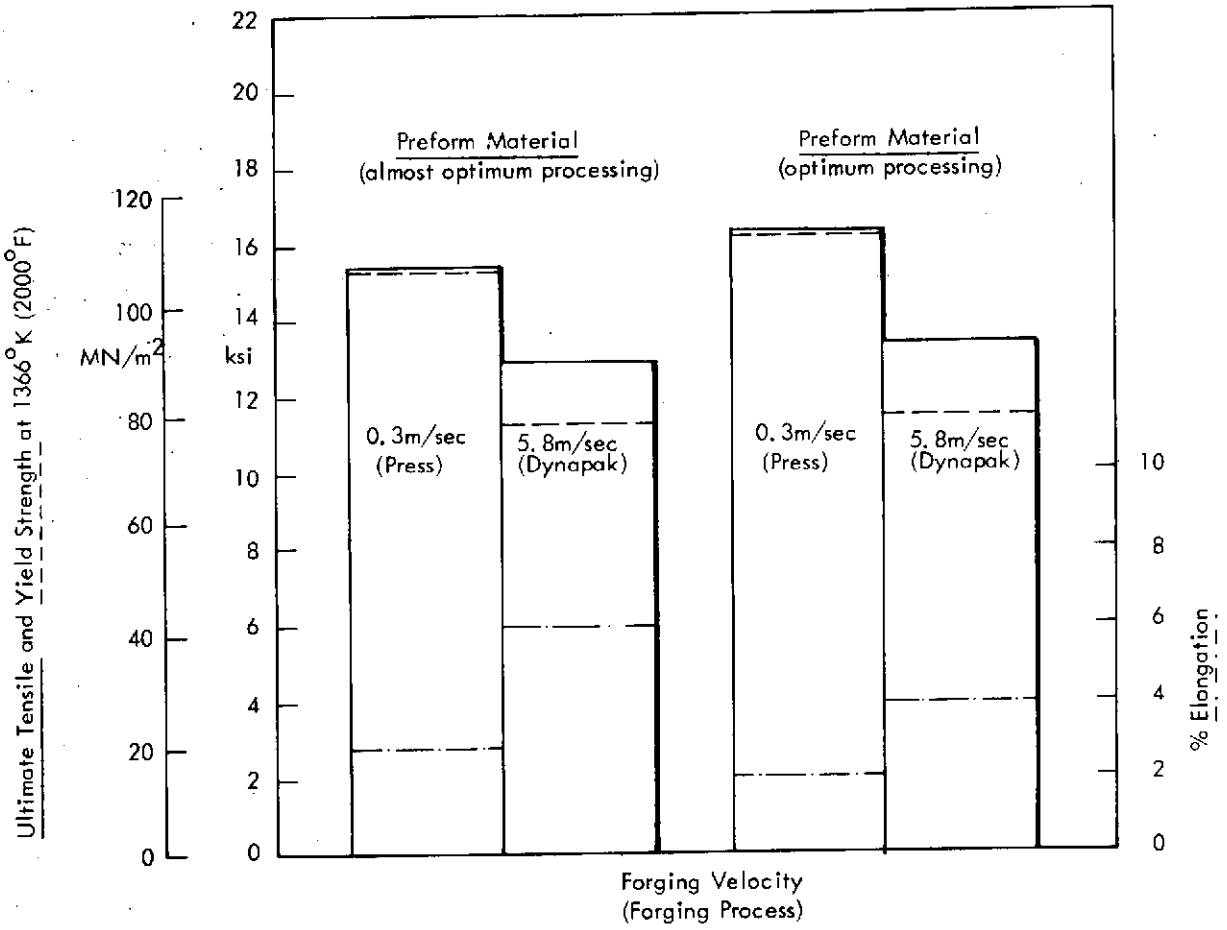

Figure 17. The Influence of Forging Velocity on Tensile Properties. Since the forgings represented by each bar data pair were processed under different conditions, any cross comparison is invalid. Specific thermomechanical details are reported in Appendix E; forgings 44, 50, 55 and 56.

A reason for the apparent influence of fabrication strain rate cannot be given. However, note that the strength advantage of lower velocity forging was on the order that obtained by parallel forging (compare to Figure 16). As such, the prior argument presented in judgment of the importance of parallel forging to strength, when compared to the influence of processing temperatures, also applies to forging velocity.

Tensile and hardness properties of shock treated material are summarized in Figure 18. Preform material, forged and annealed employing all optimized procedures, was subjected to single and double shock treatments. Tensile data for shock treated material are presented in part (a) of the figure and compared to properties displayed in the as-forged and as-annealed conditions. The benefit of annealing to high temperature strength has been discussed. Annealing results in an increase of strength at 1366°K from 19.4 to 113 MN/m^2 (2.8 to 16.3 ksi strength change at 2000°F). Shock treatment added an additional small increment of strengthening. Single and double shock treated material displayed 1366°K tensile strengths, respectively, of 133 and 117 MN/m^2 (18.2 and 16.9 ksi at 2000°F). The somewhat lower strength of double shock treated material may be associated with recovery effects related to the intermediate anneal or heat generated by the second shock treatment.

Although the strength of as-forged material was low, its room temperature hardness exceeded that of annealed material, part (b) Figure 18. This reflects its extremely fine grain size (~1 μm). Annealing, which increases the grain size by three orders of magnitude greatly improving high temperature strength, lowered hardness from that of the as-forged condition. Shock treatment caused a 100 point hardness increase due undoubtedly to the generation and entanglement of dislocations. A transmission electron micrograph of single shock treated material is displayed in Figure 19. Shock treatment did result in a major increase in dislocation density (compare with Figure 13).

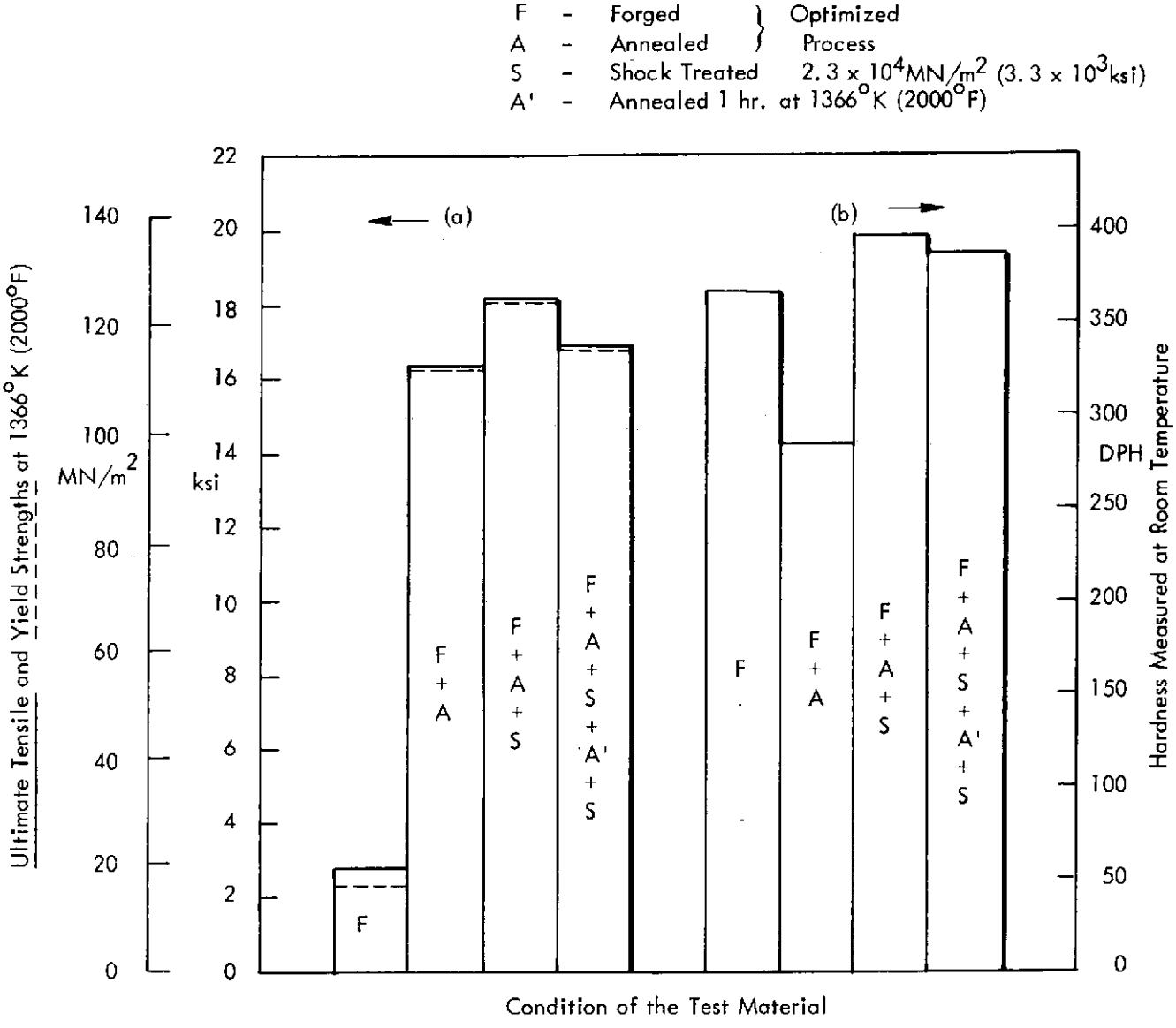

Figure 18. The Influence of Shock Treatment on the Strength and Hardness of Optimized Material. Preform forging stock. (a) Tensile data; (b) Hardness data

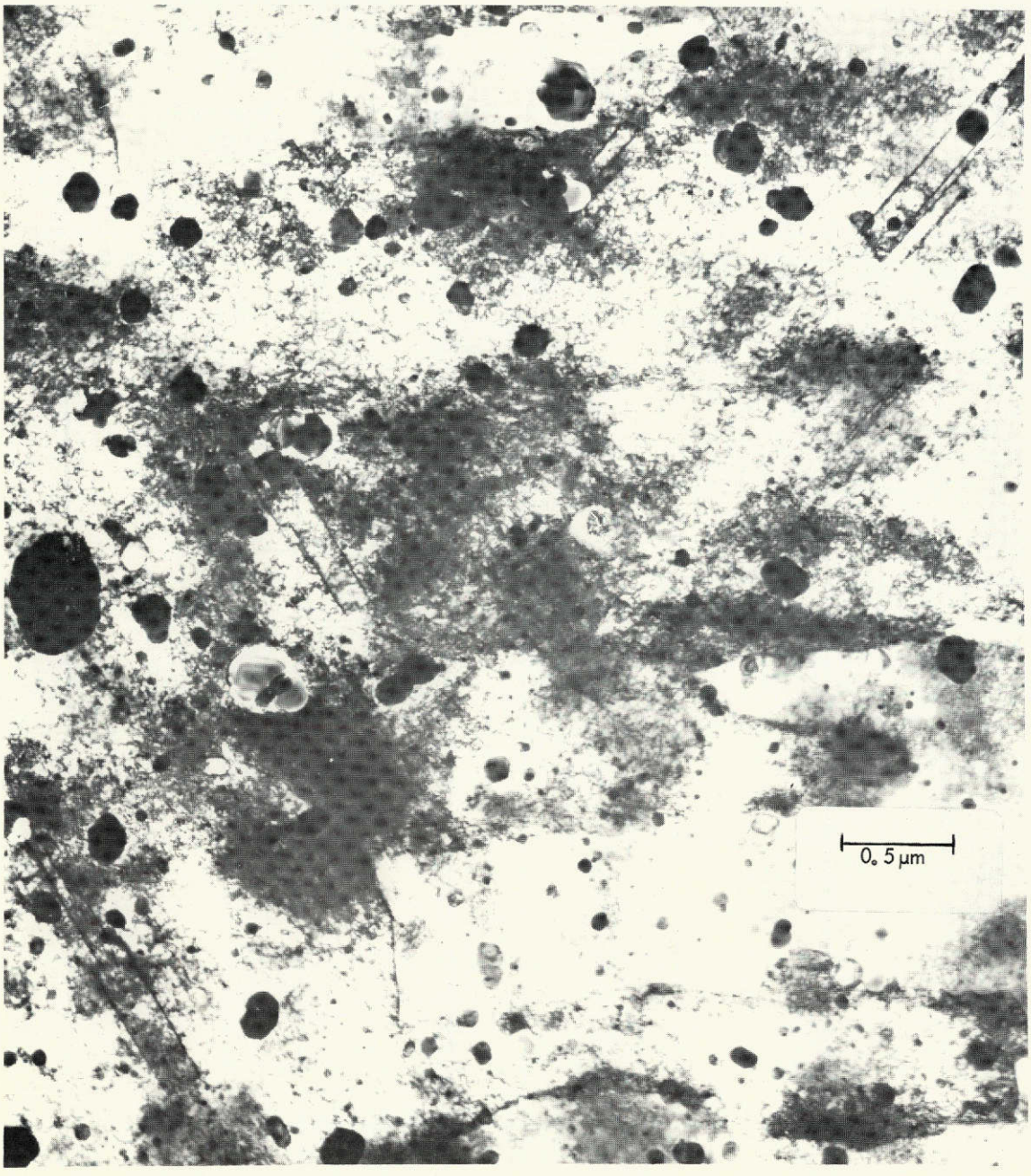

Figure 19. A Transmission Electron Micrograph of Optimally Forged and Single Shock Treated Material. Compare with Figure 13.

4.3.2 Stress-Rupture Properties

The influences that forging velocity and the relationship of forging to starting material deformation have on stress-rupture strength are summarized in parts (a) and (b) of Figure 20. Preform material was used to examine the effect of forging velocity, while deformation history was studied on extruded bar. In both cases, all forging variables other than those evaluated, were fixed at conditions which would maximize high temperature strength. Improved rupture strength was obtained by Press (lower velocity) as compared to Dynapak forging and by parallel as opposed to perpendicular forging. Forging velocity and deformation history had similar influences on tensile strength (see Figures 16 and 17).

Double shock treatment did not improve rupture strength over that of untreated material, part (c) Figure 20. Because of limited available test material*, only two tests could be made to evaluate the single shock treated condition. One test revealed a rupture strength similar to untreated material, but the other indicated an improvement in this property. A definite conclusion about the influence of single shock treatment on rupture strength can obviously not be made from this limited data.

The shock treatment experiment was designed as a relatively inexpensive preliminary effort. Its intent was to qualitatively gage whether the strength of optimally forged material might be further improved by this treatment, which is unique, in the simplified sense, that it creates some of the effects of cold work without causing major dimensional changes. As such, it could possibly be applied to finished parts. A contact explosive was used on the experiment, and the pressure produced barely reached the level at which an influence on the mechanical properties of metals is generally measured. It is concluded, with these experimental limitations under consideration, that the overall tensile and stress-rupture test results indicated that the high temperature strength of forged TDNiCr could be improved by shock treatment, and more sophisticated higher pressure experiments should be planned.

* The shock treated plates were slightly warped, and a few cracked when clamped for specimen machining resulting in a loss of some test material.

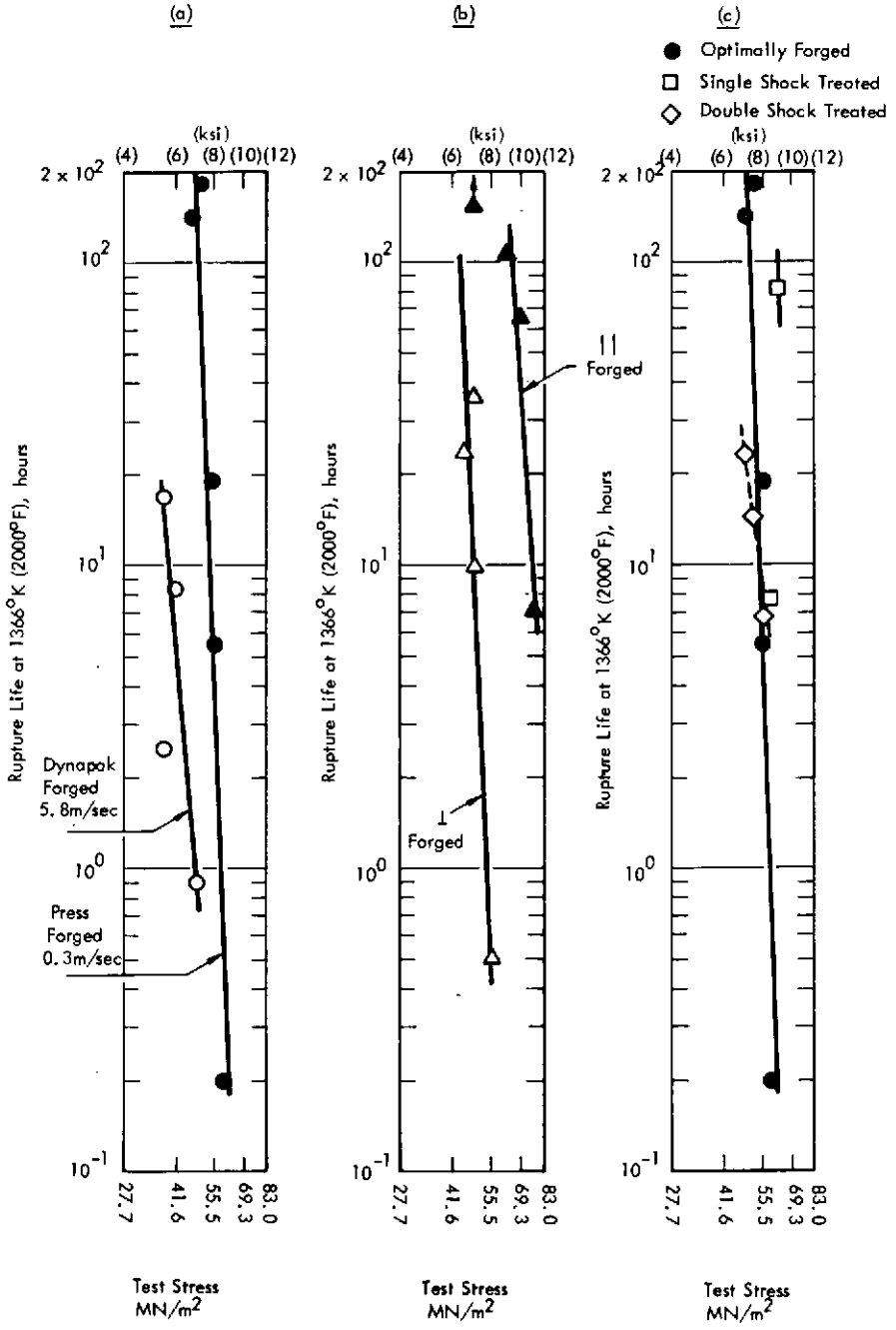

Figure 20. How Forging Velocity, Deformation History, and Shock Treatment Influence Stress-Rupture Strength
(a) Optimally forged preform material (velocity influence)
(b) Optimally forged extruded bar stock (deformation influence)
(c) Optimally forged preform material vs same plus shock treated

5.0 CONCLUSIONS

The influence of thermomechanical history and the role of microstructure in determining the high temperature tensile and stress-rupture strength levels achieved in forged TDNiCr were evaluated. The following conclusions were obtained:

1) Stress free preforms of TDNiCr can be successfully converted by forging into plates comparable in high temperature strength to extruded bar and rolled sheet material.

2) The good high temperature strength of extruded TDNiCr bar can be retained upon forging.

3) Forging temperature and final annealed condition are the most significant thermomechanical variables and influence high temperature strength by controlling grain size.

4) An increase of total forging reduction, forging which continues the metal deformation inherent in the starting material, a low forging speed and prior deformation by extrusion also promote the improvement of high temperature strength.

5) Large grained forged TDNiCr material displays a strong texture and numerous twins which may also contribute to strengthening.

6) Application of shock treatment after optimized forging could benefit high temperature strength. Pressures above the level examined on this program should be investigated.

6.0 REFERENCES

1. L. J. Klinger, W. R. Weinberger, P. G. Bailey, S. Baranow, "Development of Dispersion Strengthened Nickel-Chromium Alloy (Ni-Cr-ThO_2) Sheet for Space Shuttle Vehicles", NASA CR-120796, Final Report-Part I, December 30, 1971.

2. L. J. Klinger, et al, "Development of Dispersion Strengthened Nickel-Chromium Alloy Sheet for Space Shuttle Vehicles", NASA CR-121164, Final Report-Part II, December, 1972.

3. G. E. P. Box, K. B. Wilson, "On the Experimental Attainment of Optimum Conditions", J. Roy. Statist. Soc., Ser. B., Vol. 13, 1951, p. 1-45.

4. G. E. P. Box, J. S. Hunter, "Multi-Factor Experimental Designs for Exploring Response Surfaces", Ann. Math. Statist., Vol. 28, 1957, p. 195-241.

5. B. A. Wilcox, A. H. Clauer, W. B. Hutchinson, "Structural Stability and Mechanical Behavior of Thermomechanically Processed Dispersion Strengthened Nickel Alloys", NASA CR-72832, Final Report, March 18, 1971.

6. D. H. Killpatrick, J. D. Young, "Texture and Room Temperature Mechanical Properties of Dispersion Strengthened Ni-Cr Alloys", Met. Trans. Vol. 1, 1970, p 955-61.

DISTRIBUTION LIST FOR NASA CP-134619

CONTRACT NAS3-15548

MR. R.E. ANGLIN (5)
MS 49-3
NASA LEWIS RESEARCH CTR.
21000 BROOKPARK ROAD
CLEVELAND, OHIO 44135

MR. G.M. AULT
MS 3-13
NASA LEWIS RESEARCH CTR
21000 BROOKPARK ROAD
CLEVELAND, OHIO 44135

MR. J.C. FRECHE
MS 49-1
NASA LEWIS RESEARCH CTR
21000 BROOKPARK ROAD
CLEVELAND, OHIO 44135

MR. R.W. HALL
MS 105-1
NASA LEWIS RESEARCH CTR
21000 BROOKPARK ROAD
CLEVELAND, OHIO 44135

DR. R.V. HINER
MS 49-3
NASA LEWIS RESEARCH CTR.
21000 BROOKPARK ROAD
CLEVELAND, OHIO 44135

MR. M. QUATINETZ (2)
MS 49-3
NASA LEWIS RESEARCH CTR.
21000 BROOKPARK ROAD
CLEVELAND, OHIO 44135

MR. J.W. WEETON (2)
MS 49-3
NASA LEWIS RESEARCH CTR.
21000 BROOKPARK ROAD
CLEVELAND, OHIO 44135

DR. R.L. ASHBROOK
MS 49-3
NASA LEWIS RESEARCH CTR.
21000 BROOKPARK ROAD
CLEVELAND, OHIO 44135

MR. C.P. BLANKENSHIP
MS 105-1
NASA LEWIS RESEARCH CTR
21000 BROOKPARK ROAD
CLEVELAND, OHIO 44135

MISS T.D. GULKO
MS 49-3
NASA LEWIS RESEARCH CTR.
21000 BROOKPARK ROAD
CLEVELAND, OHIO 44135

DR. A.G. HOLMS (2)
MS 49-3
NASA LEWIS RESEARCH CTR.
21000 BROOKPARK ROAD
CLEVELAND, OHIO 44135

DR. H.B. PROBST
MS 49-3
NASA LEWIS RESEARCH CTR.
21000 BROOKPARK ROAD
CLEVELAND, OHIO 44135

MR. P.F. SIKORA (3)
MS 49-3
NASA LEWIS RESEARCH CTR.
21000 BROOKPARK ROAD
CLEVELAND, OHIO 44135

CONTRACTS SECTION B
MS 500-313
NASA LEWIS RESEARCH CTR
21000 BROOKPARK ROAD
CLEVELAND, OH 44135

LIBRARY (2)
MS 60-3
NASA LEWIS RESEARCH CTR
21000 BROOKPARK ROAD
CLEVELAND, OHIO 44135

REPORT CONTROL OFFICE
MS 5-5
NASA LEWIS RESEARCH CTR
21000 BROOKPARK ROAD
CLEVELAND, OHIO 44135

MR G. C. DEUTSCH / RW
NASA HEADQUARTERS
WASHINGTON, DC
20546

MR. H.F. HARDRATH
NASA MS 188M
LANGLEY RESEARCH CENTER
LANGLEY FIELD, VA 23365

DEFENCE DOCUMENTATION CTR
CAMERON STATION
5010 DUKE STREET
ALEXANDRIA, VIRGINIA
22314

MR. J.K. ELBAUM
AFML/LLP
HEADQUARTERS
WRIGHT PATTERSON AFB,
OH 45433

DR. P.J. APEARN AMXMR-RM
ARMY MATERIALS AND
MECHANICS RESEARCH CTR.
WATERTOWN, MA 02172

MR. T.F. WEARNS AIR-320A
NAVAL AIR SYSTEMS COMMAND
NAVY DEPARTMENT
WASHINGTON, DC 20361

PATENT COUNSEL
MS 500-113
NASA LEWIS RESEARCH CTR
21000 BROOKPARK ROAD
CLEVELAND, OHIO 44135

TECHNOLOGY UTILIZATION
MS 3-19
NASA LEWIS RESEARCH CTR
21000 BROOKPARK ROAD
CLEVELAND, OHIO 44135

MR. W. REKOS / RL
NASA HEADQUARTERS
WASHINGTON, DC
20546

ACQUISITIONS BRANCH (10)
NASA SCIENTIFIC & TECHN.
INFORMATION FACILITY
BOX 33
COLLEGE PARK, MD 20740

DR. H.M. BURTE
AFML/LL
HEADQUARTERS
WRIGHT PATTERSON AFB,
OH 45433

TECHNICAL LIBRARY
AFML/LAM
HEADQUARTERS
WRIGHT PATTERSON AFB,
OH 45433

MR. L. BURROWS
SAVDL-EU-PP
US ARMY AIR MOBILITY
R&D LABORATORY
FORT EUSTIS, VA 23604

MR. I. MACHLIN AIR-520318
NAVAL AIR SYSTEMS COMMAND
NAVY DEPARTMENT
WASHINGTON, DC 20361

DR. R. ROBERTS
NAVY DEPARTMENT
ONR CODE 439
WASHINGTON, D.C. 20525

MR. R.I. RLUEH
OAK RIDGE NATIONAL LAB
OAK RIDGE, TN 37830

DR. S.D. HARKNESS
ARGONNE NATIONAL LAB.
9700 SO. CASS AVE.
ARGONNE, IL 60439

MR. D.E. MARLOWE
EN-219
NAT. BUR. OF STANDARDS
WASHINGTON, DC 20234

MR. H.E. BOYER
AM. SOCIETY FOR METALS
METALS PARK
NOVELTY, OH 44073

MR. D.J. MAYKUTH
BATTELLE MEMORIAL INST.
COBALT INFORMATION CENTER
505 KING AVENUE
COLUMBUS, OH 43201

MR. H.R. OGDEN
BATTELLE MEMORIAL INST.
505 KING STREET
COLUMBUS, OHIO
43201

DR. E.R. PARKER
DEPT. OF MATLS. & ENGRG
UNIVERSITY OF CALIFORNIA
BERKELEY, CA 94720

MR. B.J. ROGUS
NAVAL SHIP ENG CTR
PHILADELPHIA DIV 6763 B
PHILADELPHIA, PA 19112

TECHNICAL REPORTS LIBRARY
OAK RIDGE NATIONAL LAB.
OAK RIDGE, TENN. 37830

MR. R.W. WEEKS
ARGONNE NATIONAL LAB.
9700 SO. CASS AVE.
ARGONNE, IL 60439

DR. P.G. SHEWMON
DIR. DIV. OF MTLS. RES.
NAT. SCIENCE FOUNDATION
WASHINGTON, DC 20550

DR. R.I. JAFFEE
BATTELLE MEMORIAL INST.
505 KING AVENUE
COLUMBUS OHIO 43201

MCIC
BATTELLE MEMORIAL INST.
505 KING AVENUE
COLUMBUS, OHIO 43201

DR. B. WILCOX
BATTELLE MEMORIAL INST.
505 KING AVENUE
COLUMBUS, OHIO 43201

DR. J. MOTEFF
DEPT MATLS SCI & NET ENG
LOCATION 12
UNIV OF CINCINNATI
CINCINNATI, OH 45221

DR. J.K. TIEN
HENRY KRUMB SCH. OF MINES
COLUMBIA UNIVERSITY
NEW YORK, NY 10027

PROF. J.B. NEWKIRK
METALLURGY DEPARTMENT
DENVER UNIVERSITY
DENVER, COLORADO 80210

DR. J.W. CLEGG
NORTH STAR R.&D. INST.
31000-38TH AVE SOUTH
MINNEAPOLIS, MINN. 55406

DR. E.S. WRIGHT, MANAGER
METALLURGY GROUP
STANFORD RESEARCH INST.
MENLO PARK, CALIF. 94025

DR. J. COLWELL
AEROSPACE CORPORATION
PO BOX 95085
LOS ANGELES, CA 90045

MR. R.A. LULA
ALLEGHENY LUDLUM
STEEL CORP.
BRACKENRIDGE, PENNA.
15014

LIBRARY
AVCO SYSTEMS DIVISION
LOWELL INDUSTRIAL PARK
LOWELL, MASSACHUSETTS
01851

DR. D. WEBSTER
BOEING COMPANY
M.A.S.D.
SEATTLE, WA 98124

LIBRARY
DENVER RESEARCH INSTITUTE
UNIVERSITY PARK
DENVER, COLORADO 80210

DR. N.M. PARIKH
IIT RESEARCH INSTITUTE
10 WEST 35TH STREET
CHICAGO, ILLINOIS 60616

PROF. G.S. ANSELL
RENSSELAER POLYTECHNICAL
INSTITUTE
TROY, NY 12100

PROF. O. SHERBY
DEPT. OF MATERIALS SCI.
STANFORD UNIVERSITY
PALO ALTO, CALIF. 94305

REPORTS ACQUISITION
AEROSPACE CORPORATION
P.O. BOX 95085
LOS ANGELES, CALIFORNIA
90045

MR. E.J. ZICKEFOOSE
AMSTED RESEARCH LABS
P.O. BOX 567
BENSENVILLE, ILL 60106

MR. W.E. BINZ
BOEING COMPANY
P.O. BOX 3733
SEATTLE, WA 98124

DR. R. GRIERSON
STELLITE DIVISION
CABOT CORPORATION
1020 W. PARK AVENUE
KOKOMO, IN 46901

LIBRARY
CABOT CORPORATION
STELLITE DIVISION
P.O. BOX 746
KOKOMO, INDIANA 46901

DR. D.R. MUZYKA
CARPENTER TECHNOLOGY CORP
RES. & DEV. CENTER
P.O. BOX 662
READING, PA 19603

DR. D.L. SPONSELLER
CLIMAX MOLYBDENUM COMPANY
1600 HURON PARKWAY
ANN ARBOR, MICHIGAN 48106

POWDER METALS RESEARCH
FIRTH STERLING, INC.
P.O. BOX 71
PITTSBURGH, PENNA. 15230

DR. M. ASHBY
FORDON MCKAY LABORATORY
6 OXFORD STREET
CAMBRIDGE, MA 02138

MR. B. BLACK MZ 641-30
CONVAIR AEROSPACE DIV.
GENERAL DYNAMICS CORP.
P.O. BOX 1128
SAN DIEGO, CA 92112

DR. L.A. TAPSHIS
CRD
GENERAL ELECTRIC COMPANY
P.O. BOX 8
SCHENECTADY, N.Y. 12301

DR. R.E. ALLEN
AEG/GED
GENERAL ELECTRIC COMPANY
CINCINNATI, OHIO 45215

LIBRARY
CAMERON IRON WORKS, INC
P.O. BOX 1212
HOUSTON, TX 77001

LIBRARY
CHRYSLER CORPORATION
DEFENSE-SPACE GROUP
P.O. BOX 757
DETROIT, MI 48231

MR. J.G. LEBRASSE
RESEARCH & DEVELOPMENT
FEDERAL MOGUL CORP.
ANN ARBOR, MI 48106

DR. Y.P. TELANG
MATERIALS DEVELOPMENT
FORD MOTOR COMPANY
ONE PARKLANE BOULEVARD
DEARBORN, MICHIGAN 48126

SUPERVISOR MATERIALS ENG.
GARRETT AIRESEARCH
402 E. 36TH STREET
PHOENIX, ARIZONA 85034

DR. H.E. CLINE
CRD
GENERAL ELECTRIC COMPANY
P.O. BOX 8
SCHENECTADY, N.Y. 12301

LIBRARY
ADVANCED TECHNOLOGY LAB
GENERAL ELECTRIC COMPANY
SCHENECTADY, NY 12345

MR. J.F. BARKER
AEG/GED
GENERAL ELECTRIC COMPANY
CINCINNATI, OHIO 45215

MR. L.P. JAHNKE
AEG/GED
GENERAL ELECTRIC COMPANY
CINCINNATI, OHIO 45215

DR. E.E. REYNOLDS
TECHNICAL CENTER
GENERAL MOTORS CORP.
WARREN, MI 48090

MR. L.A. MEAD
GRUMMAN AEROSPACE CORP
PLANT 25
BETHPAGE, N.Y. 11714

MR. R.J. NYLEN
HOMOGENOUS METALS INC.
WEST CANADA BLVD
HERKIMER, N.Y. 13350

DR. B. WIDMER
INDUSTR. MATLS. TECHNOL.
127 SMITH PLACE
WEST CAMBRIDGE IND. PK.
CAMBRIDGE, MASS. 02138

DR. R.F. DECKER
INTERNATIONAL NICKEL CO.
ONE NEW YORK PLAZA
NEW YORK, NY 10004

MR. C. BURLEY
GOVERNMENT RELATIONS
LADISH COMPANY
CUDAHY, WISCONSIN 53110

DR. W.S. CREMENS
RESEARCH LABORATORY
LOCKHEED-GEORGIA COMPANY
MARIETTA, GEORGIA 30060

MR.D. HANINK
ENGINEERING OPERATIONS
DETROIT DIESEL ALLISON
GENERAL MOTORS CORP.
INDIANAPOLIS,IN 46206

MRS. V. SCHMIDT
GOULD LABORATORIES
GOULD INC.
540 EAST 105TH STREET
CLEVELAND, OH 44108

LIBRARY
HERCULES, INC
910 MARKET STREET
WILMINGTON, DE 19899

MR. M. GARY
HONEYWELL INC.
AEROSPACE DIVISION
2600 RIDGWAY PARKWAY
MINNEAPOLIS, MN 55413

MR. J.V. LONG
SOLAR DIVISION
INTERNATIONAL HARVESTER
2200 PACIFIC HIGHWAY
SAN DIEGO, CAL. 92112

MR. T. MILES
KELSEY HAYES CORPORATION
7250 WHITMORE LAKE ROAD
BRIGHTON, MI 48116

MR. J.P. STROUP
LATROBE STEEL COMPANY
LATROBE, PA 15650

TECHNICAL INFORMATION CTR.
MATLS. & SCIENCE LAB.
LOCKHEED RESEARCH LABS
3251 HANOVER STREET
PALO ALTO, CAL. 94304

LIBRARY
P.R. MALLORY & CO. INC.
P.O. BOX 1115
INDIANAPOLIS, INDIANA
46206

LIBRARY MSFD
MCDONNELL DOUGLAS CORP.
3000 OCEAN PARK BLVD
SANTA MONICA, CAL. 90406

DR. J.F. RADAVICH
MICROMET LABORATORIES
202 SOUTH STREET
WEST LAFAYETTE,
INDIANA 47906

MR. R.A. HARLOW
AERONUTRONIC DIVISION
PHILCO-FORD CORPORATION
FORD ROAD
NEWPORT BEACH, CAL 92663

MR. J.R. HUMPHREY
REM METALS CORPORATION
P.O. BOX 829
ALBANY, OR 97321

LIBRARY
ROCKWELL INTERNATIONAL
ROCKETDYNE DIVISION
6633 CANOGA AVENUE
CANOGA PARK, CA 91304

DR. J.S. SMITH
CHEM & MET DIVISION
SYLVANIA ELECTRIC PROD
TOWANDA, PENNA 18848

DR. C.S. KORTOVICH
MATERIALS TECHNOLOGY
TRW EQUIPMENT GROUP
23555 EUCLID AVENUE
CLEVELAND, OHIO 44117

MR. P.E. JACKSON
MCDONNELL DOUGLAS CORP.
P.O. BOX 516
ST. LOUIS, MISSOURI 63166

MR. R. JOHNSON
MCDONNELL DOUGLAS CORP
A3-833 MS 9
HUNTINGTON BEACH, CA
92647

LIBRARY
NUCLEAR METALS INC.
WEST CONCORD, MA
01781

MR. G.J. WILE
POLYMET CORPORATION
10597 CHESTER ROAD
CINCINNATI, OH 42515

MR. L.K. CROCKETT
SPACE DIVISION
ROCKWELL INTERNATIONAL
12214 LAKEWOOD BLVD.
DOWNEY, CA. 90241

MR. W.J. BOESCH
SPECIAL METALS
CORPORATION
NEW HARTFORD, N.Y. 13413

DR. H.E. COLLINS
MATERIALS TECHNOLOGY
TRW EQUIPMENT GROUP
23555 EUCLID AVENUE
CLEVELAND, OHIO 44117

LIBRARY
MATERIALS TECHNOLOGY
TRW EQUIPMENT GROUP
23555 EUCLID AVENUE
CLEVELAND,OH 44117

DR. E.A. STEIGERWALD
TRW METALS DIVISION
MINERVA, OH 44657

DR. E.R. THOMPSON
UNITED AIRCRAFT CORP.
RESEARCH LABORATORIES
EAST HARTFORD, CONN.
06108

DR. D.N. DUHL
PRATT & WHITNEY AIRCRAFT
UNITED AIRCRAFT CORP
400 MAIN STREET
EAST HARTFORD, CT 06108

DR. B.H. KEAR
PRATT & WHITNEY AIRCRAFT
UNITED AIRCRAFT CORP
400 MAIN STREET
EAST HARTFORD, CT 06108

LIBRARY
PRATT & WHITNEY AIRCRAFT
UNITED AIRCRAFT CORP
WEST PALM BEACH, FLORIDA
33402

MR. P.J. WALL
WESTINGHOUSE ELECTRIC
STEAM DIVISION
P.O. BOX 9175
LESTER, PENNA. 19113

MR. L.G. BONAR
FALCONBRIDGE NICKEL LTD.
7 KING STREET, EAST
TORONTO, ONTARIO
CANADA

TECHNICAL LIBRARY
ROLLS ROYCE LTD
INDUSTRIAL & MARINE DIV
P.O. BOX 72 ANSTY
COVENTRY CV7 9JR ENGLAND

DR. A.I. MLAVSKY
TYCO LABORATORIES, INC
16 HICKORY DRIVE
WALTHAM, MA 02154

MR. E.F. BRADLEY
PRATT & WHITNEY AIRCRAFT
UNITED AIRCRAFT CORP
400 MAIN STREET
EAST HARTFORD CONN 06108

MR. D.J. EVANS
PRATT & WHITNEY AIRCRAFT
UNITED AIRCRAFT CORP
400 MAIN STREET
EAST HARTFORD, CT 06108

DR. W.A. OWCZARSKI
PRATT & WHITNEY AIRCRAFT
UNITED AIRCRAFT CORP
400 MAIN STREET
EAST HARTFORD, CT 06108

MR. L.W. LHERBIER
UNIVERSAL CYCLOPS STEEL
RES. & DEV. DEPARTMENT
BRIDGEVILLE, PENNA 14017

MR. W.H. COUTS
WYMAN-GORDON COMPANY
NORTH GRAFTON,MA 01436

MR. R.C. COOK
SHERRITT-GORDON MINES
FORT SASKATCHEWAN
ALBERTA
CANADA

APPENDIXES

TDNiCr (Ni-20Cr-2ThO_2) FORGING STUDIES

FOREWORD

Complete descriptions of the starting materials, methods of evaluation, and separately performed experimental projects are presented in this appendix. Test data are also tabulated. Data analysis is included only for cases where it was performed to assist in directing experiments. Statistical analysis is an example of this. Much of the information given resulted from concurrently performed experiments and is presented in actual sequence. In several cases, a brief introduction preceeds information comprising an experiment to put it in its proper prospective to other work.

All reported data were taken in common units, egs., inches, ksi, ^{o}F, hours. Data are tabulated, however, in both common and international units, the latter obtained by slide rule and/or suitable table conversions. Data in international units are shown in tables as the primary system while that in common units appears adjacent in parenthesis or separate columns. Common units were used alone only in those sections of the appendix concerned with statistical analysis. Those sections in Appendices D and E covering a statistical analysis were written by Dr. A. Holms, NASA-Lewis Research Center.

APPENDIX A

STARTING MATERIALS

Manufacturing information, chemical analysis, and mechanical properties of the starting materials are reported in Tables A-1 through A-3. What influence heat treatment at 1477 and 1589°K (2200 and 2400°F) had on the microstructure of these materials was examined, and the results are summarized in Figures A-1 through A-3.

As-received preform material required viewing at 1500X for resolution of its microstructure (compare the 500X and 1500X photomicrographs in Figure A-1). The lower magnification photomicrograph, however, did reveal the presence of large dark particles. These were actually green in appearance which suggested that they were particles of Cr_2O_3.

Both the forging* and longitudinal* plane microstructures revealed an extremely fine grain condition. A longitudinal* grain size of 1.4 μm (ASTM 14) was measured for the material. This may approximate the particle size of the alloy powders used in manufacturing.

After heat treatment at 1477 and 1589°K (2200 and 2400°F), the microstructure of preform material did not display any increase in grain size. The condition obtained after 1589°K (2400°F) annealing is displayed in Figure A-1 to illustrate this point.

Laue back reflection patterns of as-received and 1589°K (2400°F) annealed preform material are also given in Figure A-1. The Debye rings represent the (331) and (420) reflections ($\theta = 143°$ and $154°$) of CuKα radiation. The Kα doublet (the two closely spaced Debye rings resulting from the $K\alpha_1$ and $K\alpha_2$ components of CuKα radiation) are clearly resolved for both reflections in each pattern indicating a strain free state. The similarity of these patterns confirms the grain structure stability suggested by optical microscopy. In addition, because

---

* Refer to Appendixes B and C for definitions of material and grain size terms.

Table A-1. Manufacture of the Starting Materials (Fansteel Inc.)

	Forged Preforms	Extruded Bar
Dimensions	30.5 cm x 30.5 cm x 3.8 cm (12 in. x 12 in. x 1.5 in.)	2.85 cm diameter (1-1/8 in.)
Heat No.	3113-3116	3111
Powder Compaction	417 MN/m^2 (60 ksi)	417 MN/m^2 (60 ksi)
Sintering	1227°K in H_2 (1750°F)	1450°K in H_2 (2150°F)
Forging, Extrusion	At 1283°K (1850°F)	16/1 reduction at 1310°K (1900°F)
Annealing	1366°K in H_2 (2000°F)	None

Table A-2. Chemical Analysis of the Starting Material (Fansteel Inc.)

Heat No.	ppm by Weight					Weight Percent		
	C	N	S	Cu	Co	Cr	ThO_2	Ni
3111	288	100	25	10	300	19.94	2.07	Bal.
3113	405	300	52	60	100	20.23	2.44	Bal.
3114	420	60	46	60	200	20.89	2.32	Bal.
3115	426	30	39	70	100	20.24	2.63	Bal.
3116	420	70	32	30	200	21.21	2.35	Bal.

Table A-3. Mechanical Properties of the Starting Material (Fansteel Inc.)

Heat No.	Annealing Treatment	Test* Direction	Test Temperature	Ultimate Strength		Yield Strength		El.
				(MN/m^2)	(ksi)	(MN/m^2)	(ksi)	(%)
3111	1644°K (2500°F)	longitudinal	RT	850	(122.4)	483	(69.6)	46.8
	1644°K (2500°F)	longitudinal	1360°K (2000°F)	131	(18.9)	127	(18.3)	10.0
3113 to 3116	None	longitudinal	RT	1040 to 1080	(150) to (156)	1040 to 1075	(150) to (155)	6 to 12
3113 to 3116	None	longitudinal	1360°K (2000°F)	21.5 to 28.4	(3.1) to (4.1)	18.0 to 26.4	(2.6) to (3.8)	26 to 56
3115	None	transverse	1360°K (2000°F)	25.6	(3.7)	22.9	(3.3)	50.8
3114**	None	longitudinal	1360°K (2000°F)	18.8	(2.7)	15.3	(2.2)	16.5
		longitudinal	1416°K (2100°F)	14.6	(2.1)	12.5	(1.8)	15.0

* Definitions of test directions are given in Appendix B.

** Check tests run at Westinghouse.

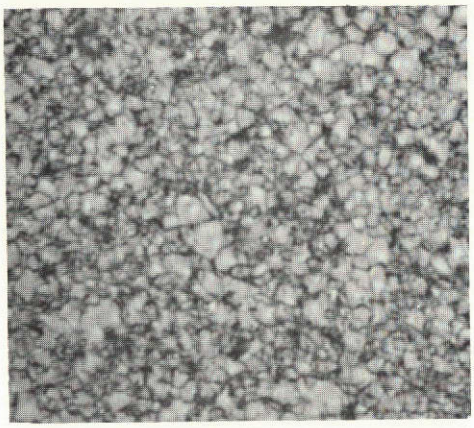

As Received

Forging Plane Surface

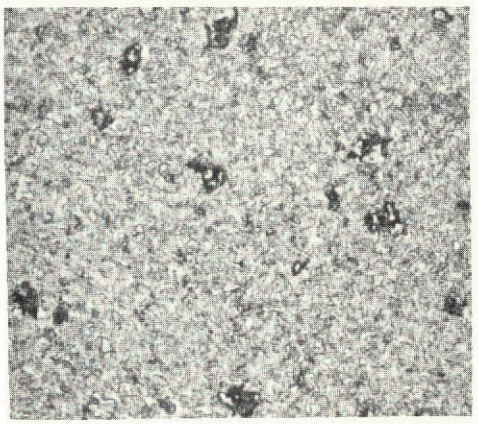

1500X

500X

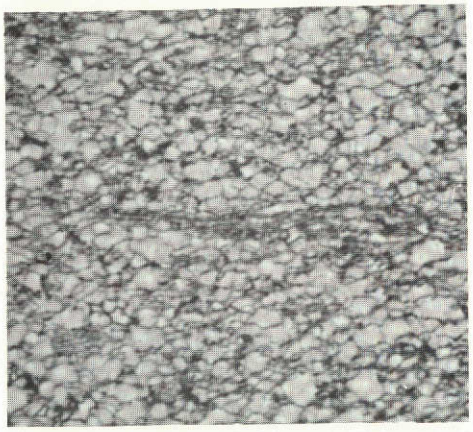

As Received

Longitudinal Surface

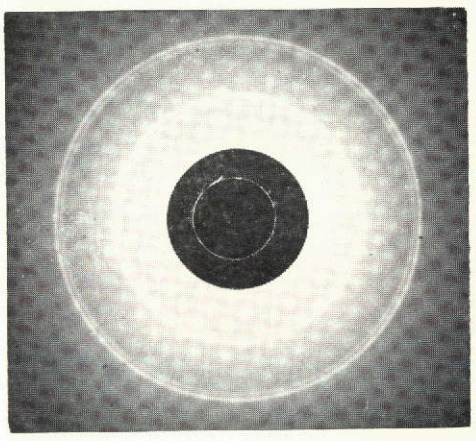

1500X

1/2 hr at 1589°K (2400°F)

Longitudinal Surface

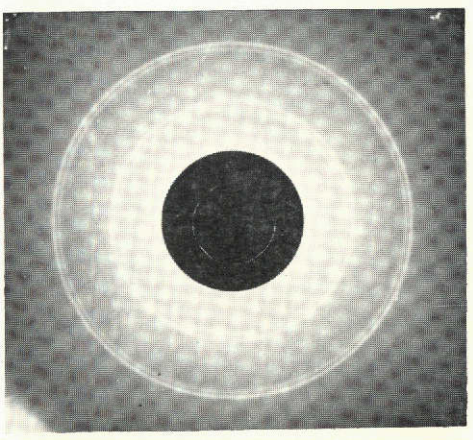

1500X

Figure A-1. Microstructure and Laue Pattern Characteristics of Preform Material

the Debye rings are continuous, they also confirm the extremely fine grain structure revealed by optical microscopy, i.e., continuous Debye rings develop when the defracting grains are so numerous that the resulting Debye spots overlap. As a general rule, a grain size of ~1 to 10 microns will produce continuous ring back reflection patterns[1]. The microscopy and diffraction results reveal that preform material is an extremely fine grain stress free product abnormally resistant to grain growth.

Microstructures and Laue patterns of extruded bar in the as-received and heat treated conditions are shown in Figure A-2. As noted for preform material, the as-received microstructure of the bar stock could not be clearly resolved by optical microscopy at 500X. Stringers of Cr_2O_3 particles were, however, apparent. The Ka doublets were almost but not quite separated in the Laue pattern of the as-received material, and the Debye rings were continuous. These results indicated the bar stock to be a very fine grain slightly cold worked product.

Heat treatment at 1477°K (2200°F) developed a large grain microstructure in material located close to the surface of the bar, while the microstructure of the interior did not display any change from that of the as-received condition. The large grain microstructure was developed across the entire bar cross section by heat treatment at 1589°K (2400°F). Note that large grains developed by heat treatment appear to contain annealing twins.

The response of hardness to heat treatment displayed by the preform and bar material is reported in Figure A-3. Only a small decrease in the level of this property was caused by annealing preform material. Preform hardness was ~365 DPH as-received and ~350 DPH after annealing at 1589°K (2400°F). Hardness of the bar stock, on the other hand, decreased from ~350 DPH

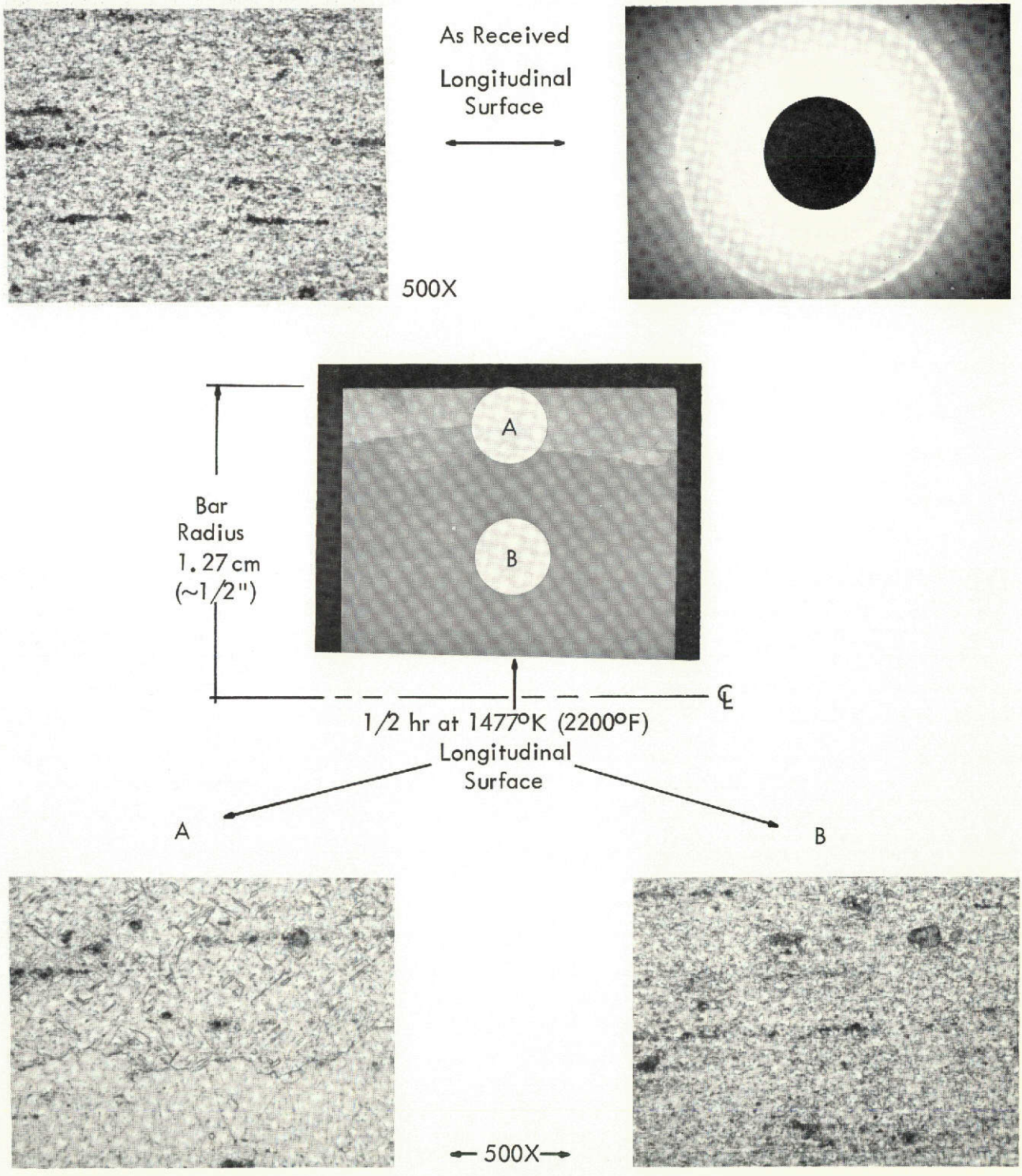

Figure A-2. Microstructure and Laue Pattern Characteristics of Extruded Bar

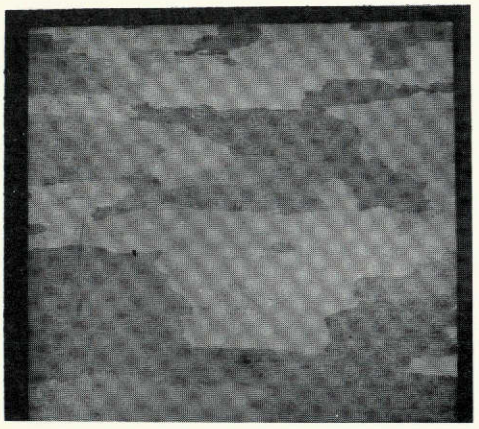

8X

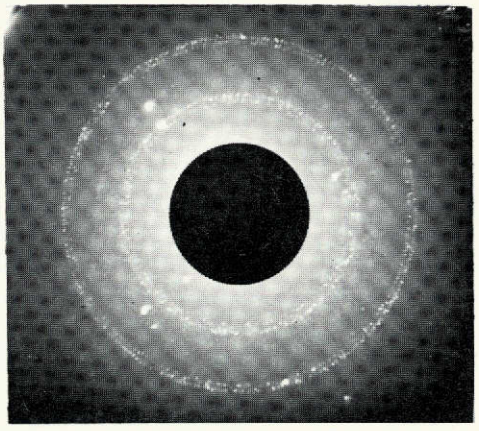

1/2 hr at 1589°K (2400°F)

Longitudinal
Surface

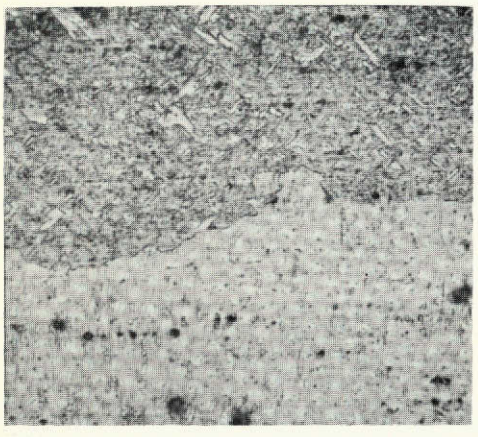

500X

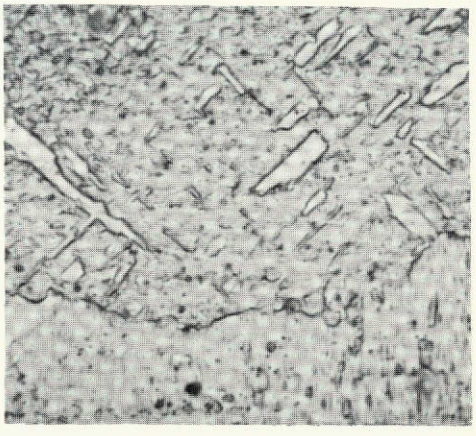

1500X

Figure A-2 (cont'd.). Microstructure and Laue Pattern Characteristics of Extruded Bar

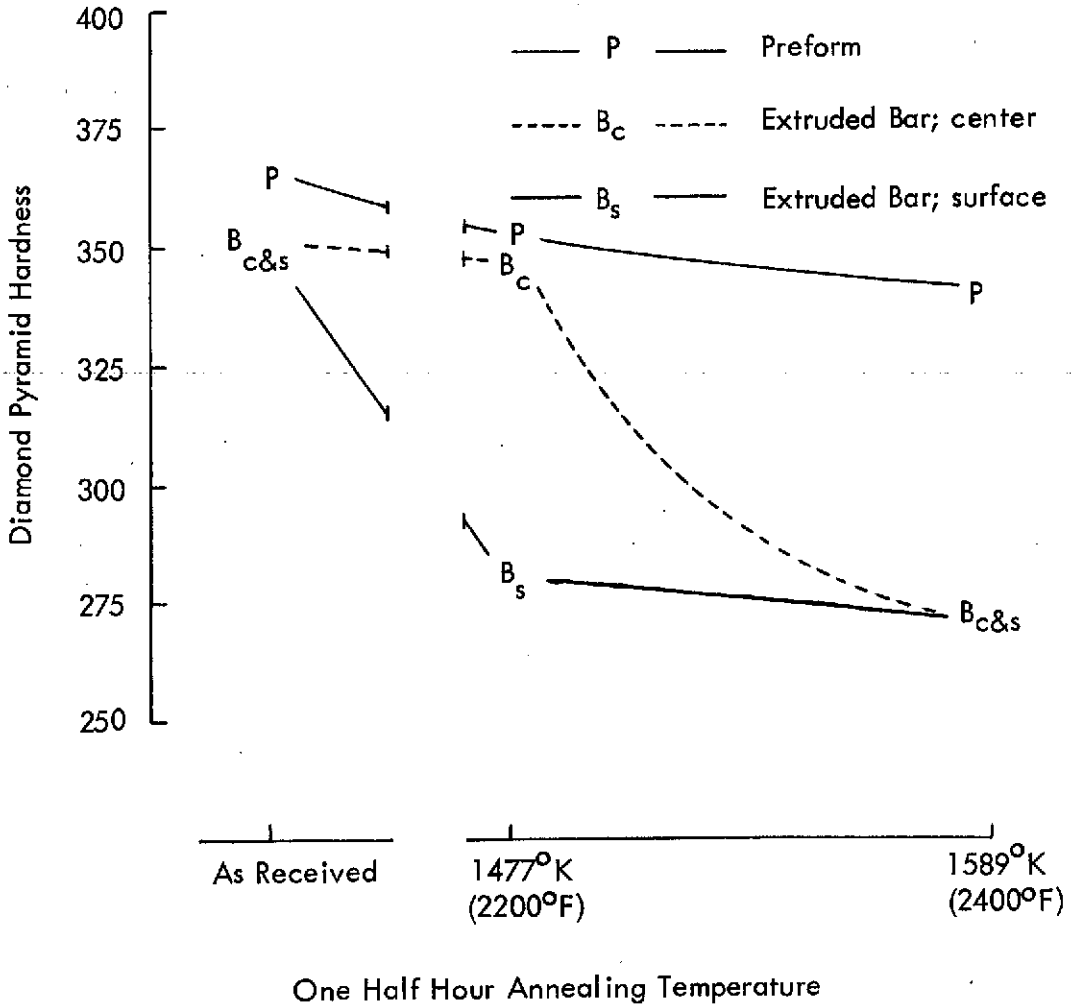

Figure A-3. Response of Hardness to Heat Treatment - Preform and Extruded Bar

as-received to ~275 DPH after heat treatment to 1589°K (2400°F). A similar hardness decrease occurred in the "surface material" of bar stock when heat treated at 1477°K (2200°F). The central portion of the bar, which resisted grain growth at the lower temperature, maintained a hardness level comparable to the as-extruded state. In spite of the decrease in hardness caused by high temperature heat treatment of the bar stock, material in this condition is reported to display at 1366°K (2000°F) tensile strength of ~132 MN/m^2 (~19 ksi), compared to ~24.3 MN/m^2 (~3.5 ksi) for the harder preform stock (refer to Table A-3).

APPENDIX B

DEFINITIONS OF MATERIAL TERMS

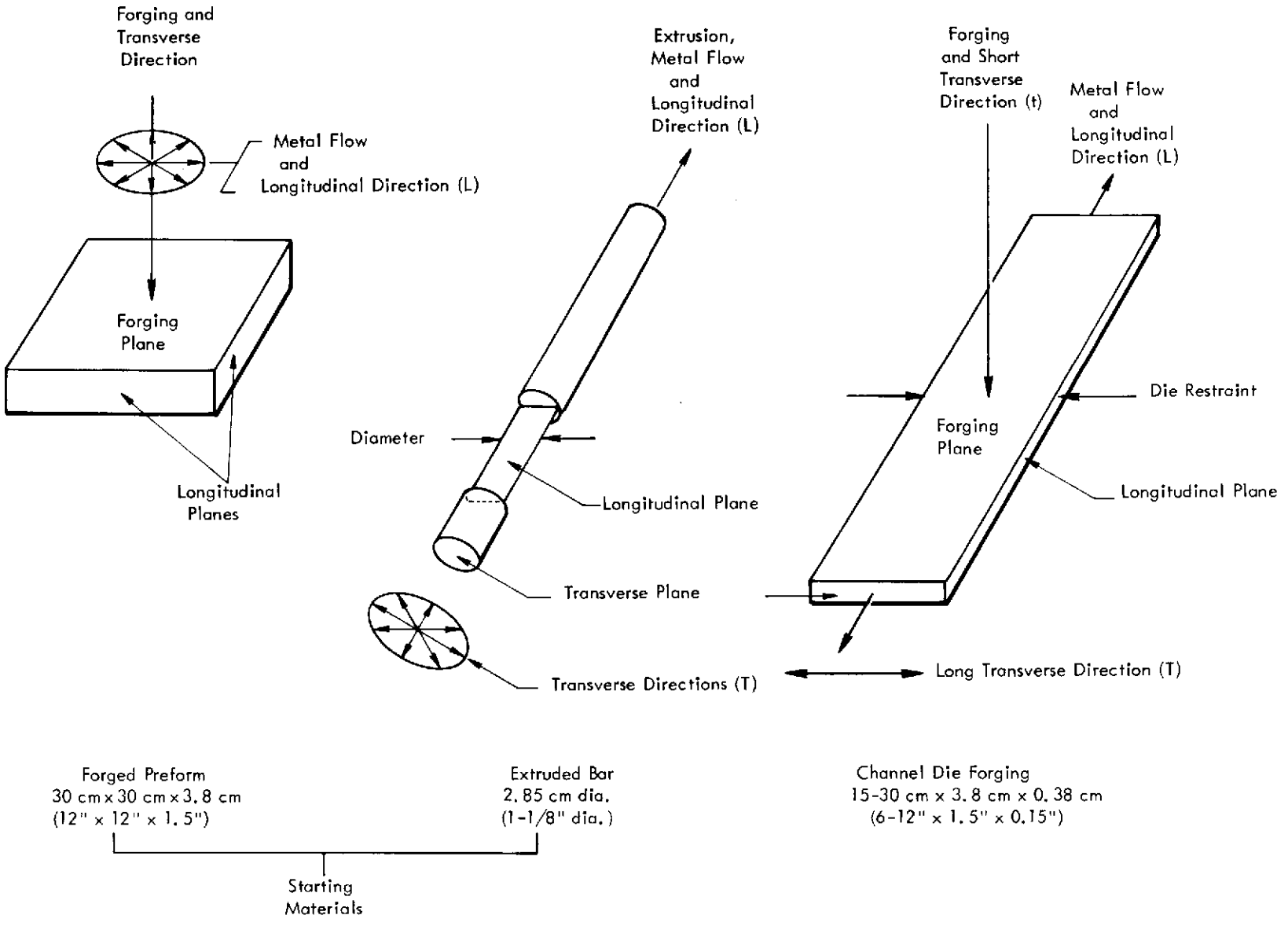

Figure B-1. Surfaces, Directions, and Letter Symbols Used in Data Presentations

APPENDIX C

DEFORMATION PROCEDURES

FORGING METHODS

The vast majority of experimental forgings produced on the program were made at the Utica, NY Division of Kelsey-Hayes using a Crank Press.* This type of forging unit is commonly employed in the manufacture of turbine blading and derives it's energy from a massive flywheel. The Crank Press used delivered 1.78×10^7 N (4×10^6 lbsf) at a tooling velocity of 0.3m/s (1.0ft/s). A few forgings were produced at the Westinghouse Astronuclear Laboratory on a model 1220C Dynapak. The Dynapak derives it's energy from the rapid expansion of a compressed gas. Forging on the Dynapak was done at conditions which delivered 8.3×10^4N (1.87×10^4 lbsf) at a tooling velocity of 5.8 m/s (19.1 ft/s).

The influence that forging and annealing conditions have on the mechanical properties of TDNiCr were examined by fabricating test plates from the starting preform and bar materials. The plates prepared were nominally 15-30 cm x 3.8 cm x 0.38 cm (6-12 in. x 1.5 in. x 0.15 in.) and were forged in a slotted or channel die. A schematic representation of channel die forging is presented in Figure C-1. The walls of the channel restrain lateral deformation, and the forged piece is essentially elongated unidirectionally along the length of the die. The method for controlling forging reduction on a fixed stroke length device such as a Crank Press by placing shims under the channel die is displayed in Figure C-1. Note that some material is extruded as flash into the gap between the walls of the channel and the punch.

Two views of a typical as-forged experimental plate are shown in Figure C-2. The serrated material along the edges of the plate is the flash formed during forging. Cracks formed in the flash propagated into the plate region in only a few instances where forging had been performed at the lowest investigated temperatures.

---

* Also commonly referred to as a Mechanical Press.

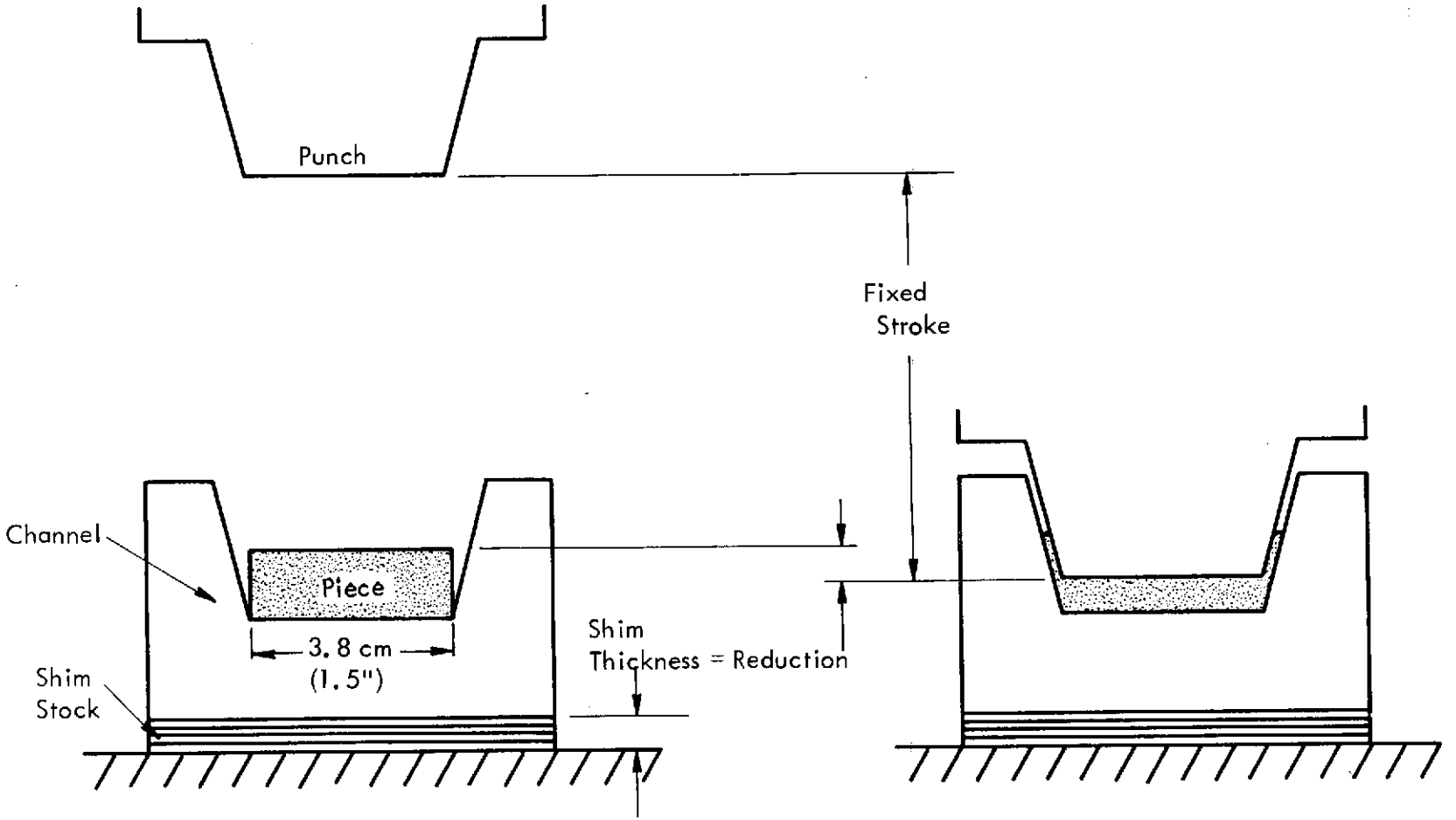

Figure C-1. A Schematic Representation of Channel Die Forging

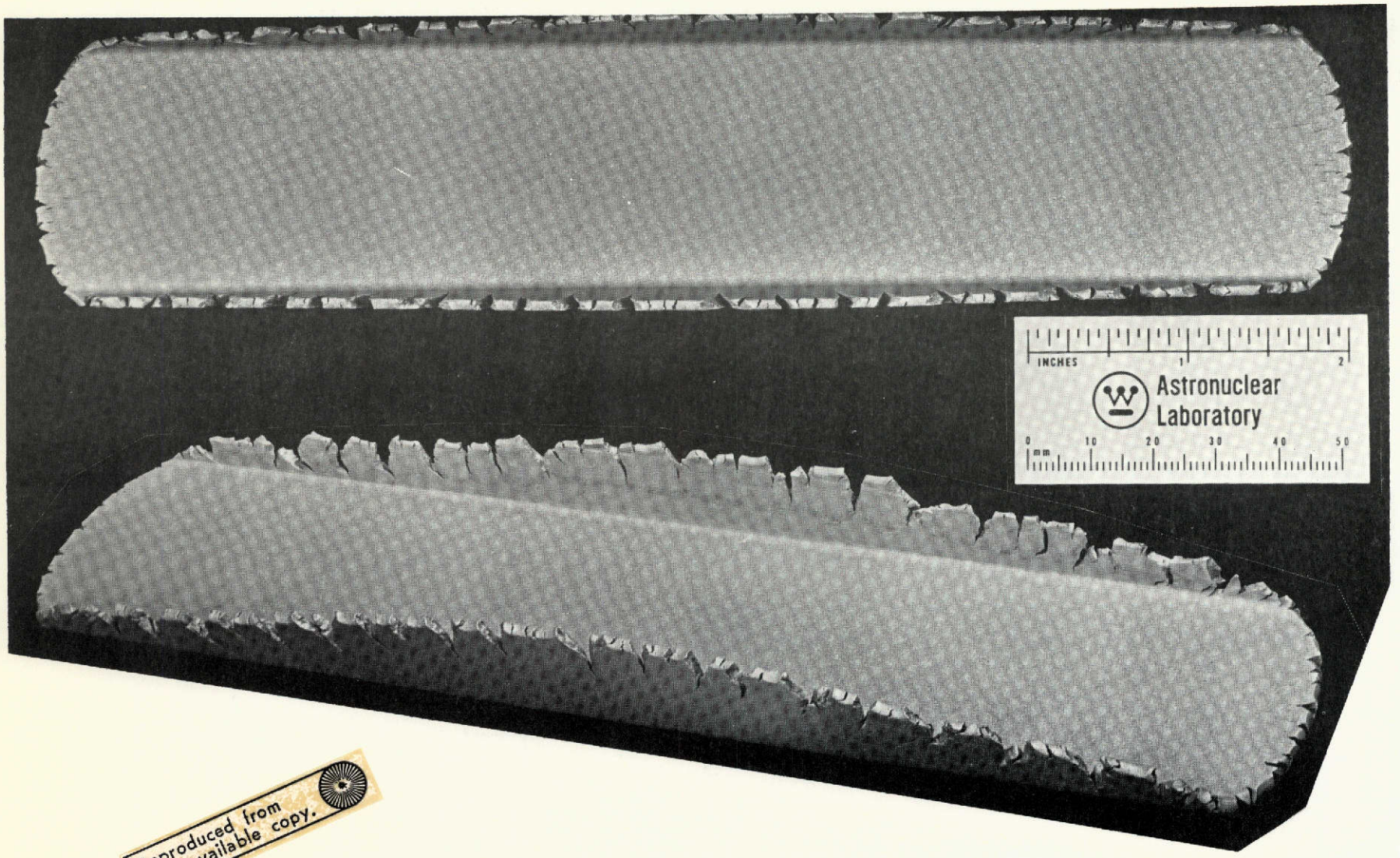

Figure C-2. Two Views of a Typical As-forged Experimental Plate

Heating for forging and in-process annealing treatments was done in SiC glo-bar and nichrome wire wound electric resistance furnaces. The pieces were held for 1800 seconds (1/2 hour) at temperature for these operations. Temperature control of the furnaces was achieved through thermocouple actuated on-off type units, while piece temperature was monitored using an optical pyrometer. Reported forging and in-process annealing temperatures are estimated to possibly be in error by $\pm$ 14°K ($\pm$25°F).

The pieces were dip coated with a commercial glass-type lubricant used for forging superalloy turbine blading. The lubricant, Acheson 347, was judged suitable for use on TDNiCr after metallographic examination of coated coupons exposed in air for 1.98×10^4 seconds at 1339°K (5.5 hours at 1950°F) did not reveal any interaction. An oil-graphite lubricant was also applied to the forging tooling. In between each forging pass, pieces were air cooled, sandblast cleaned, dimensioned, and recoated with the Acheson 347 lubricant.

SHOCK WAVE DEFORMATION

A major objective of the program was to evaluate whether the elevated temperature strength of optimally processed TDNiCr sheet could be approached by forged material. This was done by varying forging and annealing parameters and measuring their influence on high temperature mechanical properties. A shock wave deformation experiment was designed to determine if the strength of material in the best forged condition might be further improved by subjecting it to passage of a high pressure shock wave. The movement of a high pressure shock wave through a metal results in metallurgical changes somewhat similar to that of cold work without causing major dimensional changes. As such, shock wave "deformation" might lend itself to use on finished parts.

Six TDNiCr plates each measuring 3.5 cm x 7.6 cm x .25 cm (1-3/8 in. x 3 in. x 0.10 in.) were used in the experiment. They were machined from channel die forgings fabricated and annealed to optimize high temperature strength. Each plate was subjected to a pressure wave of 2.3×10^4 MN/m^2 (3.3×10^6 psi). Three were then annealed for 1800 seconds at 1366°K (1/2 hour at 2000°F) and shock treated a second time. The single and double shock wave treated plates were evaluated by electron microscopy, and tensile and stress-rupture testing at 1366°K (2000°F).

The shock wave treatments were performed at E. F. Industries, Inc., Louisville, Colorado. A contact explosive was applied to one side of each plate and detonated to create the pressure front. The plates were backed by a thick steel anvil and edged with steel strips in a picture frame fashion. A light, general purpose oil was applied at the plate-explosive interface.

A composition A-3 RDX base explosive containing 9% wax binder was used. It was pressed to a density of 1.55 gms/cm^3, a condition which upon detonation will result in a front pressure of approximately 2.3×10^4 MN/m^2 (3.3×10^6 psi).

APPENDIX D

METHODS OF EVALUATION

MECHANICAL PROPERTIES

Tensile and stress-rupture properties were evaluated using both shoulder and pin loaded specimens of designs shown in Figure D-1. Specimens removed from channel die forgings were always taken with their long axis parallel to the longitudinal forging direction.

The nominal thickness of a finished channel die forging was 0.38 cm (0.15 in.). When machining this dimension to obtain the 0.25 cm (0.10 in.) specimen thickness, care was taken to insure that equal and sufficient amounts of material were removed from both sides of the plate to eliminate any superficial cracks and thin surface layers of microstructure differing from that of more centrally located bulk. The latter condition presumably resulted from chilling due to contact with the relatively cold forging punch and die surfaces.

All mechanical property tests were run in an air environment. Elevated temperatures were obtained by use of platinum wire wound electric resistance furnaces. Precious metal thermocouples were wired at the center and ends of a specimen's gauge section to monitor and control elevated test temperatures. Temperature was controlled within $\pm 3^{\circ}K$ ($\pm 5^{\circ}F$) of nominal on tensile tests, and $\pm 6^{\circ}K$ ($\pm 10^{\circ}F$) on stress-rupture tests. Samples were held at temperature for a minimum of 1800 seconds (1/2 hour) prior to the start of testing.

The test grips were fabricated from both MAR-M200 and TDNiCr, and incorporated Al_2O_3 pins at the bearing areas in contact with the specimen. Common screw-type tensile units and stress-rupture frames of lever-arm and dead weight loading types were used. Tensile tests were performed at a crosshead speed to give a 0.05/minute strain rate.

Elongation values were determined on tensile tests from the autographically drawn machine load-displacement curves. For stress-rupture tests, this property was determined by measuring, both before and after testing, the distance between the shoulder radii at opposite ends of the specimen's gauge section.

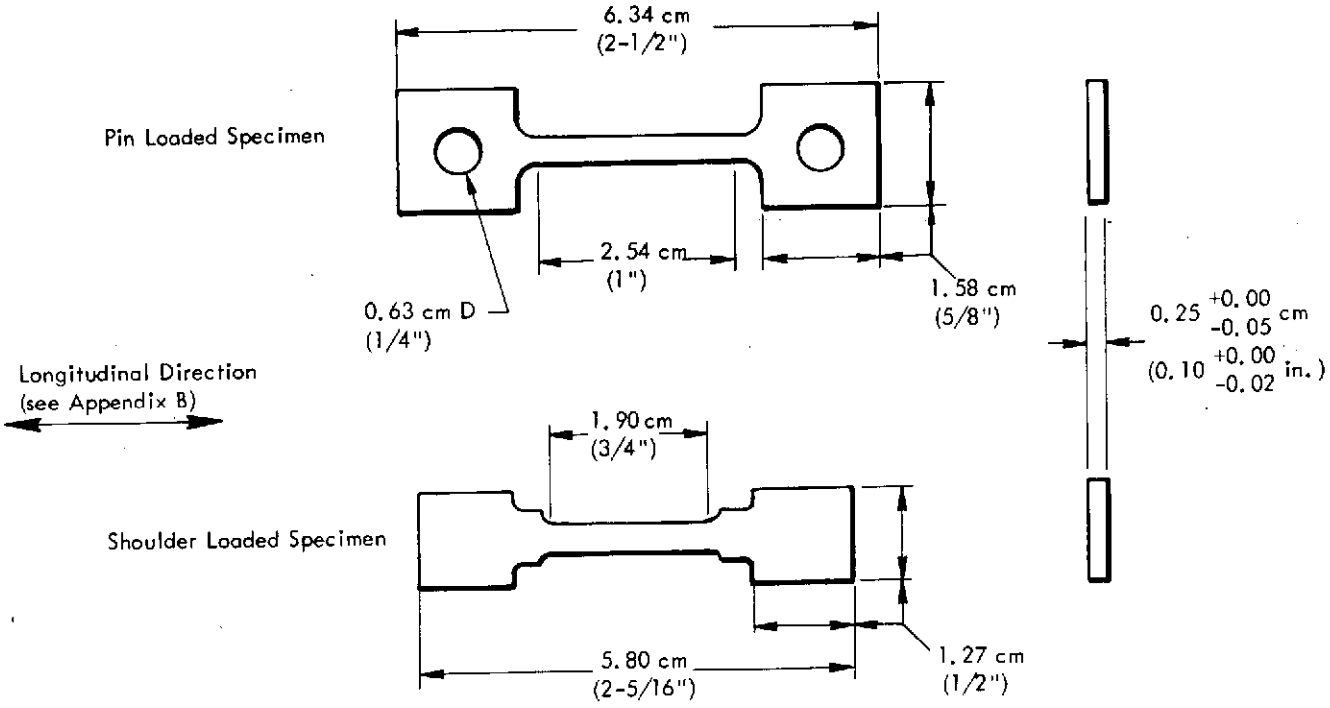

Figure D-1. Test Specimens

HEAT TREATMENT

Heat treatments of metallography and mechanical property samples were performed under vacuum of 1.3×10^{-3} to 1.3×10^{-4} N/m^2 (10^{-5} to 10^{-6} torr). All runs included a 1 to 2 hour period during which the samples were brought while under vacuum from ambient to the annealing temperature. Cooling at the conclusion of heat treatment was done much more rapidly by introducing helium into the chamber. The helium quench rate was measured between the temperatures of 1366 and 1200°K and found to be 111°K/minute (200°F/minute quench rate between 2000 and 1700°F). Temperature was measured optically employing techniques to approximate black body conditions.

OPTICAL METALLOGRAPHY

Through mostly trial-and-error efforts, several metallographic techniques were devised to define optical microstructures. Use of a particular technique was dependent upon the grain size of the sample. A tabulation of the metallographic methods found most suitable for specific grain size material is given in Table D-1.

Photomicrographs are shown in Figure D-2 to exemplify the major variation of grain size observed in channel die forged material. Grain size was demonstrated to be dependent largely upon forging and final annealing temperatures.

GRAIN SIZE MEASUREMENT

Grain size is reported as either an average grain diameter or an average grain dimension referred to a given material direction*. In the latter case, the average frequency of grain

* Definitions of directions in materials are given in Appendix B.

Table D-1. Metallographic Procedures

Grain Size	Grinding	Polishing	Etching
1 - 20 μm	Wet grind from 120 through 600 SiC paper	None	1:1, $CH_3OH:HNO_3$ Electrolytic
10 - 75 μm		.03 μm Al_2O_3 + 10% chromic acid slurry	2:1:1, glycerine:HCl:HNO_3 Electrolytic
50 - 200 μm			5:1:1, CH_3OH:HCl:HNO_3 Electrolytic
> 200 μm			2:2:5:1, H_2O:C_2H_5OH:HCl:$CuSO_4$ Immerse and Swab

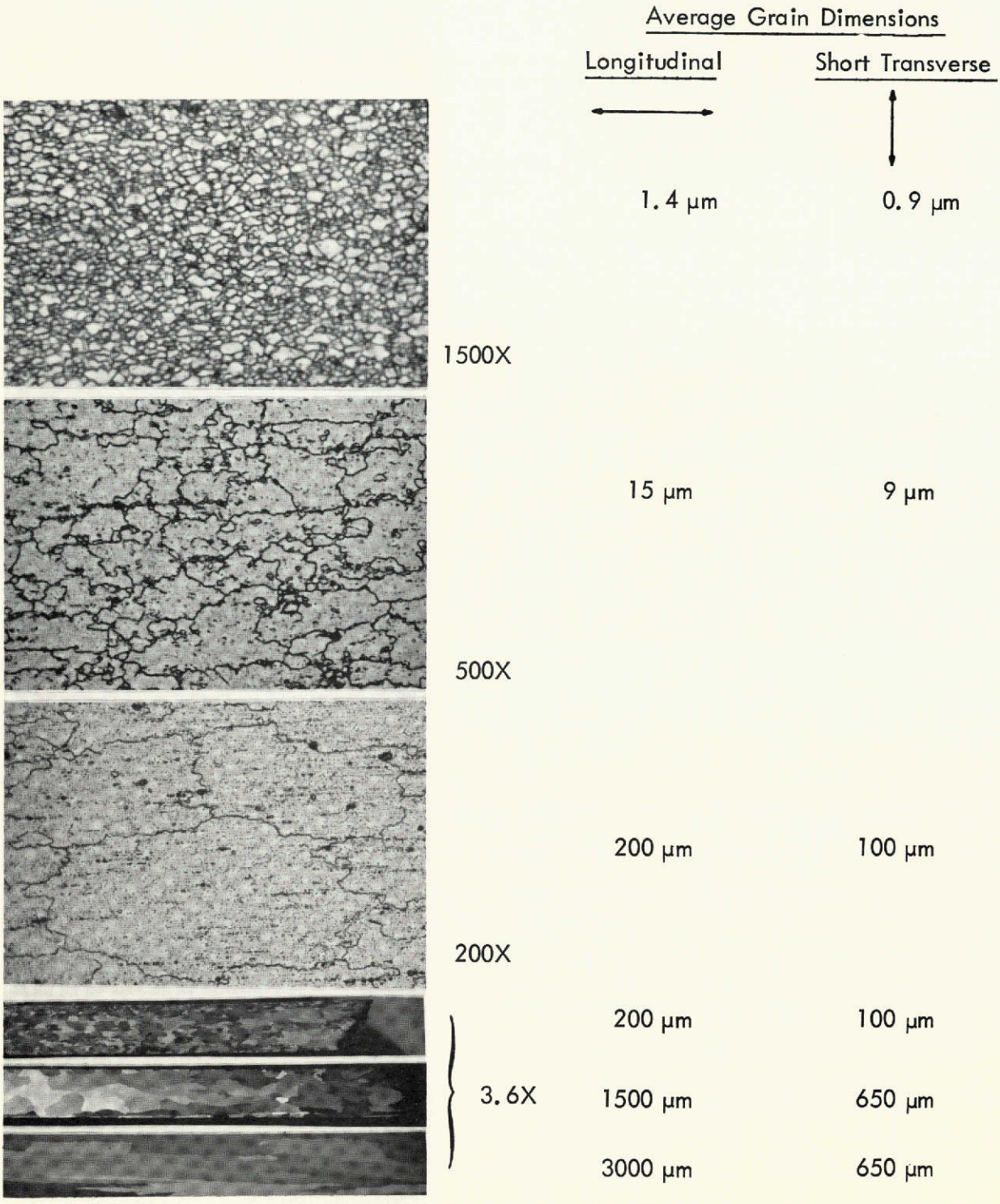

Figure D-2. Example Optical Microstructures of Channel Die Forged TDNiCr. Longitudinal surface microstructures and grain dimensions in the longitudinal and short transverse directions are shown. Surfaces and directions are defined in Appendix B.

boundary intercepts was first determined from lines drawn on a photomicrograph along the material direction of interest; intercept frequency = $\bar{f}$ = avg. no. intercepts/unit length. Intercept frequency was converted to a grain dimension by the relationship $(\bar{f}M)^{-1}$, where M is the photomicrograph magnification. Longitudinal, long transverse, and short transverse grain dimensions are symbolized in presentations as $\bar{L}$, $\bar{T}$, and $\bar{t}$, respectively.

A measure of average grain diameter involved first determining average grain dimensions along three orthogonal axes. For channel die forgings the orthogonal axes corresponded to the longitudinal, long transverse, and short transverse directions. $\bar{L}$, $\bar{T}$, and $\bar{t}$ grain dimensions were converted to average grain diameter, d, by the relationship,

$$d = \left(\frac{6}{\pi} \bar{L}\, \bar{T}\, \bar{t}\right)^{1/3}$$

Grain diameter determined as such is the diameter of a sphere of volume equivalent to the product $\bar{L}\, \bar{T}\, \bar{t}$.

ELECTRON MICROSCOPY

Selected samples were examined to qualitatively characterize densities and arrangements of dislocations. In addition, 1000 thoria particles were measured from electron micrographs of superior strength material to determine size, distribution, and spacing. This work was subcontracted to Structure Probe, Inc., West Chester, Pa. Techniques used for purposes of foil preparation were not reported.

TEXTURE DETERMINATIONS

The type and degree of preferred orientation was determined for channel die forged material of near optimum elevated temperature strength. Samples, both as-forged and annealed 3600 seconds at 1616°K (1 hour at 2450°F), were investigated. Measurements of preferred orientation were taken from surfaces prepared by machining 0.089 cm (0.035 in.) of material from the forging plane, grinding to a 600 grit SiC paper finish, and acid pickling.

Reported pole figures are oriented with the vertical axis corresponding to the longitudinal material direction. (Definitions of material directions and surfaces are given in Appendix B).

MATHEMATICAL MODELING - DR. A. HOLMS, NASA-LEWIS RESEARCH CENTER

The data for the mathematical modeling was provided by two factorial experiments and one "vector" experiment. The methodology was essentially that of the "method of steepest ascents".[2] The experiments always involved some of the variables listed in Table D-2. The variables involved in each experiment are listed in Table D-3. The dependent variable was always a high temperature ultimate tensile strength. The mathematical models chosen to relate the dependent variable to the independent variables, for each of the experiments, are given in Appendix E. Variables not listed for the particular experiments in Table D-3 were varied from one experiment to another, but were fixed within any one experiment. The conclusions obtained from the model fitting are therefore only assured to be valid for the fixed conditions (which are described in other parts of the report).

Two computer programs were used in the model fitting, both based upon techniques of regression analysis and the method of least squares. One of them, named POOLMS,[3, 4] can be used with fully saturated models (equations with the number of coefficients equal to the number of observed conditions), but the experiments and models must be suitable for Yates' analysis. The other program, named NEWRAP,[5] does not have the orthogonality requirement of POOLMS but does require that the number of estimated coefficients be less than the number of observed conditions. Both programs were applied to the first and third forging experiments. Only NEWRAP was suitable for the second experiment.

To conserve cost, few forging replicates were made; as a consequence, statistical tests of significance were not applied consistently with their operationally defined probabilistic meanings. Furthermore, the variables of final annealing condition and test temperature (X_6 and X_7 of Table D-2) were applied in a cross stratified manner to subsections of forgings rather than independently to each forging. This improves the accuracy of the estimated

influence of these variables but also distorts the usually defined meanings of tests of significance. However, although distorted from their true levels, the test of significance is considered to satisfactorily separate terms of lesser significance from those of greater significance.

Table D-2. Statistically Examined Independent Variables

Independent Variables	Design Units	Natural Units
Primary Forging Temperature	X_1	Z_1
Primary Forging Operation	X_2	Z_2
Secondary Forging Temperature	X_3	Z_3
Secondary Forging Operation	X_4	Z_4
Secondary Annealing Temperature	X_5	Z_5
Final Annealing Condition	X_6	Z_6
Test Temperature	X_7	Z_7

Table D-3. Experiments Fitted by Mathematical Models

Forging Experiment	Type of Experiment	Independent Variables
First	Fractional factorial	X_1 primary forging temp. X_3 secondary forging temp. X_4 number of secondary steps X_5 secondary annealing temp. X_6 final annealing condition X_7 test temperature
Second	Multiple vector	X_2 number of primary steps* X_3 secondary forging temp. X_5 secondary annealing temp. X_6 final annealing condition X_7 test temperature
Third	Full factorial	X_1 primary forging temp. X_2 size of primary reduction X_3 secondary forging temp. X_4 size of secondary reduction X_6 final annealing treatment

*The number of secondary steps varied in a manner dependent strictly on the number of primary steps.

APPENDIX E

A SUMMARY OF EXPERIMENTS, TEST DATA, AND STATISTICAL ANALYSIS

Descriptions of five distinguishable experiments on which 68 channel die forgings were prepared and the results of tensile and stress-rupture tests performed on these forgings comprise the major portion of this appendix. Also included are results of statistical analysis, grain size data for selected forgings, and mechanical property data for material forged to optimize high temperature strength then subjected to high pressure shock wave treatments.

DESCRIPTION AND DATA - FIRST FORGING EXPERIMENT

Eight channel die forgings were prepared on the first experiment as described in Table E-1. Differences between starting and finishing forging conditions are distinguished by the words primary and secondary. Tensile properties were measured at 1366 and 1422°K (2000 and 2100°F) on material as-forged and annealed 1800 seconds at 1589°K (1/2 hour at 2400°F). These data are presented in Tables E-2 and E-3.

STATISTICAL ANALYSIS - FIRST FORGING EXPERIMENT - DR. A. HOLMS, NASA-LEWIS RESEARCH CENTER

The conditions and results of this experiment are given in Tables E-1 through E-3. The matching of the independent variables between natural and design units is summarized in Table E-4.

A procedure for combining significance tests with Yates' method of model coefficient estimation is given in Reference 3, and a computer program (POOLMS) for doing the work in Reference 4. The Yates method requires that the observations be listed in a special order in relation to the names of the independent variables. Yates' matching between the names of the independent variables and the ordered list of observations was achieved by changing the subscripts of the independent variables (X_2 was a constant) as follows: $X_A = X_7$, $X_B = X_6$, $X_C = X_5$, $X_D = X_4$, $X_E = X_3$, $X_F = X_1$.

Table E-1. Processing Conditions - First Forging Experiment*

Forging No.	Primary Forging Conditions				In-Process Anneal Temperature		Secondary Forging Conditions			
	Steps	%R/ Step	Temperature				Steps	%R/ Step	Temperature	
			(°K)	(°F)	(°K)	(°F)			(°K)	(°F)
1	1	25	1200	(1700)	1089	(1500)	12	10	977	(1300)
2	1	25	1200	(1700)	1144	(1600)	8	10	977	(1300)
3	1	25	1311	(1900)	1144	(1600)	8	10	1089	(1500)
4	1	25	1200	(1700)	1144	(1600)	12	10	1089	(1500)
5	1	25	1311	(1900)	1089	(1500)	12	10	1089	(1500)
6	1	25	1311	(1900)	1089	(1500)	8	10	977	(1300)
7	1	25	1200	(1700)	1089	(1500)	8	10	1089	(1500)
8	1	25	1311	(1900)	1144	(1600)	12	10	977	(1300)

* Material (Appendix A): Preform Heat 3114

Total Reduction: 60%; forgings 2, 3, 6, and 7. 80%; forgings 1, 4, 5, and 8.

Forging Direction: Perpendicular to the forging direction used in preform manufacture (Appendix B)

In-process Anneal Time: 1800 seconds (1/2 hour)

Forging Operation: Mechanical press

Table E-2. 1366°K (2000°F) Tensile Data - First Forging Experiment

Forging No.	Condition	Ultimate Strength		0.2% Yield Strength		Elongation
		MN/m^2	(ksi)	MN/m^2	(ksi)	(%)
1	As-forged	65.7	(9.48)	54.8	(7.90)	3.0
1	Annealed*	50.8	(7.31)	46.2	(6.68)	6.0
2	As-forged	37.5	(5.39)	28.5	(4.12)	7.5
2	Annealed	41.4	(5.96)	37.7	(5.43)	4.5
3	As-forged	33.7	(4.86)	24.8	(3.58)	7.0
3	Annealed	45.4	(6.57)	41.2	(5.93)	6.0
4	As-forged	57.1	(8.23)	50.1	(7.22)	4.4
4	Annealed	69.1	(9.97)	61.4	(8.87)	4.4
5	As-forged	50.8	(7.32)	45.0	(6.50)	6.0
5	Annealed	47.4	(6.83)	45.2	(6.52)	7.5
6	As-forged	48.1	(6.93)	39.9	(5.77)	10.0
6	As-forged	28.9	(4.17)	18.4	(2.65)	10.5
6	Annealed	41.9	(6.02)	41.4	(5.96)	3.0
7	As-forged	41.6	(6.00)	29.2	(4.22)	10.0
7	As-forged	31.8	(4.60)	27.3	(3.94)	9.0
7	Annealed	39.7	(5.72)	37.5	(5.40)	7.5
8	As-forged	59.9	(8.62)	50.4	(7.27)	4.5
8	Annealed	62.4	(9.00)	55.0	(7.92)	1.5

* Annealing conditions: 1800 seconds at 1589°K (1/2 hr. at 2400°F)

Table E-3. 1422°K (2100°F) Tensile Data - First Forging Experiment

Forging No.	Condition	Ultimate Strength		0.2% Yield Strength		Elongation (%)
		MN/m^2	(ksi)	MN/m^2	(ksi)	
1	As-forged	41.9	(6.03)	34.4	(4.95)	7.5
1	Annealed*	46.1	(6.65)	42.1	(6.08)	4.5
2	As-forged	27.7	(3.99)	17.2	(2.47)	12.0
2	Annealed	39.1	(5.62)	36.7	(5.29)	4.5
3	As-forged	31.4	(4.52)	26.4	(3.81)	7.5
3	Annealed	35.4	(5.10)	32.2	(4.65)	9.0
4	As-forged	46.6	(6.73)	39.1	(5.63)	4.5
4	Annealed	46.4	(6.69)	44.1	(6.36)	4.5
5	As-forged	36.1	(5.20)	33.3	(4.80)	4.5
5	Annealed	36.3	(5.22)	34.9	(5.03)	4.5
6	As-forged	27.6	(3.98)	19.4	(2.79)	9.0
6	Annealed	35.4	(5.10)	33.6	(4.85)	7.5
7	As-forged	27.8	(4.02)	20.2	(2.91)	6.0
7	Annealed	31.3	(4.52)	28.6	(4.13)	6.0
8	As-forged	58.2	(8.40)	56.4	(8.13)	3.0
8	Annealed	44.6	(6.42)	43.2	(6.22)	4.5

* Annealing Conditions: 1800 seconds at 1589°K (1/2 hour at 2400°F)

Table E-4. Independent Variables - First Forging Experiment

Independent Variable	Natural Units		Design Units	
Primary Forging Temperature	Z_1	1700°F 1900°F	X_1	-1 1
Secondary Forging Temperature	Z_3	1300°F 1500°F	X_3	-1 1
Number of Secondary Steps	Z_4	8 12	X_4	-1 1
In-Process Annealing Temperature	Z_5	1500°F 1600°F	X_5	-1 1
Final Annealing Condition	Z_6	No treatment 1/2 hr., 2400°F	X_6	-1 1
Test Temperature	Z_7	2000°F 2100°F	X_7	-1 1

With the preceding matching, the tensile strength data were listed in Yates' order as shown by Table E-5. As shown in this table, the levels of X_F are not independent of the levels of the other five variables, but instead are related by $X_F = -X_C X_D X_E$. The implication of this relation is that the half replicate experiment on six variables has a defining contrast given by I = -CDEF. Correspondingly, the 64 coefficients that might be estimated by a full factorial experiment on six variables are contained in 32 alias relations among such coefficients. Where these alias relations exist between coefficients of the same order, both are listed in Table E-6; otherwise only the lower order coefficient is given.

The variables regarded as being most likely to produce interactions, in the order of such a tendency and with letter subscripts also in that order, are:

X_7	X_A	Test Temperature
X_6	X_B	Final Annealing Condition
X_5	X_C	In-process Annealing Temperature
X_4	X_D	Number of Secondary Steps
X_3	X_E	Secondary Forging Temperature
X_1	X_F	Primary Forging Temperature

Consistent with the assumed tendency of the independent variables to interact, the second parameter of each of the aliased pairs in Table E-6 was assumed to be zero. With such parameter deletions, the saturated model fitted to the data of the first forging experiment in Yates' order is:

Table E-5. Data in Yates' Order - First Forging Experiment

X_7 X_A	X_6 X_B	X_5 X_C	X_4 X_D	X_3 X_E	X_1[1] X_F	Y[2] (ksi)	Forging No.
-1	-1	-1	-1	-1	1	5.55[3]	6
1	-1	-1	-1	-1	1	3.98	6
-1	1	-1	-1	-1	1	6.02	6
1	1	-1	-1	-1	1	5.10	6
-1	-1	1	-1	-1	-1	5.39	2
1	-1	1	-1	-1	-1	3.99	2
-1	1	1	-1	-1	-1	5.96	2
1	1	1	-1	-1	-1	5.62	2
-1	-1	-1	1	1	-1	9.48	1
1	-1	-1	1	1	-1	6.03	1
-1	1	-1	1	1	-1	7.31	1
1	1	-1	1	1	-1	6.65	1
-1	-1	1	1	1	-1	8.62	8
1	-1	1	1	1	-1	8.40	8
-1	1	1	1	1	-1	9.00	8
1	1	1	1	1	-1	6.42	8
-1	-1	-1	-1	-1	1	5.30[3]	7
1	-1	-1	-1	-1	1	4.02	7
-1	1	-1	-1	-1	1	5.72	7
1	1	-1	-1	-1	1	4.52	7
-1	-1	1	-1	-1	1	4.86	3
1	-1	1	-1	-1	1	4.52	3
-1	1	1	-1	-1	1	6.57	3
1	1	1	-1	-1	1	5.10	3
-1	-1	-1	1	1	1	7.32	5
1	-1	-1	1	1	1	5.20	5
-1	1	-1	1	1	1	6.83	5
1	1	-1	1	1	1	5.22	5
-1	-1	1	1	1	-1	8.23	4
1	-1	1	1	1	-1	6.73	4
-1	1	1	1	1	-1	9.97	4
1	1	1	1	1	-1	6.69	4

(1) $X_F = -X_C X_D X_E$

(2) Ultimate tensile strength

(3) Mean of two values

Table E-6. Aliased Parameters - First Forging Experiment I = -CDEF

i.	Coefficient
0.	β_I
1.	β_A
2.	β_B
3.	β_{AB}
4.	β_C
5.	β_{AC}
6.	β_{BC}
7.	β_{ABC}
8.	β_D
9.	β_{AD}
10.	β_{BD}
11.	$\beta_{ABD} - \beta_{CEF}$
12.	$\beta_{CD} - \beta_{EF}$
13.	$\beta_{ACD} - \beta_{AEF}$
14.	$\beta_{BCD} - \beta_{BEF}$
15.	$\beta_{ABCD} - \beta_{ABEF}$
16.	β_E
17.	β_{AE}
18.	β_{BE}
19.	β_{ABE}
20.	$\beta_{CE} - \beta_{DF}$
21.	$\beta_{ACE} - \beta_{ADF}$
22.	$\beta_{BCE} - \beta_{BDF}$
23.	$\beta_{ABCE} - \beta_{ABDF}$
24.	$\beta_{DE} - \beta_{CF}$
25.	$\beta_{ADE} - \beta_{ACF}$
26.	$\beta_{BDE} - \beta_{BCF}$
27.	$\beta_{ABDE} - \beta_{ABCF}$
28.	$-\beta_F$
29.	$-\beta_{AF}$
30.	$-\beta_{BF}$
31.	$-\beta_{ABF}$

$$
\begin{aligned}
Y = {} & \beta_0 + \beta_1 X_7 + \beta_2 X_6 + \beta_3 X_6 X_7 \\
& + \beta_4 X_5 + \beta_5 X_5 X_7 + \beta_6 X_5 X_6 + \beta_7 X_5 X_6 X_7 \\
& + \beta_8 X_4 + \beta_9 X_4 X_7 + \beta_{10} X_4 X_6 + \beta_{11} X_4 X_6 X_7 \\
& + \beta_{12} X_4 X_5 + \beta_{13} X_4 X_5 X_7 + \beta_{14} X_4 X_5 X_6 + \beta_{15} X_4 X_5 X_6 X_7 \\
& + \beta_{16} X_3 + \beta_{17} X_3 X_7 + \beta_{18} X_3 X_6 + \beta_{19} X_3 X_6 X_7 \\
& + \beta_{20} X_3 X_5 + \beta_{21} X_3 X_5 X_7 + \beta_{22} X_3 X_5 X_6 + \beta_{23} X_3 X_5 X_6 X_7 \\
& + \beta_{24} X_3 X_4 + \beta_{25} X_3 X_4 X_7 + \beta_{26} X_3 X_4 X_6 + \beta_{27} X_3 X_4 X_6 X_7 \\
& - \beta_{28} X_1 - \beta_{29} X_1 X_7 - \beta_{30} X_1 X_6 - \beta_{31} X_1 X_6 X_7
\end{aligned} \tag{1}
$$

The data given in Table E-5 were used to estimate the coefficients of equation 1. Decision procedures described in Reference 3 were invoked to eliminate insignificant coefficients. Equation 1, written with only significant coefficients and presented in the order of their absolute values, is:

$$
\begin{aligned}
Y = {} & 6.260 \\
& + 1.121 X_4 \\
& - 0.748 X_7 \\
& + 0.369 X_5 \\
& - 0.279 X_4 X_6 \\
& - 0.258 X_5 X_6 X_7 \\
& + 0.257 X_4 X_5 \\
& - 0.216 X_4 X_7 \\
& - 0.210 X_3 \\
& - 0.208 X_4 X_5 X_6 X_7
\end{aligned} \tag{2}
$$

The test temperature of 2000°F was of greatest interest. Equation 2, specialized to this temperature by setting $X_7 = -1$, is:

$$\begin{aligned} Y &= 7.008 \\ &+ 1.337\, X_4 \\ &+ 0.369\, X_5 \\ &- 0.279\, X_4X_6 \\ &+ 0.258\, X_5X_6 \\ &+ 0.257\, X_4X_5 \\ &- 0.210\, X_3 \\ &+ 0.208\, X_4X_5X_6 \end{aligned} \qquad (2a)$$

Equation 2a shows that greatest strengthening would be achieved at the larger secondary reduction, namely 12 steps, which is equivalent to $X_4 = 1$. A strength increment of 1.34 ksi (over $X_4 = 0$) was obtained by imposing this condition, and the relationship reduces to:

$$\begin{aligned} Y &= 8.345 \\ &+ 0.626\, X_5 \\ &+ 0.466\, X_5X_6 \\ &- 0.279\, X_6 \\ &- 0.210\, X_3 \end{aligned} \qquad (3)$$

A strength increment of 0.63 ksi (over $X_5 = 0$) can be obtained from equation 3 by setting $X_5 = 1$, which is equivalent to the higher in-process annealing temperature, namely, 1600°F. This reduces the relationship to:

$$\begin{aligned} Y &= 8.971 \\ &- 0.210\, X_3 \\ &+ 0.187\, X_6 \end{aligned}$$

Use of the lower secondary forging temperature, $X_3 = -1$, and the final annealing condition of 1/2 hour at 2400°F, $X_6 = 1$, is suggested by the above equation. The individual strength increments obtained by imposing these two conditions are 0.21 and 0.19 ksi.

The four calculated strength increments given in the order of the above arguments are: 1.34, 0.63, 0.21, and 0.19 ksi. Of these, the first is regarded as significant, the second as probably significant, and the last two as of very doubtful significance.

In no case was the distinction between 1700 and 1900°F primary forging temperatures significant.

The major conclusion drawn from this analysis was that, within the bounds of the first forging experiment, an increase in the number of secondary forging steps and, to a lesser extent, in-processing annealing temperature, improved strength. An increase of secondary forging steps simply corresponded to an increase of total reduction. A general strength improvement with increase of total reduction can be verified by careful examination of the raw data (Tables E-1 through E-3).

To obtain a check on the above computations and conclusions, a model was fitted to the same data using the NEWRAP program of reference 5. This procedure was used with the strategy of pooling all insignificant mean squares into the residual, which was used as an estimate of the error mean square. The imposed nominal confidence level for the tests of significance was 0.900. The model fitted to the data was abreviated from that used with the chain pooling procedure (which can use a saturated model - equation 1) so that there would be a starting number of degrees of freedom greater than zero. The model equation used has four initial degrees of freedom for the residual and is:

$$
\begin{aligned}
Y = {} & \beta_0 + \beta_1 X_1 + \beta_2 X_3 + \beta_3 X_4 + \beta_4 X_5 \\
& + \beta_5 X_6 + \beta_6 X_7 + \beta_7 X_1 X_6 + \beta_8 X_1 X_7 \\
& + \beta_9 X_3 X_4 + \beta_{10} X_3 X_5 + \beta_{11} X_3 X_6 \\
& + \beta_{12} X_3 X_7 + \beta_{13} X_4 X_5 + \beta_{14} X_4 X_6 \\
& + \beta_{15} X_4 X_7 + \beta_{16} X_5 X_6 + \beta_{17} X_5 X_7 \\
& + \beta_{18} X_6 X_7 + \beta_{19} X_1 X_3 X_7 + \beta_{20} X_1 X_6 X_7 \\
& + \beta_{21} X_3 X_4 X_6 + \beta_{22} X_3 X_4 X_7 + \beta_{23} X_3 X_5 X_6 \\
& + \beta_{24} X_3 X_5 X_7 + \beta_{25} X_3 X_6 X_7 + \beta_{26} X_4 X_5 X_6 \\
& + \beta_{27} X_4 X_6 X_7 + \beta_{28} X_5 X_6 X_7
\end{aligned} \tag{4}
$$

Table E-6 had listed the coefficients - β_{AEF} and β_{ACD} as being an aliased set (not separately estimable). In equation (1), the corresponding estimate was assumed to be the coefficient of $X_4X_5X_7$, whereas in equation (4) the same estimate was assumed to be the coefficient of $X_1X_3X_7$. The significant terms resulting from the fitting of equation (4) to the data, in decreasing order of the absolute values of the coefficients, were:

$$
\begin{aligned}
Y = {} & 6.260 \\
& + 1.121\, X_4 \\
& - 0.748\, X_7 \\
& + 0.369\, X_5 \\
& - 0.279\, X_4 X_6 \\
& - 0.258\, X_5 X_6 X_7 \\
& + 0.257\, X_4 X_5 \\
& - 0.216\, X_4 X_7 \\
& - 0.210\, X_3
\end{aligned} \tag{5}
$$

Except for the absence of the smallest term, equation (5) is an exact confirmation of equation (2).

Equation (5) was used to predict the tensile strength for all of the conditions of the first experiment. The highest predicted value was 9.203 and occurred for the coordinates (X_1, X_3, X_4, X_5, X_6, X_7) = (1, -1, 1, 1, -1, -1) which are:

Primary Forging Temperature	1900°F
Secondary Forging Temperature	1300°F
Number of Secondary Steps	12
In-process Annealing Temperature	1600°F
Final Annealing Condition	None
Test Temperature	2000°F

The conclusions obtained from equation (2) are consistent with the preceding list of conditions, with the understanding that primary forging temperature was concluded to be insignificant, and the final annealing condition and secondary forging temperature were thought to be of doubtful significance.

The conclusion that the amount of secondary forging is the most potent variable raises the question: "How much forging can be done without causing cracking or other deterioration?" Increasing the secondary forging temperature from 1300°F to 1500°F caused a strength reduction of doubtful significance. Can significance for this supposedly important variable be clearly demonstrated by investigating it over a wider temperature interval? Should the increased total reduction be mainly at the primary or at the secondary forging temperature, and what will be needed in the way of in-process annealing? The first degree and interaction effects of the primary forging temperature were insignificant between 1700°F and 1900°F, suggesting that the primary forging temperature should be fixed at 1800°F. Under this condition, the investigation of practical limits for the total reduction should be done in a manner that will answer the preceding questions on processing temperatures. The questions

on temperatures can be answered by a small experiment, and the points of such an experiment can be regarded as establishing discrete vectors with distance along the vectors being the achievable total reduction. The appropriate experiment is described in the next section.

DESCRIPTION AND DATA - SECOND FORGING EXPERIMENT

Nine forgings were prepared on the second experiment as described in Table E-7. The results of elevated temperature tensile tests are given in Tables E-8 and E-9. Photographs of the nine forgings in the as-forged condition are presented in Figure E-1. A direct dependence of material soundness on the magnitude of forging and annealing temperatures was noted on this experiment and is discussed in this figure.

STATISTICAL ANALYSIS - SECOND FORGING EXPERIMENT - DR. A. HOLMS, NASA-LEWIS RESEARCH CENTER

This experiment and the resulting test data are summarized in Tables E-7 through E-9. Note that a five-fold replication of test data was obtained for forging number 16 (Table E-8). The median value of this data was used in analysis. Independent variables are matched to natural and design units for the second experiment in Table E-10.

Because the total number of reductions and the amount of total reduction was constant for this experiment, the variables X_2 and X_4, defined in Table D-2, are completely correlated and cannot be included simultaneously in the fitted model. The choice of which to include is arbitrary. The first on the list, X_2, was chosen.

Table E-7. Processing Conditions - Second Forging Experiment*

Forging No.	Primary Forging Conditions				In-Process Anneal Temperature		Secondary Forging Conditions			
	Steps	%R/ Step	Temperature (°K)	Temperature (°F)	(°K)	(°F)	Steps	%R/ Step	Temperature (°K)	Temperature (°F)
9	2	15	1255	(1800)	None		12	15	922	(1200)
10	4	15	1255	(1800)	None		10	15	922	(1200)
11	6	15	1255	(1800)	None		8	15	922	(1200)
12	2	15	1255	(1800)	1144	(1600)	12	15	922	(1200)
13	4	15	1255	(1800)	1144	(1600)	10	15	922	(1200)
14	6	15	1255	(1800)	1144	(1600)	8	15	922	(1200)
15	2	15	1255	(1800)	None		12	15	1144	(1600)
16	4	15	1255	(1800)	None		10	15	1144	(1600)
17	6	15	1255	(1800)	None		8	15	1144	(1600)

* Material (Appendix A): Preform heat 3114

Total Reduction: 85-90%

Forging Direction (Appendix C): Parallel to the forging direction used in preform manufacture.

In-process Anneal Time: 1800 seconds (1/2 hour)

Forging Operation: Mechanical press

Table E-8. 1366°K (2000°F) Tensile Data - Second Forging Experiment

Forging No.	Condition	Ultimate Strength		0.2% Yield Strength		Elongation (%)
		MN/m^2	(ksi)	MN/m^2	(ksi)	
9	As-forged	21.4	(3.08)	20.9	(3.02)	3.0
10	As-forged	32.0	(4.62)	25.2	(3.64)	1.5
10	Annealed*	33.7	(4.86)	30.6	(4.42)	3.0
11	As-forged	34.5	(4.97)	31.9	(4.60)	3.0
11	Annealed	34.6	(4.99)	31.1	(4.48)	6.0
12	As-forged	51.8	(7.47)	43.9	(6.32)	4.5
12	Annealed	43.3	(6.22)	42.6	(6.14)	2.0
13	As-forged	53.1	(7.66)	37.7	(5.43)	6.0
13	Annealed	49.0	(7.08)	46.7	(6.73)	2.0
14	As-forged	57.1	(8.22)	46.2	(6.68)	6.0
14	Annealed	54.3	(7.83)	53.7	(7.72)	1.5
15	As-forged	60.8	(8.76)	59.4	(8.58)	3.5
15	Annealed	68.9	(9.92)	67.6	(9.74)	3.5
16	As-forged	77.8	(11.20)	75.8	(10.90)	3.0
16	As-forged	88.1	(12.70)	86.8	(12.50)	3.0
16	As-forged	84.0	(12.10)	81.1	(11.70)	2.0
16	As-forged	88.1	(12.70)	86.8	(12.50)	2.0
16	As-forged	75.7	(10.90)	75.0	(10.80)	3.0
16	Annealed	65.0	(9.38)	63.9	(9.20)	3.0
17	As-forged	58.2	(8.40)	57.1	(8.22)	6.0
17	Annealed	56.9	(8.20)	55.6	(8.00)	3.0

* Annealing conditions: 1800 seconds at 1589°K (1/2 hour at 2400°F)

Table E-9. 1422°K (2100°F) Tensile Data - Second Forging Experiment

Forging No.	Condition	Ultimate Strength		0.2% Yield Strength		Elongation (%)
		MN/m^2	(ksi)	MN/m^2	(ksi)	
12	Annealed*	45.5	(6.57)	43.4	(6.26)	3.0
13	As-forged	36.4	(5.24)	28.3	(4.08)	3.0
13	Annealed	32.8	(4.73)	32.8	(4.73)	0.8
14	As-forged	42.0	(6.07)	34.3	(4.95)	4.5
14	Annealed	39.4	(5.68)	36.4	(5.25)	1.5
15	As-forged	53.6	(7.73)	52.2	(7.54)	4.5
15	Annealed	52.0	(7.50)	51.5	(7.43)	3.0
16	As-forged	63.5	(9.16)	63.1	(9.10)	4.5
16	Annealed	49.6	(7.17)	48.8	(7.03)	2.0
17	As-forged	65.6	(9.47)	64.8	(9.35)	5.0
17	Annealed	62.0	(8.95)	62.0	(8.95)	1.5

* Annealing Conditions: 1800 seconds at 1589°K (1/2 hour at 2400°F)

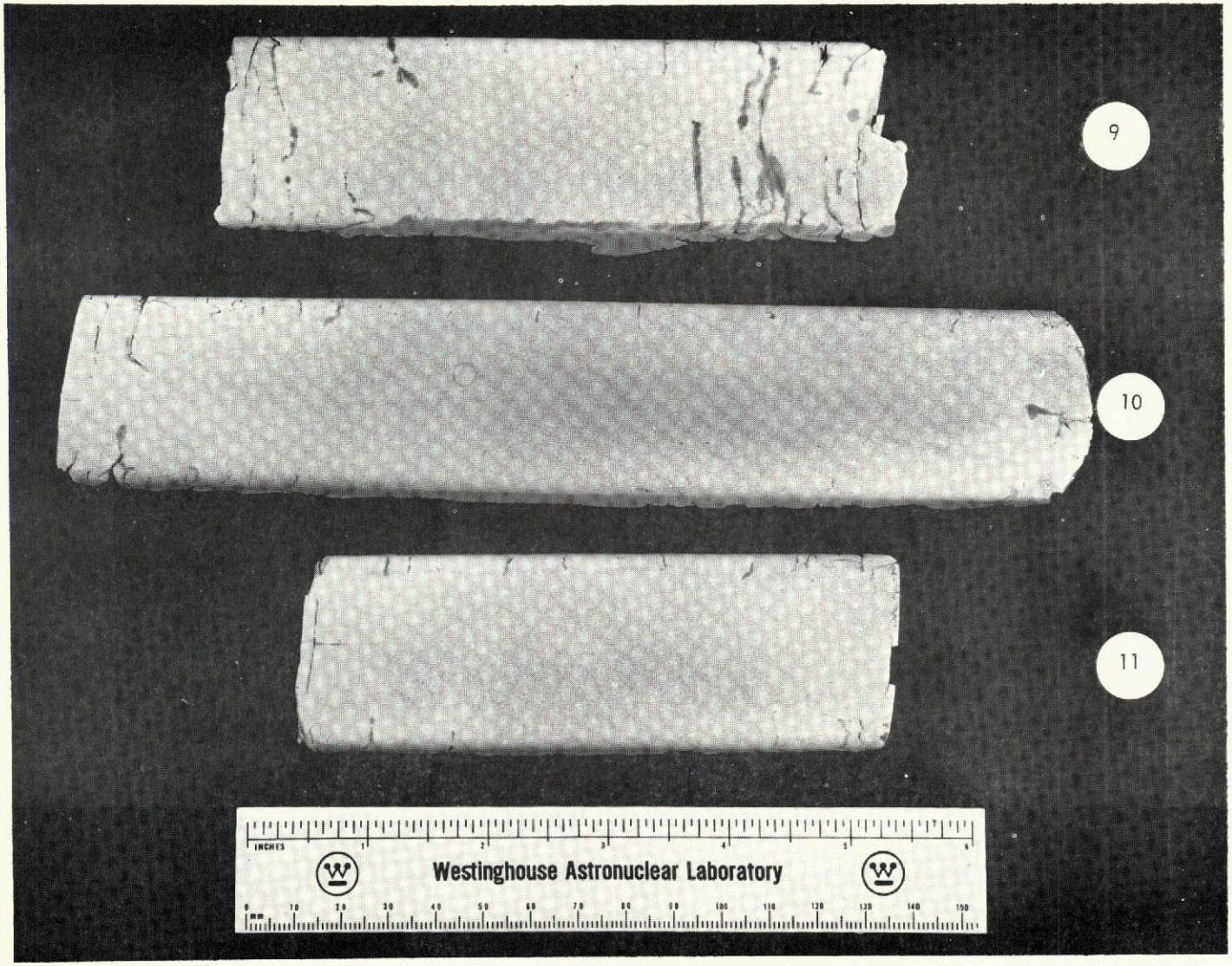

Figure E-1, Part (a). Forgings 9, 10, and 11.
The condition of these forgings was the poorest of the 68 prepared on the entire program. They were secondary forged at the lowest temperature investigated, 922°K (1200°F), without higher temperature in-process annealing. (Dye penetrant used to accentuate cracks).

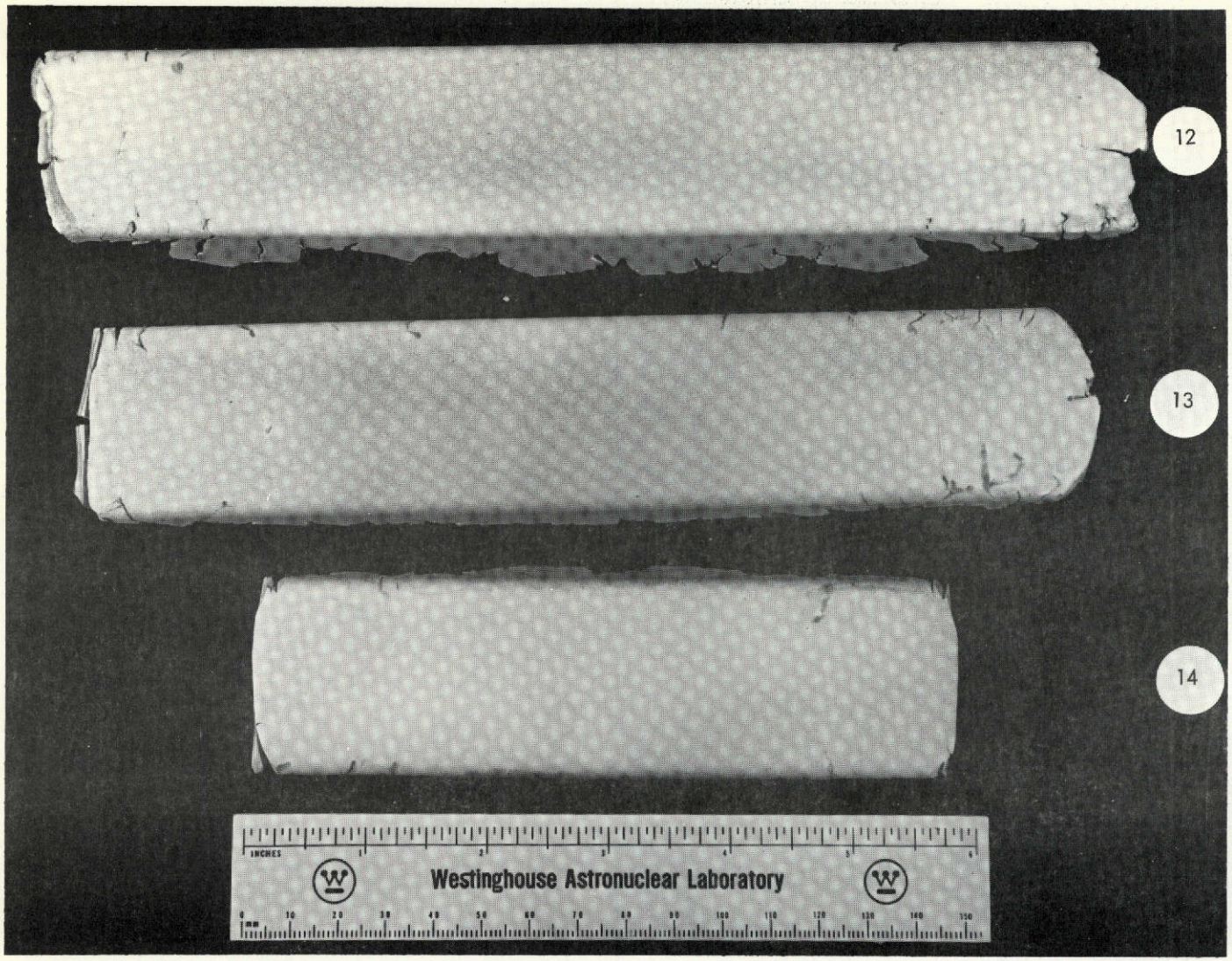

Figure E-1, Part (b). Forgings 12, 13, and 14.
These were secondary forged at 922°K (1200°F) and in-process annealed at 1144°K (1600°F). Lesser cracking in comparison to forgings 9, 10, and 11 is attributed to in-process annealing. (Dye penetrant inspection used to accentuate cracks).

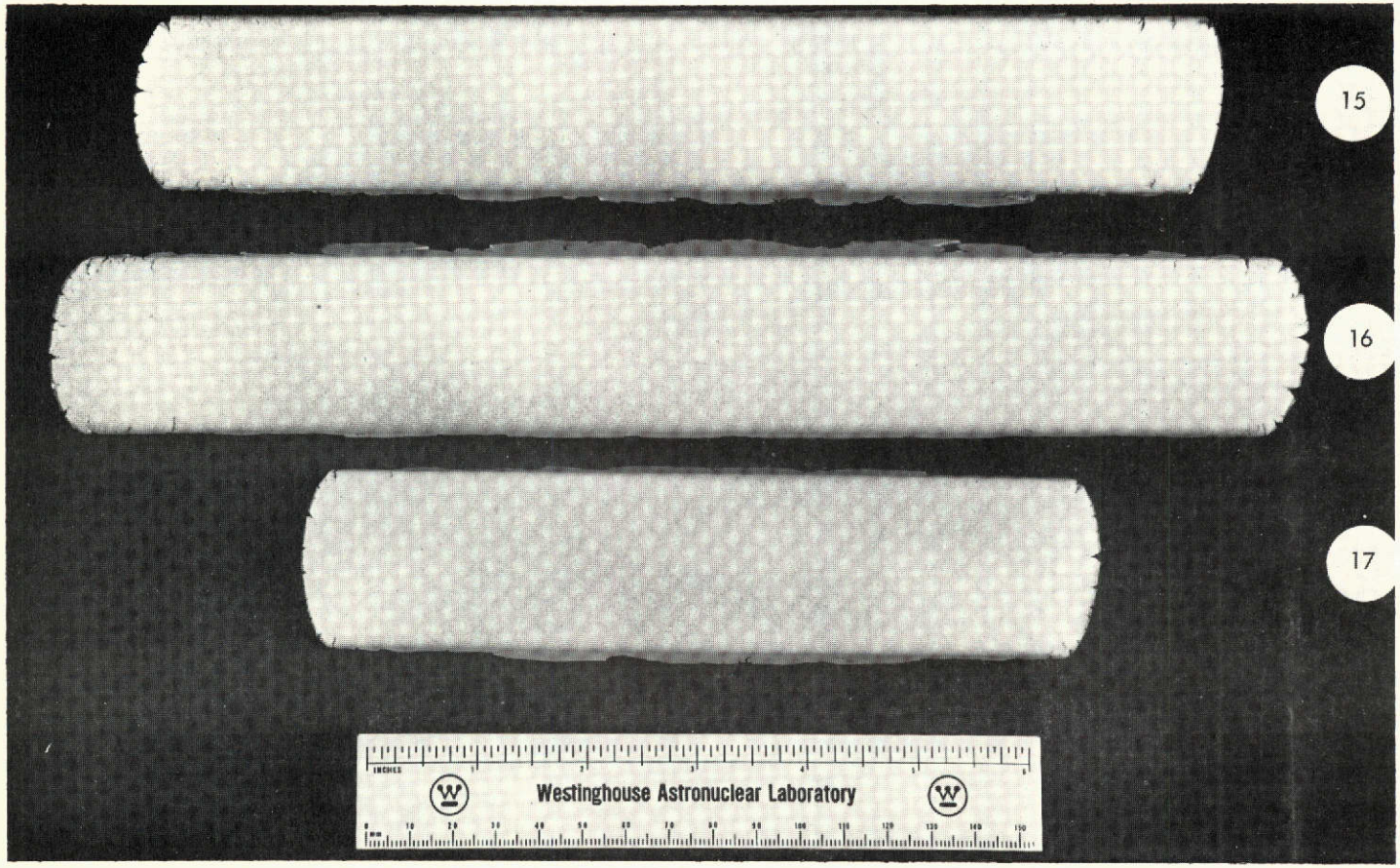

Figure E-1, Part (c). Forgings 15, 16, and 17.
These were secondary forged at 1144°K (1600°F). Lesser cracking in comparison to forgings 9 to 14 is attributed to use of a higher forging temperature. The quality of these forgings typifies the wide majority of those prepared on the program. (Dye penetrant used to accentuate cracks).

Because X_2 was present in the experiment at three levels, coefficients could be estimated for terms of both first and second degree in this variable. The actual combinations of variables investigated are shown by Table E-11. In general, two factor and some higher order interaction coefficients could be estimated. One exception concerns X_3 and X_5. Only one level of X_5 was investigated at the upper level of X_3 so that neither the two factor coefficient for these variables nor any higher order interaction coefficient involving them could be estimated. Similar remarks apply to the combination of X_5 and X_7 where only the lower level of X_7 was investigated at the lower level of X_5. A careful study of the levels of the independent variables actually present in the experiment as shown in Table E-11, suggested that the following model could be fitted to the data:

$$
\begin{aligned}
Y = {} & \beta_0 + \beta_1 X_2 + \beta_2 X_3 + \beta_3 X_5 + \beta_4 X_6 \\
& + \beta_5 X_7 + \beta_6 X_2^2 + \beta_7 X_2 X_3 + \beta_8 X_2 X_5 \\
& + \beta_9 X_2 X_6 + \beta_{10} X_2 X_7 + \beta_{11} X_3 X_6 \\
& + \beta_{12} X_3 X_7 + \beta_{13} X_5 X_6 + \beta_{14} X_6 X_7 \\
& + \beta_{15} X_2 X_3 X_6 + \beta_{16} X_2 X_3 X_7 + \beta_{17} X_2 X_5 X_6 \\
& + \beta_{18} X_2 X_6 X_7 + \beta_{19} X_3 X_6 X_7 + \beta_{20} X_2^2 X_3 \\
& + \beta_{21} X_2^2 X_5 + \beta_{22} X_2^2 X_6 + \beta_{23} X_2^2 X_7 \\
& + \beta_{24} X_2 X_3 X_6 X_7
\end{aligned}
\qquad (6)
$$

Table E-10. Independent Variables - Second Forging Experiment

Independent Variable	Natural Units		Design Units	
Number of Primary Reductions	Z_2	2	X_2	-1
		4		0
		6		1
Secondary Forging Temperature	Z_3	1200°F	X_3	-1
		1600°F		1
In-Process Annealing Temperature	Z_5	1200°F	X_5	-1
		1600°F		1
Final Annealing Condition	Z_6	No treatment	X_6	-1
		1/2 hr., 2400°F		1
Test Temperature	Z_7	2000°F	X_7	-1
		2100°F		1

Table E-11. Data in Statistical Form - Second Forging Experiment

X_2	X_3	X_5	X_6	X_7	Y	Forging No.	Test Temp. (°F)
-1	-1	-1	-1	-1	3.08	9	2000
-1	-1	1	-1	-1	7.47	12	2000
-1	-1	1	1	-1	6.22	12	2000
-1	-1	1	1	1	6.57	12	2100
-1	1	1	-1	-1	8.76	15	2000
-1	1	1	-1	1	7.73	15	2100
-1	1	1	1	-1	9.92	15	2000
-1	1	1	1	1	7.50	15	2100
0	-1	-1	-1	-1	4.62	10	2000
0	-1	-1	1	-1	4.86	10	2000
0	-1	1	-1	-1	7.66	13	2000
0	-1	1	-1	1	5.24	13	2100
0	-1	1	1	-1	7.08	13	2000
0	-1	1	1	1	4.73	13	2100
0	1	1	-1	-1	12.10	16	2000
0	1	1	-1	1	9.16	16	2100
0	1	1	1	-1	9.38	16	2000
0	1	1	1	1	7.17	16	2100
1	-1	-1	-1	-1	4.97	11	2000
1	-1	-1	1	-1	4.99	11	2000
1	-1	1	-1	-1	8.22	14	2000
1	-1	1	-1	1	6.07	14	2100
1	-1	1	1	-1	7.83	14	2000
1	-1	1	1	1	5.68	14	2100
1	1	1	-1	-1	8.40	17	2000
1	1	1	-1	1	9.47	17	2100
1	1	1	1	-1	8.20	17	2000
1	1	1	1	1	8.95	17	2100

The experiment was planned for 36 conditions;but eight were not achieved, so only 28 conditions were available for estimating the 25 coefficients of equation (6). The data were fitted by the model of equation (6) using the NEWRAP procedure of Reference 5 in which the mean squares for rejected coefficients are pooled into the residual variance, which, in turn, is used as the estimate of the error mean square. The nominal confidence level used was 0.900. The significant terms of equation (6) were as follows:

$$
\begin{aligned}
Y = {} & 6.343 \\
& + 1.597 X_3 \\
& + 1.446 X_5 \\
& - 0.386 X_6 \\
& - 1.280 X_7 \\
& - 0.284 X_5 X_6 \\
& + 0.632 X_2 X_3 X_7 \\
& - 0.737 X_2^2 X_3 \\
& + 0.475 X_2^2 X_6 \\
& + 0.949 X_2^2 X_7
\end{aligned}
\qquad (7)
$$

Equation (7) shows an absence of the first degree term in X_2, the number of primary forging steps. The second degree term in X_2 is present but not as the pure term X_2^2. Instead, it is coupled with X_3, X_6, and X_7. This implies that there exists a maximum or a minimum on X_2, depending on the values of X_3, X_6, and X_7.

The large positive coefficient of X_3 (the secondary forging temperature) suggests that its upper level ($X_3 = 1$) would be preferred. The same statement applies to X_5, the in-process annealing temperature. The first degree coefficient of X_6 (the final annealing condition) was of the same order of magnitude as some of the interaction terms containing X_6. This would imply that the effect of X_6 is very much dependent upon the levels of the other variables. The first degree effect of X_7 (the test temperature) is quite large, as would be expected.

At the lower test temperature, $X_7 = -1$, equation (7) specializes to:

$$\begin{aligned} Y &= 7.623 \\ &- 0.949 X_2^2 \\ &+ 1.597 X_3 \\ &+ 1.446 X_5 \\ &- 0.386 X_6 \\ &- 0.632 X_2 X_3 \\ &- 0.737 X_2^2 X_3 \\ &+ 0.475 X_2^2 X_6 \\ &- 0.284 X_5 X_6 \end{aligned} \qquad (8)$$

The large negative coefficient of X_2^2 suggests that among the test levels, $X_2 = -1$, 0, or 1, the level of zero is preferred. This conclusion becomes doubly applicable in view of (1) the coefficient of X_3, which is large and positive, suggesting the level of $X_3 = 1$ would be favored, and (2) the interaction $X_2^2 X_3$ is negative for $X_3 = 1$, but setting $X_2 = 0$ would nullify this term. Using the preferred values of $X_2 = 0$ and $X_3 = 1$, equation 8 reduces to:

$$Y = 9.220 + 1.446X_5 - 0.386X_6 - 0.284X_5X_6 \quad (9)$$

The strong positive coefficient of X_5 suggests that it be set at its upper level. In this case, because the coefficients of the remaining terms are negative, X_6 should be set at its lower level.

In summary, the results for lower test temperature of 2000°F indicated that an optimum partitioning of the primary and secondary forging process occurred at four primary reductions at 1800°F followed by 10 secondary reductions at the higher secondary temperature of 1600°F. The higher secondary annealing temperature of 1600°F was generally preferred, but the final annealing condition of 1/2 hour at 2400°F was detrimental.

At the upper test temperature, $X_7 = 1$, equation (7) becomes:

$$Y = 5.063 + 1.597X_3 + 1.446X_5 - 0.386X_6 + 0.949X_2^2 + 0.632X_2X_3 - 0.737X_2^2X_3 + 0.475X_2^2X_6 - 0.284X_5X_6 \quad (10)$$

The large positive coefficients of X_3 and X_5 suggest that they should be set at their upper levels reducing the equation to:

$$\begin{aligned} Y &= 8.106 \\ &+ 0.632\,X_2 \\ &+ 0.212\,X_2^2 \\ &- 0.670\,X_6 \\ &+ 0.475\,X_2^2X_6 \end{aligned} \qquad (11)$$

The experiment was run at the following (X_2, X_6) combinations: (-1, -1), (0, -1), (1, -1), (-1, 1), (0, 1), and (1, 1). Substitution into equation (11) revealed the best combination to be (1, -1), i.e., six primary reductions and no final annealing treatment.

The preferred levels for maximumizing strength at the upper test temperature, which are $X_3 = 1$, $X_5 = 1$, $X_2 = 1$, $X_6 = -1$, correspond to use of the highest secondary forging and in-process annealing temperatures, six step primary forging, and no final annealing treatment. Processing for the development of optimum strength at 2100°F compared to 2000°F differed only in the partitioning of primary and secondary forging steps. Four primary and 10 secondary steps were preferred for 2000°F strength, while 6 and 8 was the optimum partitioning for strength at the higher temperature.

The really significant conclusion obtained from this analysis was that within the bounds of the second forging experiment, an increase of secondary and in-process annealing temperatures improved strength. These observations can be verified by careful examination of the raw data (Tables E-8 and E-9). Such a conclusion on the effect of secondary and in process annealing temperatures leaves unanswered such questions as:

1. Can an increase in strength be achieved by going to primary forging temperatures much higher than those investigated thus far?

2. Can an increase in strength be achieved by going to higher secondary forging temperatures?

3. If the primary forging temperature is to be higher than the secondary forging temperature, what is an ideal partitioning of the amount of reduction at each temperature?

The investigation thus far has been concerned with the optimization of strength as a function of process variables without regard to how the forging cost would vary with these variables. An important cost factor is the number of steps, which can be reduced by going to large step sizes. Successful forging at large step sizes might depend upon the temperature and thus any investigation of low cost forging practices should be coupled with an extensive investigation of temperature effects. These considerations suggest the question:

4. What is the effect of step size and what are the interactions between step size and the temperature variables discussed in the previous three questions?

The preceding four interrelated questions call for the design and performance of a factorial experiment as will be described in the next section.

DESCRIPTION AND DATA - THIRD FORGING EXPERIMENT

Twenty-three channel die forgings were produced on this experiment as described in Table E-12. Some assessment of what influence forge piece orientation and prior extrusion have on properties was included in this experiment (Forgings 36-40). The results of 1366°K (2000°F) tensile tests are given in Table E-13.

Table E-12. Processing Conditions - Third Forging Experiment*

Forging No.	Primary Forging Conditions				Secondary Forging Conditions			
	Steps	%R/ Step	Temperature (°K)	Temperature (°F)	Steps	%R/ Step	Temperature (°K)	Temperature (°F)
18	1	39	1577	(2200)	4	39	1577	(2200)
19	1	39	1394	(2050)	4	39	1394	(2050)
20	1	28	1394	(2050)	6	28	1144	(1600)
21	1	28	1394	(2050)	3	48	1144	(1600)
22	1	28	1394	(2050)	6	28	1255	(1800)
23	1	28	1394	(2050)	3	48	1255	(1800)
24	1	28	1255	(1800)	6	28	1144	(1600)
25	1	28	1255	(1800)	3	48	1144	(1600)
26	1	28	1255	(1800)	6	28	1255	(1800)
27	1	28	1255	(1800)	3	48	1255	(1800)
28	1	48	1394	(2050)	6	28	1144	(1600)
29	1	48	1394	(2050)	3	48	1144	(1600)
30	1	48	1394	(2050)	6	28	1255	(1800)
31	1	48	1394	(2050)	3	48	1255	(1800)
32	1	48	1255	(1800)	6	28	1144	(1600)
33	1	48	1255	(1800)	3	48	1144	(1600)
34	1	48	1255	(1800)	6	28	1255	(1800)
35	1	48	1255	(1800)	3	48	1255	(1800)
36	1	39	1325	(1925)	4	39	1200	(1700)
37	1	39	1325	(1925)	4	39	1200	(1700)
38	1	39	1325	(1925)	4	39	1200	(1700)
39	1	39	1325	(1925)	4	39	1200	(1700)
40	1	39	1325	(1925)	4	39	1200	(1700)

* Material (Appendix A): Forgings 18-39; preform heat 3115. Forging No. 40, extruded bar heat 3111

Total Reduction: 85-90%.

Forging Direction (Appendix B): Forgings 18-37; parallel to preform forging direction. Forgings 38 & 39; perpendicular to preform forging direction. Forging 40; perpendicular to the extrusion axis. Material placed with the extrusion axis parallel to the length of the channel die.

Forging Operation: Mechanical press

Table E-13. 1366°K (2000°F) Tensile Data - Third Forging Experiment

Forging No.	Condition	Ultimate Strength		0.2% Yield Strength		Elongation (%)
		MN/m^2	(ksi)	MN/m^2	(ksi)	
18	As-forged	13.8	(1.99)	7.8	(1.13)	42.4
	Annealed*	106.5	(15.20)	106.5	(15.20)	3.0
19	As-forged	14.8	(2.13)	9.2	(1.33)	40.2
	Annealed	102.0	(14.70)	102.0	(14.70)	3.0
20	As-forged	60.4	(8.71)	59.1	(8.52)	4.6
	Annealed	60.3	(8.70)	57.7	(8.31)	4.5
21	As-forged	55.4	(7.99)	54.5	(7.86)	4.5
	Annealed	56.6	(8.17)	54.4	(7.85)	4.5
22	As-forged	109.5	(15.80)	109.5	(15.80)	1.5
	Annealed	118.5	(17.10)	118.5	(17.10)	3.0
23	As-forged	102.0	(14.70)	99.1	(14.30)	3.7
	Annealed	114.4	(16.50)	113.7	(16.40)	2.3
24	As-forged	70.0	(10.10)	70.0	(10.10)	1.4
	Annealed	68.2	(9.85)	66.9	(9.65)	5.3
25	As-forged	63.5	(9.16)	62.6	(9.02)	4.4
	Annealed	69.0	(9.97)	68.6	(9.90)	2.3
26	As-forged	122.0	(17.60)	122.0	(17.60)	1.4
	Annealed	111.7	(16.10)	111.7	(16.10)	3.8
27	As-forged	89.4	(12.90)	89.4	(12.90)	1.5
	Annealed	116.4	(16.80)	116.4	(16.80)	2.3
28	As-forged	61.7	(8.78)	61.7	(8.78)	5.0
	Annealed	73.5	(10.60)	-	-	3.0
29	As-forged	61.6	(8.77)	61.6	(8.77)	2.8
	Annealed	59.6	(8.60)	59.6	(8.15)	4.6
30	As-forged	111.0	(16.00)	111.0	(16.00)	2.2
	Annealed	95.7	(13.80)	95.7	(13.80)	2.3
31	As-forged	102.0	(14.70)	101.0	(14.60)	2.2
	Annealed	102.0	(14.70)	102.0	(14.70)	2.3
32	As-forged	71.4	(10.30)	67.0	(9.68)	5.3
	Annealed	66.9	(9.66)	64.5	(9.30)	4.5
33	As-forged	76.2	(11.00)	75.6	(10.90)	5.3
	Annealed	72.1	(10.40)	71.4	(10.30)	3.8
34	As-forged	112.2	(16.20)	112.2	(16.20)	2.3
	Annealed	102.0	(14.70)	102.0	(14.70)	1.5
35	As-forged	101.0	(14.60)	101.0	(14.60)	2.3
	Annealed	83.1	(13.00)	83.1	(13.00)	3.0
36	As-forged	80.5	(11.60)	80.5	(11.60)	3.8
	Annealed	73.5	(10.60)	73.5	(10.60)	6.0
37	As-forged	85.1	(12.30)	85.1	(12.30)	3.0
	Annealed	89.5	(12.90)	89.5	(12.90)	3.8
38	As-forged	64.3	(9.28)	63.1	(9.10)	3.0
	Annealed	53.3	(7.69)	51.6	(7.44)	3.8
39	As-forged	73.5	(10.60)	65.4	(9.43)	2.2
	Annealed	71.4	(10.30)	71.4	(10.30)	1.5
40	As-forged	70.0	(10.10)	68.4	(9.88)	3.0
	Annealed	88.8	(12.80)	84.6	(12.20)	4.5

* Annealing Conditions: 3600 seconds at 1616°K (1 hour at 2450°F)

Of the forgings prepared, those numbered 20 through 37 comprised the statistical portion of the experiment. Forgings 18 and 19 were prepared using conditions suggested by the results of microstructural examinations made on material forged on the first and second experiments, which uncovered a correlation between grain size and strength and suggested that very high forging temperatures be investigated. Forgings 18 and 19 were simply fabricated at the highest practical temperatures using five equal reductions. Very similar fabrication was concluded after additional statistical work to be adequate for achieving superior strength in forged material. (Superior strength is developed by combining high temperature forging and final annealing.)

STATISTICAL ANALYSIS - THIRD FORGING EXPERIMENT - DR. A. HOLMS, NASA-LEWIS RESEARCH CENTER

The statistical portion of the third forging experiment was a two-level on five variable investigation. The matching of independent variables is shown in Table E-14. The model ordinarily fitted to this experiment is:

$$
\begin{aligned}
Y = {} & \beta_0 + \beta_1 X_1 + \beta_2 X_2 + \beta_3 X_3 + \beta_4 X_4 + \beta_5 X_6 \\
& + \beta_6 X_1 X_2 + \beta_7 X_1 X_3 + \beta_8 X_1 X_4 + \beta_9 X_1 X_6 \\
& + \beta_{10} X_2 X_3 + \beta_{11} X_2 X_4 + \beta_{12} X_2 X_6 \\
& + \beta_{13} X_3 X_4 + \beta_{14} X_3 X_6 \\
& + \beta_{15} X_4 X_6
\end{aligned}
$$

Table E-14. Independent Variables - Third Forging Experiment

Independent Variable	Natural Units		Design Units	
Primary Forging Temperature	Z_1	1800°F	X_1	-1
		1925°F		0
		2050°F		1
Primary Step Reduction	Z_2	28%	X_2	-1
		39%		0
		48%		1
Secondary Forging Temperature	Z_3	1600°F	X_3	-1
		1700°F		0
		1800°F		1
Secondary Step Reduction	Z_4	28%	X_4	-1
		39%		0
		48%		1
Final Annealing Condition	Z_6	None	X_6	-1
		1 hr., 2450°F		1

$$
\begin{aligned}
&+\beta_{16}X_1X_2X_3 + \beta_{17}X_1X_2X_4 + \beta_{18}X_1X_2X_6 \\
&+\beta_{19}X_1X_3X_4 + \beta_{20}X_1X_3X_6 + \beta_{21}X_1X_4X_6 \\
&+\beta_{22}X_2X_3X_4 + \beta_{23}X_2X_3X_6 + \beta_{24}X_2X_4X_6 \\
&+\beta_{25}X_3X_4X_6 + \beta_{26}X_1X_2X_3X_4 + \beta_{27}X_1X_2X_3X_6 \\
&+\beta_{28}X_1X_2X_4X_6 + \beta_{29}X_1X_3X_4X_6 \\
&+\beta_{30}X_2X_3X_4X_6 + \beta_{31}X_1X_2X_3X_4X_6
\end{aligned}
\tag{12}
$$

The fitted equation using the NEWRAP program[4] with coefficients listed in the order of their absolute magnitudes is:

$$
\begin{aligned}
Y = \; & 12.316 \\
& + 2.951\,X_3 \\
& - 0.477\,X_2X_3 \\
& - 0.376\,X_4 \\
& + 0.360\,X_1X_3 \\
& - 0.348\,X_2X_6 \\
& - 0.328\,X_2X_3X_6 \\
& + 0.284\,X_1X_3X_4 \\
& - 0.273\,X_1 \\
& + 0.272\,X_3X_4X_6 \\
& + 0.261\,X_1X_2X_3X_4X_6 \\
& + 0.228\,X_4X_6 \\
& - 0.219\,X_2X_4X_6 \\
& - 0.211\,X_3X_4 \\
& + 0.189\,X_1X_2X_4X_6
\end{aligned}
\tag{13}
$$

If the data from the center point forgings (forgings 36 and 37) are omitted, the model given by equation (12) can also be fitted by the methods of references 3 and 4. Such a procedure was followed using the ordering of the data shown in Table E-15. The consequence was that the 15 largest absolute value coefficients were decided to be significant. In the order of the absolute values of these coefficients, the fitted equation is:

$$
\begin{aligned}
Y = \; & 12.374 \\
& + 2.951 X_3 \\
& - 0.477 X_2X_3 \\
& - 0.376 X_4 \\
& + 0.360 X_1X_3 \\
& - 0.348 X_2X_6 \\
& - 0.328 X_2X_3X_6 \\
& + 0.284 X_1X_3X_4 \\
& - 0.273 X_1 \\
& + 0.272 X_3X_4X_6 \\
& + 0.261 X_1X_2X_3X_4X_6 \\
& + 0.228 X_4X_6 \\
& - 0.219 X_2X_4X_6 \\
& - 0.211 X_3X_4 \\
& + 0.189 X_1X_2X_4X_6 \\
& - 0.172 X_1X_4X_6
\end{aligned}
\qquad (14)
$$

The term $-0.172 X_1X_4X_6$ was found in equation (14) and not (13); but except for this, the two relationships were identical.

The variable X_3, secondary forging temperature, is most potent in equation (13). Setting $X_3 = 1$ yields:

Table E-15. Data in Yates' Order - Third Forging Experiment

$$X_1 = X_{E'}\ X_2 = X_{D'}\ X_3 = X_{C'}\ X_4 = X_{B'}\ X_6 = X_A$$

Forging No.	Treatment	Strength (ksi)	Forging No.	Treatment	Strength (ksi)
24	(1)	10.10	20	e	8.71
24	a	9.85	20	a e	8.70
25	b	9.16	21	b e	7.99
25	a b	9.97	21	a b e	8.17
26	c	17.60	22	c e	15.80
26	a c	16.10	22	a c e	17.10
27	b c	12.90	23	b c e	14.70
27	a b c	16.80	23	a b c e	16.50
32	d	10.30	28	d e	8.78
32	a d	9.66	28	a d e	10.60
33	b d	11.00	29	b d e	8.77
33	a b d	10.40	29	a b d e	8.60
34	c d	16.20	30	c d e	16.00
34	a c d	14.70	30	a c d e	13.80
35	b c d	14.60	31	b c d e	14.70
35	a b c d	13.00	31	a b c d e	14.70

$$
\begin{aligned}
Y = \; & 15.325 \\
& - 0.477 X_2 \\
& - 0.585 X_4 \\
& + 0.087 X_1 \\
& - 0.676 X_2 X_6 \\
& + 0.284 X_1 X_4 \\
& + 0.500 X_4 X_6 \\
& + 0.450 X_1 X_2 X_4 X_6 \\
& - 0.219 X_2 X_4 X_6
\end{aligned}
\qquad (16)
$$

Equation (16) was specialized to the upper secondary forging temperature of 1800°F. Conspicuously large terms revealed by this were: $-0.676 X_2 X_6$, $-0.585 X_4$, $0.500 X_4 X_6$, and $-0.477 X_2$. The first degree terms in X_4 and X_2 indicated they should be used at their lower levels, but the preferred level of X_6 was less clear. Because the coefficient of the first degree term of X_4 is numerically larger than that of X_2, the next step was to set $X_4 = -1$.

With the size of the secondary forging step set at the lower level, $X_4 = -1$, equation (16) reduces to:

$$
\begin{aligned}
Y = \; & 15.910 \\
& - 0.477 X_2 \\
& - 0.197 X_1 \\
& - 0.457 X_2 X_6 \\
& - 0.500 X_6 \\
& - 0.450 X_1 X_2 X_6
\end{aligned}
\qquad (17)
$$

In equation (17), the largest coefficient is that of the first degree term in X_6. For $X_6 = -1$, no final annealing treatment, equation (17) reduces to:

$$Y = 16.410 - 0.020X_2 - 0.197X_1 + 0.450X_1X_2 \quad . \quad (18)$$

Equation (18) indicates that X_1 and X_2 should both be set at -1. This corresponds to the primary forging conditions of 1800°F and 28% reduction.

The preferred levels of the independent variables, approximately in order of their relative importance, are:

Secondary Forging Temperature	1800°F
Secondary Forging Step Size	28%
Final Annealing Condition	None
Primary Forging Temperature	1800°F
Primary Forging Step Size	28%

Of the five variables examined, increasing the secondary forging temperature caused an overwhelmingly large improvement in strength. This was apparent in the sign and magnitude of the coefficient of this variable, X_3, in equations (13) and (14). It can be verified simply by examination of the raw data (Tables E-12 and E-13), which will consistently reveal higher strength for material secondary forged at the highest temperature investigated, 1800°F. Because of this, still higher forging temperatures were investigated on the fourth experiment. Also, since the influence of primary forging temperature on strength was small, it was eliminated as a variable. Experiment 4 investigated a 1800 to 2050°F forging temperature range, and a 16 to 28% range of forging reductions. Forging reductions at and below the minimum level examined on the third experiment were chosen. The basis for this was the statistical conclusion obtained from the third experiment, namely, that forging reductions in the range of 39 to 48% might be too large.

REMARKS ON STRATEGIES OF FIRST THREE FORGING EXPERIMENTS - DR. A. HOLMS, NASA-LEWIS RESEARCH CENTER

The individual tensile values are each subject to random experimental errors (such as material variability, processing variability, and testing variability), and are, therefore, by themselves not suitable measures of the progress that has been made in an optimum seeking investigation. Predicted values, from the model equations, are less subject to such errors, and will, therefore, be used as the basis of the following discussion.

The predicted value for the mid-point (design center) of the experimental space is given by the constant term of the model equation because that point is the point for which all of the x-values are zero.

THE OUTPUT OF THE NEWRAP program contains predicted values for each of the points of the experiment as computed from the final model equation (the equation with insignificant terms deleted). From such outputs, the maximum values for each experiment were noted.

Forging Experiment	Condition	Equation	Ultimate Tensile, ksi 2000°F
First	Design center	2.a	7.008
	Maximum	5	9.203
Second	Design center	8	7.623
	Maximum	7	11.336
Third	Design center	13	12.316
	Maximum	13	17.021

The preceding tabulation illustrates the fact that the strategy of alternate performance of small designed experiments and mathematical modeling of the results assures that steady progress will be made.

DESCRIPTION AND DATA - FOURTH FORGING EXPERIMENT

Eleven forgings were prepared on this experiment as described in Table E-16. Assessments of how forged properties are influenced by prior extrusion (forgings 42, 45, 48, and 51), and by Dynapak forging and piece orientation (forgings 44, 50, and 51), were included in this experiment. The results of 1366°K (2000°F) tensile tests are given in Table E-17.

STRESS-RUPTURE EVALUATION - SELECTED THIRD AND FOURTH EXPERIMENT FORGINGS

A few selected forgings prepared on the third and fourth experiments were tested to evaluate stress-rupture properties at 1366°K (2000°F). Selection was made to test material ranging in 1366°K tensile strength from 69.4 to 128.1 MN/m^2 (test material ranging in 2000°F tensile strength from 10 to 18.5 ksi). The results of stress-rupture tests are summarized in Table E-18. All evaluated material was annealed at 1616°K for 3600 seconds prior to testing (annealed at 2450°F for 1 hour).

GRAIN SIZE EVALUATION - SELECTED FORGINGS

Metallographic examination was made to define the grain size of selected material forged on the first four experiments. The entire ranges of high temperature tensile strength observed for as-forged and annealed material were represented in the sample selection. Grain dimensions were measured in the three orthogonal longitudinal, long transverse, and short transverse directions.

Grain size data are reported in Table E-19. The samples examined are identified by forging number, condition, and 1366°K (2000°F) tensile strength. Data for the starting materials and calculated average grain diameters and aspect ratios are included in the table. The method of grain size measurement is described in Appendix D.

Table E-16. Processing Conditions - Fourth Forging Experiment*

Forging No.	Forging Conditions			
	Steps	%R/Step	Temperature (°K)	Temperature (°F)
41	7	28	1255	(1800)
42	7	28	1255	(1800)
43	7	28	1283	(1850)
44	9	22	1311	(1900)
45	9	22	1311	(1900)
46	9	22	1339	(1950)
47	13	16	1366	(2000)
48	13	16	1366	(2000)
49	13	16	1394	(2050)
50	9	22	1311	(1900)
51	9	22	1311	(1900)

* Material (Appendix A): Forgings 41, 43, 44, 46, 47, 49, and 50; preform heat 3115. Forgings 42, 45, 48, and 51; extruded bar heat 3111.

Total Reduction: 85-90%

Forging Direction (Appendix B): Forgings 41, 43, 44, 46, 47, 49, and 50; parallel to the preform forging direction. Forgings 42, 45, and 48; perpendicular to the extrusion axis. Material placed with the extrusion axis parallel to the length of the channel die.

Forging 51; perpendicular to the extrusion axis. Material placed with the extrusion axis perpendicular to the length of the channel die.

Forging Operation: Forgings 41 to 49; mechanical press
Forgings 50 and 51; Dynapak

Table E-17. 1366°K (2000°F) Tensile Data - Fourth Forging Experiment

Forging No.	Condition	Ultimate Strength		0.2% Yield Strength		Elongation
		MN/m^2	(ksi)	MN/m^2	(ksi)	(%)
41	As-forged	79.9	(11.50)	76.3	(11.0)	3.0
41	Annealed*	84.0	(12.10)	84.0	(12.10)	4.6
42	As-forged	88.9	(12.80)	73.6	(10.60)	6.9
42	Annealed	77.8	(11.20)	71.5	(10.30)	6.2
43	As-forged	18.3	(2.64)	13.1	(1.88)	19.2
43	Annealed	111.7	(16.10)	109.5	(15.80)	3.0
44	As-forged	64.4	(9.28)	64.4	(9.28)	3.8
44	Annealed	106.5	(15.40)	106.5	(15.40)	3.0
45	As-forged	80.5	(11.60)	64.0	(9.22)	5.4
45	Annealed	72.9	(10.50)	72.9	(10.50)	2.3
46	As-forged	17.6	(2.54)	11.4	(1.65)	43.8
46	Annealed	114.4	(16.50)	114.4	(16.50)	3.0
47	As-forged	19.8	(2.86)	15.8	(2.28)	23.0
47	Annealed	128.1	(18.50)	119.1	(17.20)	5.4
48	As-forged	15.9	(2.29)	13.2	(1.90)	26.2
48	Annealed	113.0	(16.30)	106.8	(15.40)	10.0
49	As-forged	13.4	(1.93)	8.9	(1.28)	36.2
49	Annealed	113.0	(16.30)	109.5	(15.80)	9.2
50	As-forged	81.1	(11.70)	64.8	(9.32)	6.2
50	Annealed	89.5	(12.90)	78.5	(11.30)	6.2
51	As-forged	71.5	(10.30)	64.4	(9.28)	5.4
51	Annealed	78.5	(11.30)	72.2	(10.40)	6.2

* Annealing conditions: 3600 seconds at 1616°K (1 hour at 2450°F)

Table E-18. 1366°K (2000°F) Stress-Rupture Data* - Thermomechanical Studies

Forging No.	Stress MN/m^2	Stress (ksi)	Rupture Time (hours)**	Elongation (%)
18	48.5	7.0	453.4	***
18	55.4	8.0	41.6	***
22	48.5	7.0	28.7	***
22	34.7	5.0	596.0	
	to	to	+	
	43.6	6.3	240.0	
	to	to	+	
	48.5	7.0	73.3	***
24	48.5	7.0	0.07	***
24	41.6	6.0	0.23	3.1
26	48.5	7.0	20.8	***
26	43.6	6.3	95.0	***
27	48.5	7.0	0.85	***
27	41.6	6.0	24.9	1.0
37	48.5	7.0	0.08	***
37	31.2	4.5	1.4	1.7
44	48.5	7.0	1.7	0.7
44	45.0	6.5	6.3	0.6
46	69.3	10.0	0.51	1.1
46	62.4	9.0	5.9	***
46	55.4	8.0	5.8	***
46	48.5	7.0	159.3	0.5
47	48.5	7.0	334.6	
	to	to	+	
	69.3	10.0	94.9	***
47	55.4	8.0	215.3	
	to	to	+	
	72.8	10.5	35.0	***
47	65.9	9.5	155.8	1.9
49	52.0	7.5	282.5	
	to	to	+	
	62.4	9.0	277.1	***
49	76.2	11.0	0.03	***
49	69.3	10.0	0.50	2.2

* Specimens annealed 1 hour at 1616°K (2450°F).

** On tests involving stress changes, rupture time is the value given for the highest stress level. The time periods over which these tests were held at lower stresses are also reported.

*** These specimens could not be suitably reassembled to allow measurement of rupture elongation.

Table E-19. Grain Size Data - Selected Forgings

Forging No.	Sample Condition	1366°K (2000°F) T.S.		Avg. Grain Dimensions*, μm			Avg. Grain Dia., μm	Grain Aspect Ratios	
		MN/m^2	(ksi)	$\bar{L}$	$\bar{T}$	$\bar{t}$	$d=(\frac{6}{\pi}\bar{L}\bar{T}\bar{t})^{1/3}$	$\bar{L}/\bar{T}$	$\bar{T}/\bar{t}$
Preform	Tensile tested**	18.6	(2.68)	1.4	1.1	-	1.6***	(L/T = 1.3)	-
1	Forged	65.7	(9.48)	8.7	6.4	4.2	7.6	2.1	1.5
4	+	57.1	(8.23)	9.1	7.1	5.1	8.6	1.8	1.4
5	Tensile**	50.9	(7.32)	8.5	6.8	5.9	8.7	1.4	1.2
10	Tested	32.0	(4.62)	3.1	4.7	2.0	3.8	1.5	2.4
18	"	13.8	(1.99)	1.4	1.2	0.9	1.4	1.6	1.3
22	"	109.5	(15.80)	231	182	83.8	189	2.7	2.2
24	"	70.0	(10.10)	14.8	7.6	6.9	11.3	2.1	1.1
37	"	85.1	(12.30)	30.5	23.8	16.6	28.6	1.8	1.4
40	"	70.0	(10.10)	18.8	7.9	8.8	11.0	2.1	0.9
46	"	17.6	(2.54)	1.1	1.1	0.7	1.2	1.6	1.6
48	"	15.8	(2.27)	1.1	0.9	1.1	1.3	1.0	0.8
49	"	13.4	(1.93)	1.5	1.7	0.8	1.3	1.9	2.1
Extruded bar	Annealed+	-	(18.9)	3000	1200	-	2000++	(L/T = 2.5)	-
1	Forged	50.8	(7.31)	10.3	6.7	5.2	8.8	2.0	1.3
4	+	69.0	(9.97)	13.5	5.5	7.4	10.2	1.8	0.7
5	Annealed+	47.4	(6.83)	8.2	4.8	5.0	7.2	1.6	1.0
10	"	33.7	(4.83)	6.7	4.8	3.7	6.1	1.8	1.3
18	"	105.4	(15.20)	2950	1410	660	1724	4.5	2.1
22	"	118.5	(17.10)	210	101	103	161	2.0	1.0
24	"	68.2	(9.85)	14.0	9.1	6.9	11.9	2.0	1.3
26	"	111.7	(16.10)	219	103	75.5	148	2.8	1.4
37	"	89.2	(12.90)	14.2	11.7	8.9	14.2	1.6	1.3
40	"	88.8	(12.80)	10.9	5.1	10.2	10.3	1.1	0.5
46	"	114.3	(16.50)	1265	945	316	898	4.0	3.0
47	"	128.1	(18.50)	1620	990	1040	1470	1.6	1.0
48	"	113.0	(16.30)	1520	880	642	1180	2.4	1.4
49	"	113.0	(16.30)	1160	718	533	945	2.2	1.3

* $\bar{L}$, $\bar{T}$, $\bar{t}$; average grain dimensions in the longitudinal, long transverse, and short transverse directions. (Refer to Appendix D.)

** Tensile tested at 1366°K (2000°F).

*** $\bar{d}=(\frac{6}{\pi}\bar{L}\bar{L}\bar{T})^{1/3}$ Mutually orthogonal directions are L, L, T for preform material. (See Appendix B.)

\+ Annealed at 1589 - 1644°K (2400-2500°F).

++ $d=(\frac{6}{\pi}\bar{L}\bar{T}\bar{T})^{1/3}$ Mutually orthogonal directions are L, T, T for extruded bar stock. (See Appendix B.)

EVALUATION OF OPTIMUM FORGED MATERIAL

Data gathered on the first four experiments demonstrated, unequivocally, that the high temperature strength of forged TDNiCr depends largely upon forging temperature and final heat treat condition. Material displaying the best combination of elevated temperature tensile and stress rupture strength was produced by forging in the temperature range of 1255 to 1577°K (1800 to 2200°F) followed by annealing at ~1616°K (~2450°F). In this condition, forged TDNiCr closely approached or surpassed optimally rolled sheet in elevated temperature strength. As a result, a more thorough investigation of the properties of optimally forged TDNiCr was made.

Seventeen channel die forgings were prepared to thoroughly evaluate optimally forged material. A summary of the processing conditions used is given in Table E-20. Further assessments of how forged properties are influenced by prior extrusion, forge piece orientation, and Dynapak forging were also included in this experiment (forgings 52-55).

The "optimum forging temperature" was chosen as 1366°K (2000°F). This is simply the midpoint of the forging temperature range which produced material of superior elevated temperature strength*. Forging involved seven steps each of nominally 28%, accomplishing a total reduction of 85 to 90%. Material prepared on the prior four experiments, which displayed good high temperature strength, was produced using anywhere from 5 to 14 forging steps. Use of seven forging steps for "optimum processing" simply represented a compromise toward the more practical lower extreme of this range.

The results of tests run to assess how prior fabrication history, forge piece orientation, and forging methods influence the tensile and stress-rupture behavior of optimally forged material are reported in Tables E-21 and E-22. Data defining the temperature dependency of the tensile properties of optimally forged preform stock are presented in Table E-23. Optimally forged preform stock was also tested to determine the temperature dependency of stress-rupture properties, and evaluated by electron microscopy to measure the distribution of ThO_2 particles. These data are summarized in Tables E-24 and E-25.

* Superior strength after high temperature annealing.

Table E-20. Processing Conditions Used for Optimum Forging

Forging No.	Starting Material*	Forging Material**	Optimized Forging Conditions		
			Steps	%R/ Step	Temperature
52 - 54	Bar Heat 3111	Mechanical Press			
55	Preform Heat 3116	Dynapak	7	28	1366°K (2000°F)
56 - 68		Mechanical Press		***	

* Appendix A.

** Forging Direction: (Appendix B)
Forgings 52 & 53; perpendicular to the extrusion axis. Material placed with the extrusion axis perpendicular to the length of the channel die.

Forging 54; perpendicular to the extrusion axis. Material placed with the extrusion axis parallel to the length of the channel die.

Forgings 55 - 68; parallel to the perform forging direction.

*** 85 - 90% total forging reduction.

Table E-21. 1366°K (2000°F) Tensile Properties* - Optimum Forged Bar and Preform Stocks

Forging No.	Starting Material	Forging Method	Forging** Direction	Ultimate Strength		0.2% Yield Strength		Elongation
				MN/m^2	(ksi)	MN/m^2	(ksi)	%
53	Extruded Bar	Mechanical Press	⊥ , ⊥	105.3	(15.2)	94.1	(13.6)	0.9
54			⊥ , II	128.1	(18.5)	114.2	(16.5)	7.5
55	Preform	Dynapak	II	92.9	(13.4)	80.4	(11.6)	4.0
56		Mechanical Press	II	113.0	(16.3)	113.0	(16.3)	2.2

* Samples annealed 3600 seconds at 1616°K (1 hour at 2450°F).

** ⊥ , ⊥ Forging direction perpendicular to the extrusion axis. Material placed with the extrusion axis perpendicular to the length of the the channel die.

⊥ , II Forging direction perpendicular to the extrusion axis. Material placed with the extrusion axis parallel to the length of the channel die.

II Forging direction parallel to the preform forging direction.

Table E-22. 1366°K (2000°F) Stress-Rupture Properties* - Optimum Forged Bar and Preform Stocks

Forging No.	Starting Material	Forging Method	Forging** Direction	Stress MN/m^2	Rupture Time (ks)	Stress (ksi)	Rupture Time (hours)	Elongation %
52	Extruded Bar	Mechanical Press	⊥,⊥	41.6 to 48.5	504 + 130	6.0 to 7.0	140.0 + 36.0	- 3.6
52				55.4	1.8	8.0	0.5	1.1
53				48.5	36.0	7.0	10.0	1.3
53				45.0	84.0	6.5	23.3	1.5
54	Extruded Bar	Mechanical Press	⊥, II	48.5	>550+	7.0	>153+	***
				62.4	380	9.0	105.5	***
				69.2	225	10.0	62.4	3.2
				71.2	25.2	11.0	7.0	***
55	Preform	Dynapak	II	48.5	3.2	7.0	0.9	1.2
				41.6	30.2	6.0	8.4	2.0
				38.1	60.8	5.5	16.9	***
				38.1	9.0	5.5	2.5	***
62	Preform	Mechanical Press	II	48.5	522	7.0	140.5	1.9
				52.0	655	7.5	182.0	1.4
				55.4	19.8	8.0	5.5	1.8
				55.4	69.0	8.0	19.1	1.1
				59.0	0.7	8.5	0.2	1.5

* Samples annealed 3600 seconds at 1616°K (1 hour at 2450°F).

** ⊥,⊥ Forging direction perpendicular to the extrusion axis. Material placed with the extrusion axis perpendicular to the length of the channel die.

⊥, II Forging direction perpendicular to the extrusion axis. Material placed with the extrusion axis parallel to the length of the channel die.

II Forging direction parallel to the preform forging direction.

*** These specimens could not be suitably reassembled to permit measurement of elongation.

\+ Test terminated due to a temperature excursion and melting resulting from control thermocouple failure.

Table E-23. Temperature Dependency of Tensile Properties - Optimum Forged Preform Stock

Forging No.*	Condition**	Test Temperature (°K)	Test Temperature (°F)	Ultimate Strength MN/m^2	Ultimate Strength (ksi)	0.2% Yield Strength MN/m^2	0.2% Yield Strength (ksi)	Elongation (%)
56	As-f	R. T.	(R. T.)	1080	(155.6)	979	(141.5)	9.1
56	A			880	(126.9)	525	(75.8)	17.5
57	As-f	364	(200)	1045	(150.2)	965	(139.7)	8.8
57	A			854	(122.6)	508	(73.2)	18.0
58	As-f	476	(400)	920	(142.3)	899	(129.7)	7.4
58	A			795	(114.2)	459	(66.2)	14.6
59	As-f	588	(600)	980	(140.7)	828	(119.2)	7.2
59	A			799	(115.1)	539	(77.8)	14.0
60	As-f	700	(800)	888	(127.9)	805	(116.0)	5.9
60	A			758	(109.2)	414	(59.7)	15.8
61	As-f	811	(1000)	725	(104.4)	667	(96.1)	3.8
61	A			662	(95.7)	384	(55.3)	17.6
62	As-f	922	(1200)	152	(22.5)	121	(17.5)	29.0
62	A			455	(65.6)	323	(46.6)	9.6
63	As-f	1033	(1400)	60.2	(8.7)	55.4	(8.0)	53.7
63	A			278	(40.1)	269	(38.9)	4.8
64	As-f	1144	(1600)	40.9	(5.9)	34.0	(4.9)	33.3
64	A			192	(27.7)	181	(26.0)	4.7
65	As-f	1255	(1800)	27.0	(3.9)	23.6	(3.4)	36.3
65	A			146	(21.0)	142	(20.6)	2.8
58	As-f	1366	(2000)	19.4	(2.8)	16.0	(2.3)	44.0
56	A			113	(16.3)	113	(16.3)	2.2
57	A	1477	(2200)	81.0	(11.7)	-	-	0.1

* All of these forgings were fabricated from the same starting material in an identical manner. Forging numbers were assigned to test specimens so that any forging, which might differ significantly in mechanical properties from the others, could be identified.

** As-f - As-forged. A - Annealed 3600 seconds at 1616°K (1 hour at 2450°F).

Table E-24. Temperature Dependency of Stress-Rupture Properties* - Optimum Forged Perform Stock

Forging No.	Test Temperature (°K)	Test Temperature (°F)	Stress MN/m^2	Rupture Time (ks)	Stress (ksi)	Rupture Time (hours)	Elongation %
65	1033	(1400)	243	0.07	35.0	0.02	**
65			208	0.29	30.0	0.08	2.1
65			174	5.1	25.0	1.4	2.9
61			156	1.44	22.5	0.4	1.3
61			152	53.7	22.0	14.9	2.7
61			149	217	20.0	60.3	1.8
60	1255	(1800)	83.0	16.9	12.0	4.7	0.7
63			83.0	3.6	12.0	1.0	0.9
60			76.1	124	11.0	34.5	1.4
63			76.1	13.0	11.0	3.6	0.9
60			69.2	2550	10.0	709.3	1.2
57			73.0	270	10.5	74.9	1.6
57			86.8	0.04	12.5	0.01	**
62	1366	(2000)	48.5	522	7.0	140.5	1.9
62			52.0	655	7.5	182.0	1.4
62			55.4	19.8	8.0	5.5	1.8
62			55.4	69.0	8.0	19.1	1.1
60			59.0	0.7	8.5	0.2	1.5
64	1489	(2200)	48.5	0.4	7.0	0.1	1.3
64			41.6	2.5	6.0	0.7	1.0
64			34.7	0.7	5.0	0.2	**
64			27.7	64.5	4.0	17.9	**
65			24.3	332	3.5	92.1	**
65			20.8	227	3.0	63.3	1.1

* Samples annealed 3600 seconds at 1616°K (1 hour at 2450°F).

** Specimen could not be suitable reassembled to measure elongation.

Table E-25. Particle Size Distribution in Optimally Forged TDNiCr*

Diameter Range $m \times 10^{10}$ (Angstoms)	Number of Particles
0 - 50	94
50 - 100	256
100 - 150	287
150 - 200	178
200 - 250	86
250 - 300	36
300 - 350	17
350 - 400	10
400 - 450	6
450 - 500	6
500 - 550	5
550 - 600	3
600 - 650	3
650 - 700	3
700 - 750	4
750 - 800	1
800 - 850	1
850 - 900	2
900 - 950	1
950 - 1000	3
1000 - 1050	0
1050 - 1100	0
1100 - 1150	2
1150 - 1200	0
1200 - 1250	1
1250 - 1300	1
1300 - 1350	0
1350 - 1400	2
1750 - 1800	1
2350 - 2400	1
TOTAL	1010

* Preform forging stock

EVALUATION OF OPTIMUM FORGED AND SHOCK TREATED MATERIAL

Preform stock channel die forged to plate and annealed to optimize high temperature strength was shock treated then examined to evaluate what influence this would have on mechanical properties. The material used for the experiment was taken from channel die forgings 66 through 68. Forging conditions are reported in Table E-20. The shock treatment experiment is summarized in Figure E-2. Results of hardness, tensile, and stress-rupture evaluations of the shock treated material are given in Tables E-26 and E-27.

TURBINE VANE FORGING

This experiment was intended to qualitatively judge the feasibility of forging turbine parts from TDNiCr. It involved forging an inlet guide compressor vane normally produced from a stainless steel. The part chosen is made by Kelsey-Hayes Company of Utica, New York. Fabrication from TDNiCr involved the same die setups and reductions used for stainless steel forging. Forging stock, 1.27 cm diameter rod (1/2 inch diameter), was prepared by swaging extruded bar at 1366°K (2000°F).

The sequence of forging operations involved is illustrated in Figure E-3. (TDNiCr parts are shown at the various forging stages.) Forging was done at 1339 - 1366°K (1950 - 2000°F). Each upset was accomplished using five blows, but the two subsequent forging operations were each single blow steps. Slight cracking occurred during upset forging, but the manufacturer felt minor die modifications could have eliminated it. A total of five vanes were forged with the results generally concluded to indicate it would be feasible to produce similar turbine parts by forging TDNiCr.

Tensile and stress-rupture properties were evaluated for vane forged material at 1366°K (2000°F). These data are reported in Table E-28. The high temperature strength of these forgings fell far short of the best level achieved on channel die forged material.

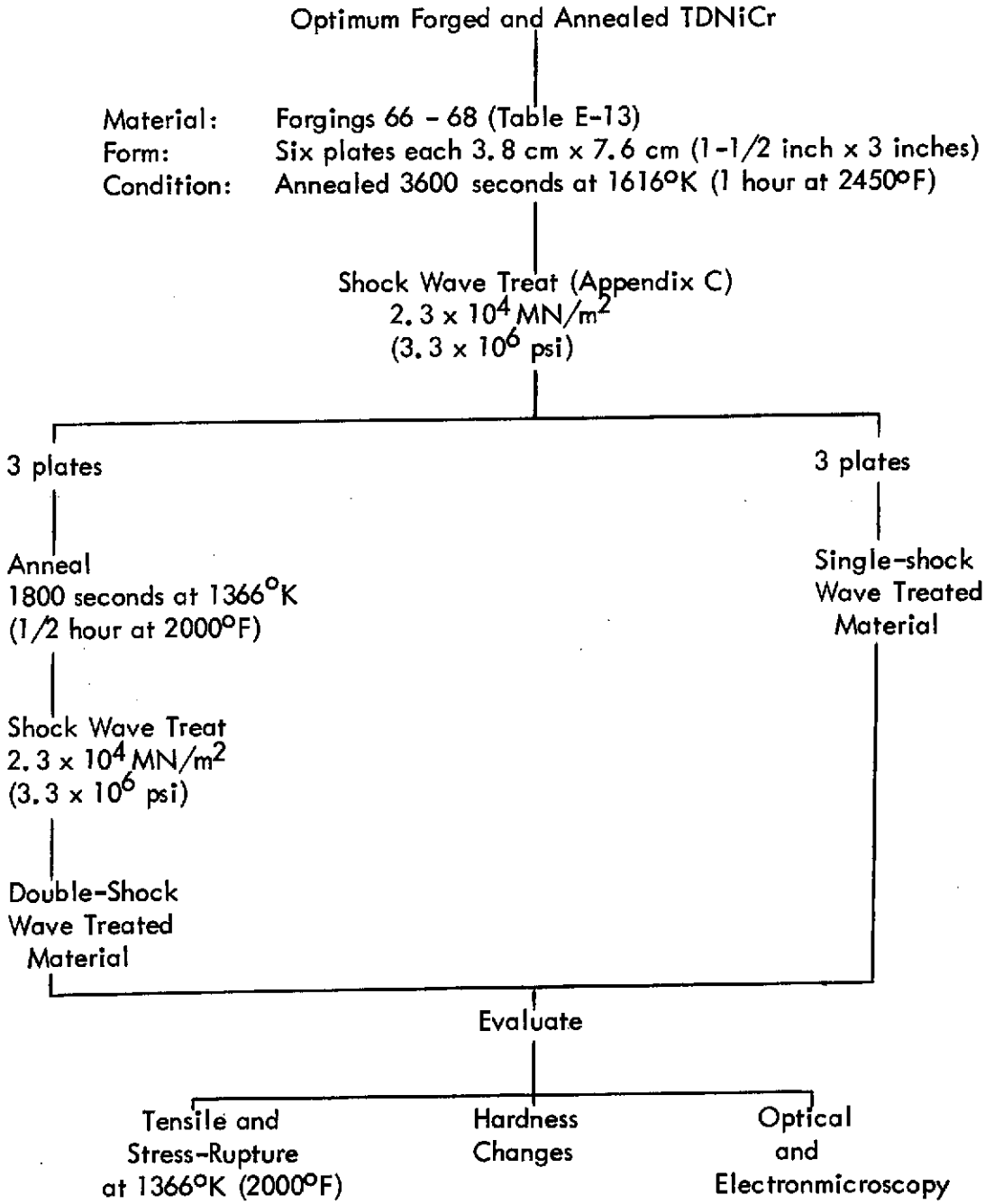

Figure E-2. A Summary of the Shock Treatment Experiment

Table E-26. Hardness and 1366°K (2000°F) Tensile Properties - Shock Treated Material

Material Condition	Δ Hardness* Δ DPH	Ultimate Strength		0.2% Yield Strength		Elongation
		MN/m^2	(ksi)	MN/m^2	(ksi)	%
Single-shock treated	285 to 396	125.5	(18.1)	125.5	(18.1)	0.0
Double-shock treated	285 to 388	117.0	(16.9)	117.0	(16.9)	0.0

* Hardness of the forged plus 1 hour 1616°K (2450°F) annealed material was 285 DPH. Hardness prior to annealing was 365 DPH.

Table E-27. 1366°K (2000°F) Stress-Rupture Properties - Shock Treated Material

Material Condition	Stress MN/m^2	Rupture Time (ks)	Stress (ksi)	Rupture Time (hours)	Elongation %
Single-shock treated	62.3	292	9.0	81.0	1.3
	59.0	28.1	8.5	7.8	1.0
Double-shock treated	48.5	84.2	7.0	23.4	1.5
	52.0	53.0	7.5	14.7	1.3
	55.4	24.8	8.0	6.9	1.6

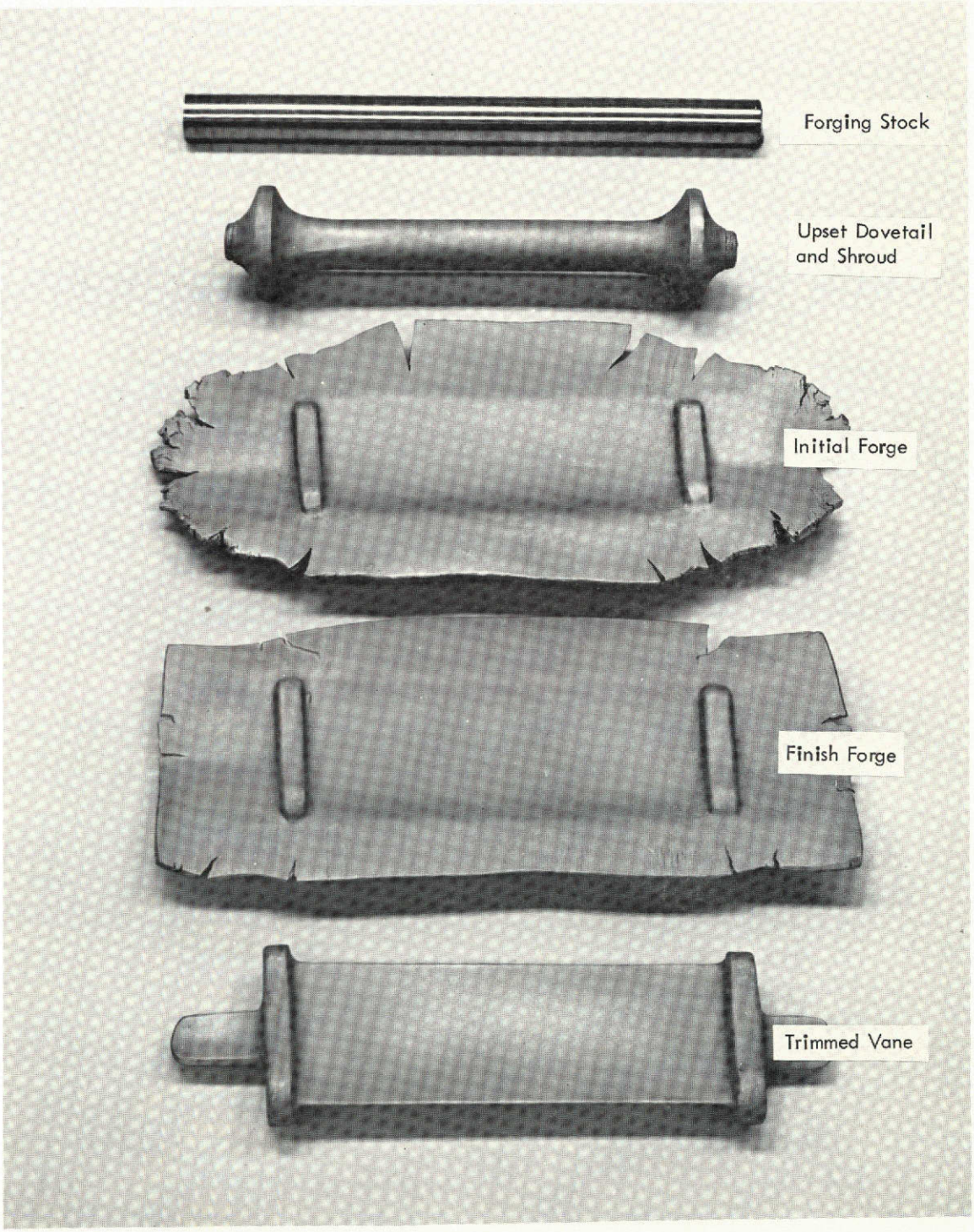

Figure E-3. Turbine Vane Forging Stages.
1X TDNiCr parts are shown for each forging stage.

Table E-28. 1366°K (2000°F) Tensile and Rupture Properties* - Turbine Vanes

Ultimate Strength		Yield Strength		Rupture Stress		Rupture Time		Elongation
MN/m^2	(ksi)	MN/m^2	(ksi)	MN/m^2	(ksi)	ks	(hrs.)	%
88.0	(12.7)	86.8	(12.5)	-	-	-	-	1.5
-	-	-	-	34.7	(5.0)	21.3	(5.9)	1.7
-	-	-	-	41.6	(6.0)	42.5	(11.8)	1.4

* Material annealed 3600 seconds at 1616°K (1 hour at 2450°F)

APPENDIX F

AN EXPERIMENT RELATING MICROSTRUCTURE TO FORGING HISTORY

INTRODUCTION AND SUMMARY

TDNiCr coupons were forged on this study at 1200, 1311, and 1422°K (1700, 1900, and 2100°F). Reductions up to 85% were covered. Macro and microstructures were examined for as-forged material and for material subsequently annealed at 1450, 1533, and 1616°K (2150, 2300, and 2450°F). Microstructures ranging from extremely fine to grossly coarse were produced by the spectrum of conditions examined. Grain sizes spanned from very nearly suboptical to ~500 μm. The results displayed conclusively that increasing the forging reduction and annealing temperature favored development of coarse grain microstructures. Evidence was also obtained to indicate extremely coarse TDNiCr microstructures of ~200 to 500 μm grain size are developed by secondary recrystallization.

EXPERIMENTAL APPROACH

Separate sets of TDNiCr coupons machined from preform stock were upset forged at 1200, 1311, and 1420°K (1700, 1900, and 2100°F). A typical set of coupons is shown in Figure F-1. Four coupons were cylinders, and the other was a very flat truncated cone. Each was forged to approximately 0.50 cm (.20 in.) thick discs. A continuous range of reduction from maximum at the center to essentially zero at the edge was obtained by forging the truncated cone. This coupon was used to cover the low range of reductions for material forged at 1311 and 1420°K (1900 and 2100°F). The cylinders were employed to span reductions from ~50 to 85% in increments of 10 to 15%. Only the four cylindrical coupons were forged at 1200°K (1700°F), and the reduction range from 15 to 75% was covered. Reported forging reductions are accurate to within ± 5%.

The coupons were heated at temperature for 1 hour in an air furnace. They were placed on large Inconel plates used to transfer them to the forge to minimize loss of temperature. Also in an effort to minimize cooling, three very small nichrome tabs were welded in a tripod pattern onto the bottom of each coupon preventing the surface from contacting the cold

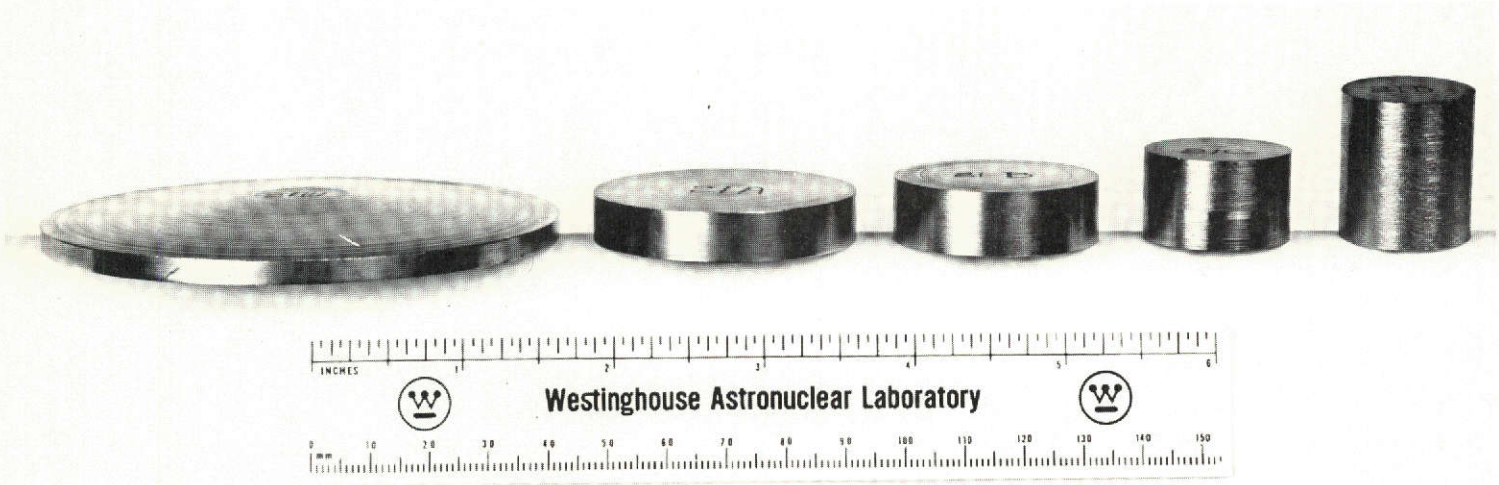

Figure F-1. A Set of Forging Coupons

forge platten. Lubrication was provided by coating the forge plattens with an oil-graphite suspension and the coupons with a glass compound. These coatings also serve as insulating barriers. In spite of the precautions taken, some heat loss must occur from the time a coupon is taken out of the furnace to the forging impact; approximately 10 seconds elapse during this period. This unavoidable heat loss was anticipated to be in the neighborhood of 56°K (100°F); and to compensate for it, furnace temperatures were set by this amount above the reported forging temperatures. Forging temperatures are conservatively estimated to be accurate within ± 23°K (± 50°F). Each coupon was upset forged on a model 1220C Dynapak in one blow.

A summary of the procedures used to fabricate, sample, and examine a forged disc is presented in Figure F-2. Four samples of "pie wedge" configuration were removed from each disc by sawing along radial directions. These were used to characterize macro and microstructures in the as-forged condition and after one hour anneals at 1450, 1533, and 1616°K (2150, 2300, and 2450°F). Note that examination was made on a radial plane.

RESULTS AND DISCUSSION

Macrostructure

All samples were first examined in a macroetched condition. A uniform grain appearance was obtained for material in the as-forged state, but grossly heterogeneous grain conditions were uncovered in several samples given large reductions prior to annealing. A typically observed heterogeneous grain condition is displayed in Figure F-3. Note that a central band of coarse grains formed in that region of the sample nearest the original center of the forged disk. This band spread into two forks at approximately mid-radius. By comparison, a much finer structure formed in regions near the original surfaces and edge of the forging.

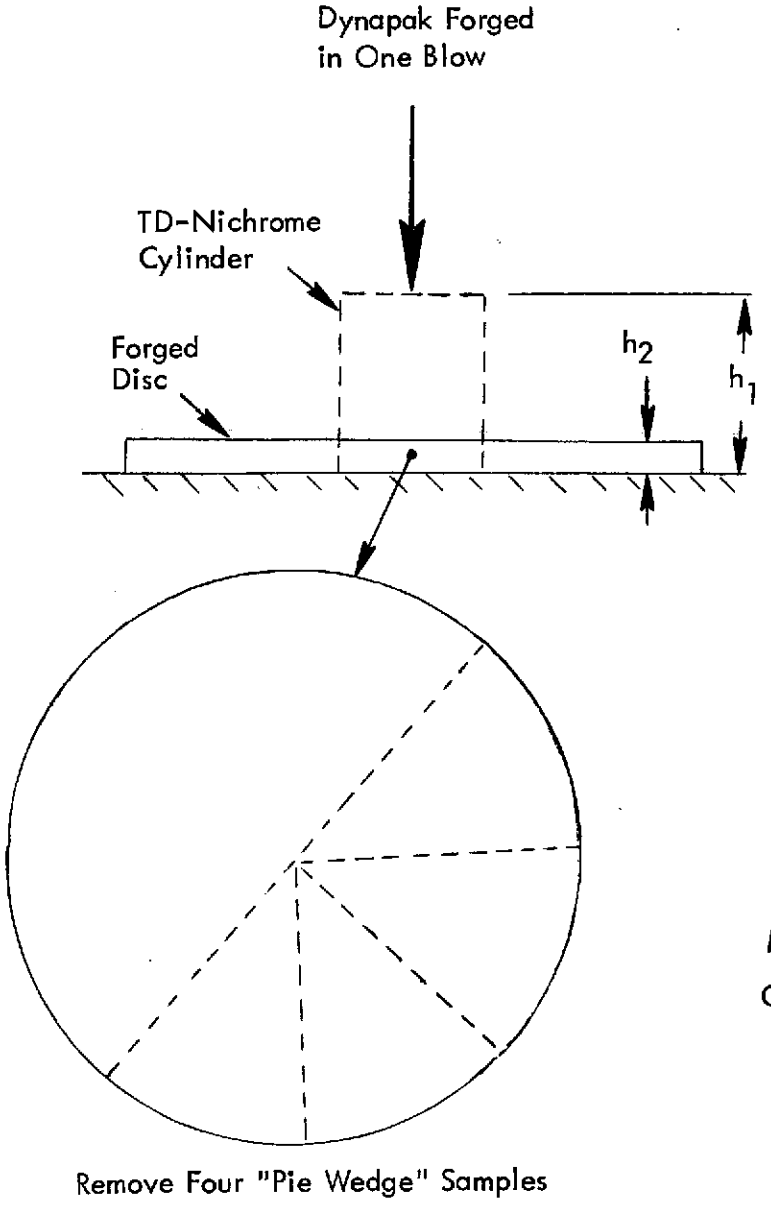

$$\% R = \frac{h_1 - h_2}{h_1} \times 100$$

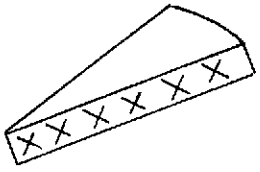

Examine Radial
Macrostructure and Microstructure

Conditions: As-forged
1 hr/1450°K (2150°F)
1 hr/1533°K (2300°F)
1 hr/1616°K (2450°F)

Figure F-2. Experimental Fabrication, Sampling, and Examination Procedures

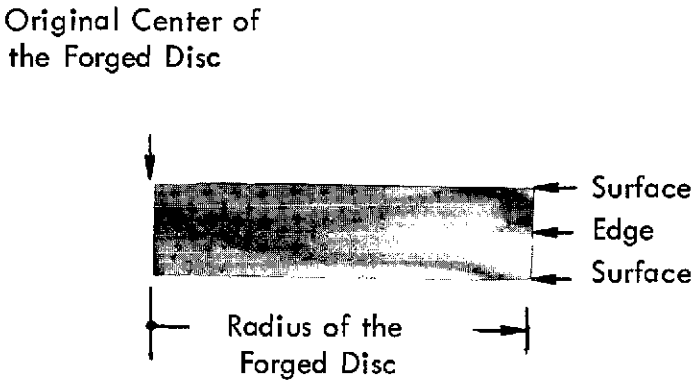

Figure F-3. The Radial Macrostructure of a Typical Heterogeneous Grain Sample. 2X. The material received a nominal forging reduction of 75% and was annealed for 1 hour at 1616°K (2450°F).

The upset forging procedure used on the experiment is believed responsible for development of the heterogeneous grain conditions. If during this process lubrication is not perfect, the frictional constraint placed on top and bottom surfaces of the forging billet causes nonuniform deformation. A schematic representation of this effect[6] is presented in Figure F-4. Deformation is uniform throughout the cross section of a billet upset forged under conditions of ideal lubrication; part (a), Figure F-4. In real cases, however, perfect lubrication is not achieved, and the resulting restraint can cause surface and edge regions to undergo little deformation while a reduction greater than nominal is produced in the central area; part (b).

Radial sections of material forged under conditions of high surface friction are shown in part (c), Figure F-4. The regions of high and low deformation match, respectively, the coarse and fine grain areas noted in heterogeneous grain material; compare the schematics given in part (c) with the macrostructure shown in Figure 3. This is taken as evidence that formation of heterogeneous grain structures is a consequence of nonuniform deformation resulting from surface friction present during upset forging.

The relationship $\frac{h_1 - h_2}{h_1 - h_\gamma}$ gives the approximate reduction obtained in the central region of material upset forged under conditions of high surface restraint (h_1 and h_2 are the original and final forging heights, and γ is the thickness of the slightly deformed surface regions). A calculation based upon this relationship for the sample whose macrostructure is shown in Figure F-3 revealed that the actual deformation obtained in the central portion was close to 90% as opposed to the nominal 75% level.

Microstructure

Microstructural and diffraction characteristics of the TDNiCr perform forging stock were presented in Figure A-1. The material displayed longitudinal and transverse grain dimensions of 1.4 and 1.1 μm (Table E-9). Continuous Debye rings obtained on a Laue' back reflection diffraction pattern confirmed its fine grain size, and separation of the rings into Ka_1 and Ka_2 doublets indicated a stress relieved condition. Room temperature hardness of the material was a rather high 365 Vickers, probably a reflection of its extremely fine grain state.

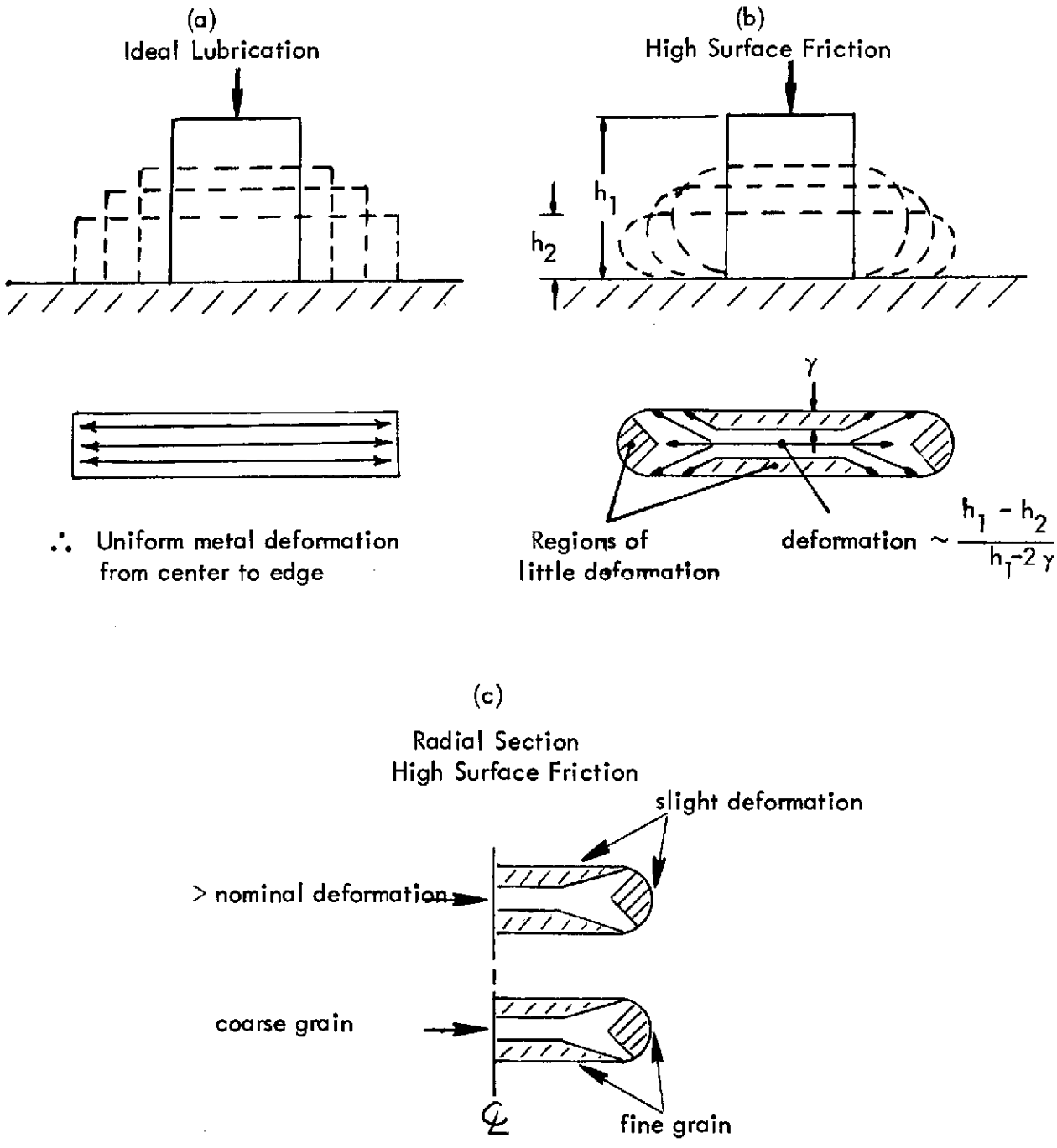

Figure F-4. The Influence of Friction on Metal Deformation and Macrostructure
Friction causes little deformation in surface and edge regions while the central area receives a reduction greater than nominal; part (b). Regions of high and low deformation match coarse and fine grain areas found in some samples, part (c).

Microstructures of forged and annealed material ranged from extremely fine to grossly coarse grained but could be separated into a few categories. A duplex grain condition composed one of these categories and was most frequently observed. One grain constituent of this microstructure type was 1.3 μm or smaller in size. The other displayed a single grain size falling in the range of approximately 5 to 20 μm.

Typical duplex grain microstructures are displayed in Figure F-5. The microstructure shown in part (a) of the figure was observed in material forged 60% at 1311°K (1900°F). The very fine grain constituent is not resolved in the photomicrograph and appears dark. This constituent, classified as type A, had an appearance and grain size identical to that of the starting material in some samples. In others, it displayed a smaller grain size, and frequently, grain features could not be resolved*.

The second constituent in the duplex microstructure shown in part (a) of Figure F-5 was composed of distinct grains of white appearance which average ~5 μm in size. This constituent is classified as type B. The size of B grains observed in A + B duplex microstructures spanned from ~5 to 20 μm.

Heat treatment had the effect of increasing the B grain proportion in many samples which displayed the A + B microstructure as-forged. This is exemplified by the other microstructures shown in Figure F-5. The B grain proportion in material forged 60% at 1311°K (1900°F) is only approximately 10%, part (a) Figure F-5. Heat treatment for one hour at 1450°K (2150°F)and 1616°K (2450°F) increased the amount of B grain to roughly 50 and 90%; parts (b) and (c), Figure F-6. Note also the associated decrease in hardness with increased B grain proportion. This was a general observation made on material which underwent a change in dominant microstructural feature from the A to the B constituent.

---

* Grain features indistinct at 1500 magnification.

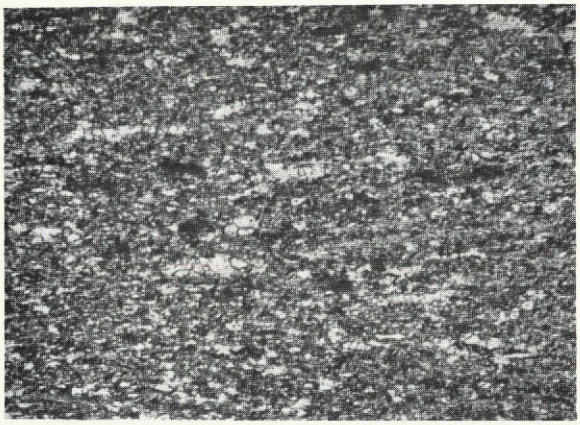

(a)

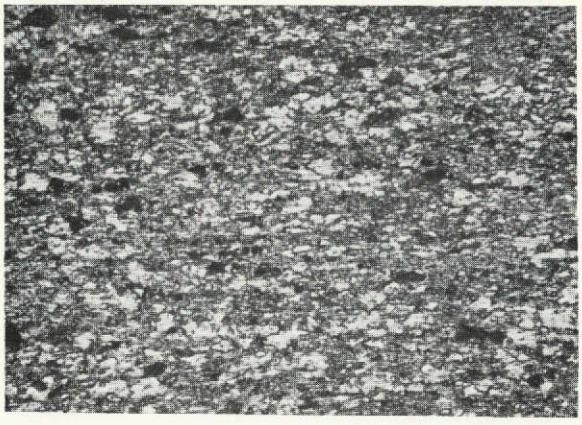

(b)

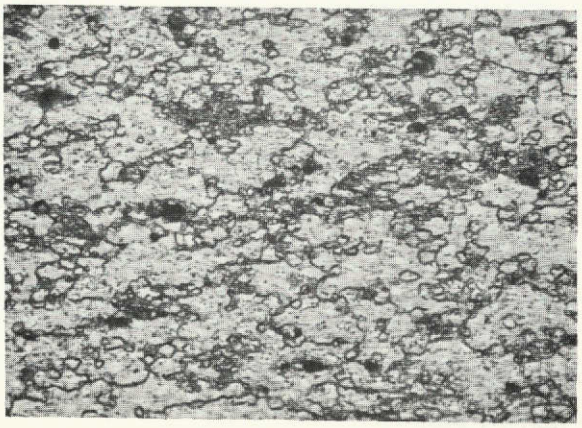

(c)

Figure F-5. Typical Duplex Grain Microstructures, 500X. (a) forged 60% at 1311°K (1900°F), 368 Vickers hardness, the type A grain constituent (dark) occupies 90% of the microstructure; (b) a+1 hour at 1450°K (2150°F), 349 hardness, B grains (light) and the A constituent each occupy 50% of the microstructure; (c) a+1 hour at 1616°K (2450°F), 278 hardness, 90% of the microstructure is composed of type B grains. (Black spots are voids which once contained Cr_2O_3 particles.)

Annealing in some instances caused microstructural changes beyond A-to-B grain transition. Microstructures of grain size averaging greater than 20 μm, classified as type C, were formed in these cases.

Type C microstructures displayed a very broad grain size range. Grains 20 to 50 μm in size composed the microstructure of samples in which structural change had proceeded only slightly beyond the point at which B grain formation eliminated the A constituent. Where structural change proceeded far beyond A-to-B grain transition, type C microstructures dominated by 200 to 500 μm grains were developed. Because of this, type C microstructures will be subdivided into two categories, C_1 for the initially formed 20 to 50 μm structure, and C_2 for the grossly coarse grain condition. Grain characteristics of the various TDNiCr microstructures observed are summarized in Table F-1.

Heterogeneous grain samples displayed the A + B and C_1 or C_2 microstructures. Examples of these conditions are shown in Figure F-6. Material forged 75% at 1200°K (1700°F) then annealed at 1533°K (2300°F) developed a type C_1 microstructure in the severely deformed central portion of the sample, and the A + B condition in the lesser deformed areas, part (a) Figure F-6. Microstructure types C_2 and A + B developed in correspondingly similar locations in material forged 75% at 1311°K (1900°F) then annealed at 1533°K (2300°F), part (b), Figure F-6.

Microstructures formed as a function of forging and annealing conditions are summarized in Table F-2. Predominent microstructure or grain types arbitrarily defined as occupying 70% or more of a sample are underlined. Two microstructures are reported for samples displaying a heterogeneous grain condition.

Table F-1. Observed Microstructural Characteristics

Microstructure	Grain Condition	Grain Size Range*
A	Uniform	Unresolved** to 1.3 μm
A + B	Duplex	A as above B 5 to 20 μm
C_1	Mixed	20 to 50 μm
C_2	Mixed	200 to 500 μm

* Microstructures were generally slightly elongated, and grain sizes are an average of length and width dimensions. Reported grain sizes are estimated to be accurate within ± 50%.

** Grain features indistinguishable by optical microscopy at 1500X.

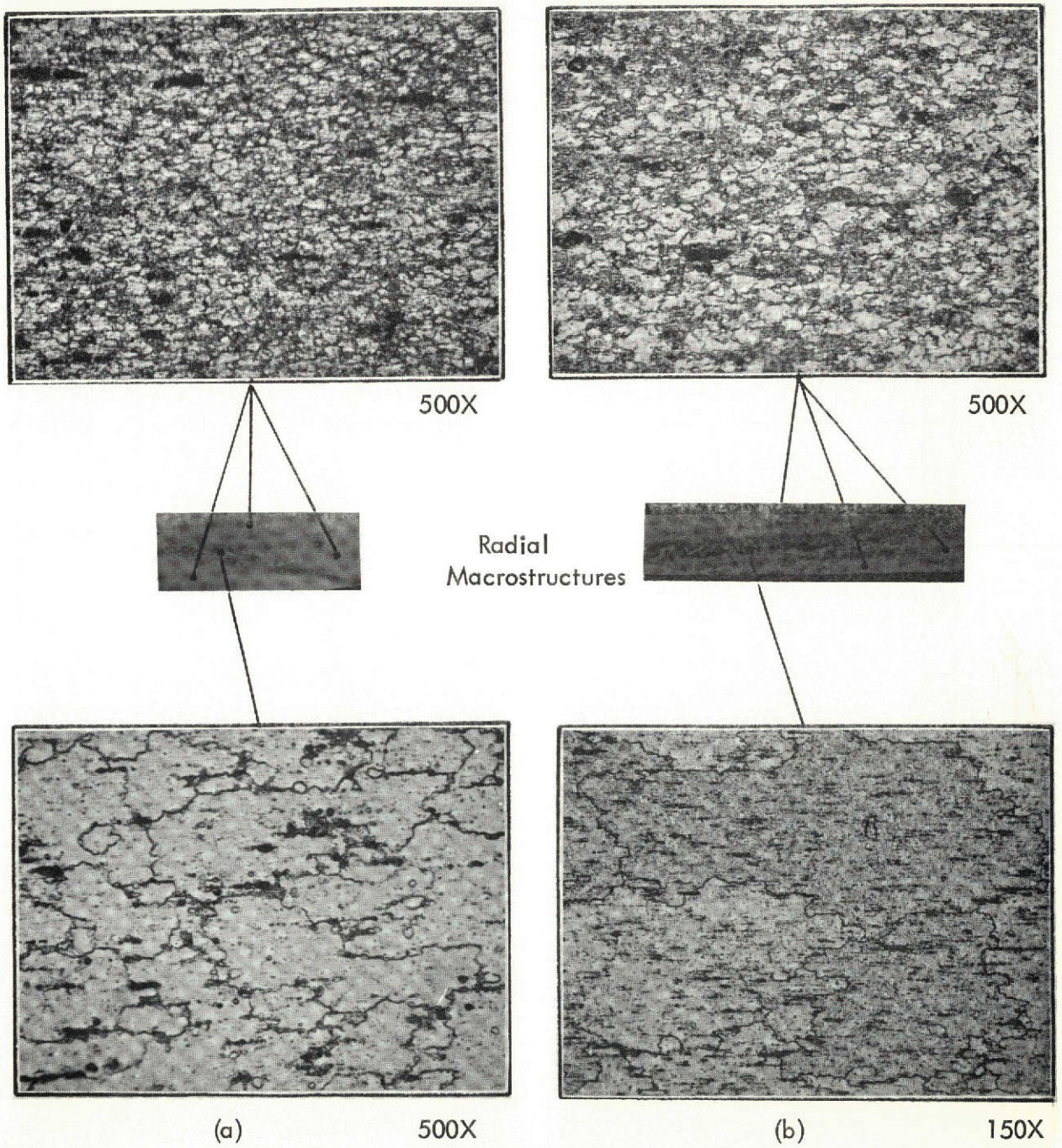

Figure F-6. The Microstructures of Two Heterogeneous Grain Samples. The macrostructures are oriented as shown in Figure F-3. (a) forged 75% at 1200°K (1700°F) and annealed 1 hour at 1533°K (2300°F), microstructural change in the severely deformed central region progressed slightly beyond the A-to-B grain transition developing a type C_1 structure; (b) the extremely coarse type C_2 microstructure formed in the central region. Both samples displayed the A + B microstructure in surface and edge areas.

Table F-2. Relationship of Microstructure to Thermomechanical Condition

Forging Conditions		Annealing Conditions and Microstructures Developed*			
Temp.	Nominal % Red.	As-forged	1 hr. at 2150°F (1450K)	1 hr. at 2300°F (1533K)	1 hr. at 2450°F (1616K)
1700°F (1200K)	15	A	A	A + B	A + B
	25	A + B	A + B	A + B	A + B
	55	A + B	A + B	A + B	A + B
	75	A + B	A + B & C_1	A + B & C_1	A + B & C_1
1900° F (1311K)	15	A	A + B	A + B	A + B
	25	A + B	A + B	A + B	A + B
	40	A + B	A + B	A + B	A + B
	50	A + B	A + B	A + B	A + B
	65	A + B	A + B	A + B	A + B
	75	A + B	A + B	A + B & C_2	A + B & C_2
	84	A + B	A + B & C_2	A + B & C_2	A + B & C_2
2100°F (1422K)	15	A	A + B	A + B	C_1
	25	A + B	A + B	A + B	C_2
	45	A + B	A + B	A + B	C_2
	60	A + B	A + B	A + B	C_2
	70	A + B	A + B	A + B & C_2	A + B & C_2
	84	A + B	A + B	A + B & C_2	A + B & C_2

* Refer to Table A-1 for a description of the microstructure codes.
Constituents occupying 70% or more of a sample are underlined.
Two microstructures are reported for samples displaying a heterogeneous grain condition.

The microstructure of material forged 15% at the three study temperatures was A type and similar in appearance to that of the starting stock. Material given higher reductions displayed the A + B microstructure with the A constituent generally predominant. Grain features in the A constituent of these microstructures became increasingly indistinct* as forging reductions increased, indicating development of a heavily strained condition.

Specimens forged at 1200°K (1700°F) then annealed at the three study temperatures displayed the A + B microstructure or the heterogeneous A + B and C_1 condition. A change in dominant feature in the A + B microstructures from the A to the B constituent generally occurred with increasing annealing temperature.

Annealing at increasingly higher temperatures also promoted an A-to-B grain transition in material forged up to 65% at 1311°K (1900°F). The heterogeneous grain A + B and C_2 condition generally developed in material more severely deformed at this temperature.

The microstructures of samples forged up to 60% at 1422°K (2100°F) changed insignificantly upon subsequent heat treatment at the two lower temperatures. However, the coarse type C microstructures developed in these samples when heat treated at 1616°K (2450°F). Annealing at 1533 and 1616°K (2300 and 2450°F) promoted the heterogeneous grain A + B and C_2 condition in samples forged 70 and 84% at 1422°K (2100°F).

In summary, an increase of annealing temperature generally produced coarser grain conditions. This was represented by an increase of B grain proportion in A + B microstructures and formation of type C microstructures.

---

* Indistinct at 1500 magnification.

Similar grain conditions developed in as-forged material regardless of forging temperature. The influence forging temperature had on the microstructures developed by subsequent annealing was mixed. In some instances, formation of coarse grain conditions (type C microstructures) appears favored by a low forging temperature; compare data for samples annealed at 2150°F (1450°K) after forging 75 to 84%. Formation of coarse grain microstructures appears to be promoted by a high forging temperature in other cases; compare data for material annealed at 2450°F (1616°K).

Data is compared at constant reduction and annealing temperature to evaluate a forging temperature influence. However, the assumption that nominal reduction is an exact measure of deformation may be incorrect in some cases. The possibility that nonuniform deformation occurred during forging resulting in deformation being less than nominal in some locations and greater than this level in others has been pointed out. As a consequence, the actual deformation conditions may differ between samples even though they were given the same nominal reduction making it impossible to conclusively evaluate any forging temperature effect. However, results obtained from studies reported in Appendix E definitely established that development of coarse grain annealed microstructures is promoted by higher forging temperatures.

The influence reduction had on annealed microstructures can be obtained from data on heterogeneous grain samples. This condition developed in material given very high nominal forging reductions prior to annealing. It has been postulated to result from nonuniform deformation and characterized by formation of the A + B microstructure in regions of low deformation and type C grain structures where deformation exceeded the nominal level. It follows that a large amount of deformation must favor the formation of type C (coarse grain) microstructures upon subsequent annealing.

MECHANISMS

The increase of B grain proportion with increasing annealing temperature noted in the A + B grain microstructures of many samples resembles a primary recrystallization process. A decrease in hardness observed as the amount of B grain increased in these microstructures, and the extremely fine grain or highly strained appearance of the A constituent both lend support to the operation of this mechanism. Furthermore, development of the A + B microstructures in material as-forged 25 to 84% would be difficult to account for by a mechanism other than B grain formation by recrystallization. The heat and strain energy present at the conclusion of a forging event were presumably sufficient in these cases to begin the recrystallization process.

It follows logically that the processes of grain growth and secondary recrystallization occurred to form the coarser grain type C microstructures. However, neither mechanism is likely to account alone for the broad approximately 20 to 500 μm type C grain size range. Secondary recrystallization is undoubtedly responsible for formation of the huge 200 to 500 μm grains in microstructures designated as type C_2. Microstructures of type C_1, one order of magnitude smaller in grain size, could represent a stage of grain growth.

APPENDIX G

REFERENCES

1. Cullity, B. D., Elements of X-ray Diffraction, Addison Wesley (1956).

2. Box, G. E. P., and Wilson, K. B., "On the Experimental Attainment of Optimum Conditions", J. Roy. Statist. Soc., Ser. B., Vol. 13, 1951, pp. 1-45.

3. Holms, A. G., and Berrettoni, J. N., "Multiple Decision Procedures for ANOVA of Two-Level Factorial Fixed-Effects Replication-Free Experiments," NASA TN D-4272, 1969.

4. Amling, G. E., and Holms, A. G., "POOLMS - A Computer Program for Fitting and Model Selection for Two-Level Facorial Replication-Free Experiments", NASA TM X-2706 (1973).

5. Sidik, S. M., "An Improved Multiple Linear Regression and Data Analysis Computer Program Package", NASA TN D-6770.

6. Dieter, G. E., Jr., Mechanical Metallurgy, McGraw-Hill (1961), pp. 479-480.